CYBER-PHYSICAL SYSTEMS WITH MULTI-UNMANNED AERIAL VEHICLE-BASED COOPERATIVE SOURCE SEEKING AND CONTOUR MAPPING

by

Jinlu Han

A dissertation submitted in partial fulfillment
of the requirements for the degree

of

DOCTOR OF PHILOSOPHY

in

Electrical Engineering

Approved:

Dr. YangQuan Chen Major Professor	Dr. Mac McKee Committee Member
Dr. David Geller Committee Member	Dr. Donald Cripps Committee Member
Dr. Koushik Chakraborty Committee Member	Dr. Mark R. McLellan Vice President for Research and Dean of the School of Graduate Studies

UTAH STATE UNIVERSITY
Logan, Utah

2014

Abstract

Cyber-Physical Systems with Multi-Unmanned Aerial Vehicle-
Based Cooperative Source Seeking and Contour Mapping

by

Jinlu Han, Doctor of Philosophy
Utah State University, 2014

Major Professor: Dr. YangQuan Chen
Department: Electrical and Computer Engineering

This dissertation focuses on the design, simulation, and execution of multi-unmanned aerial vehicle (UAV)-based cooperative source seeking and contour mapping with cyber-physical systems (CPS). Both fixed-wing UAVs and vertical takeoff and landing (VTOL) UAVs are developed as the flight platforms. Compared with single UAV, multi-UAV formation with advanced cooperative control strategies has more advantages for radiative source detection, especially in urgent tasks, for example, detecting nuclear radiation before deploying the salvage. A contour mapping algorithm for the nuclear radiation is proposed, and practical predefined waypoint-based formation flights are realized. Then, four scenarios are developed for multi-UAV-based cooperative source seeking and contour mapping of radiative signal fields. The fixed wing UAVs are more suitable for widespread detection, while VTOL UAVs are better for accurate detection. The flight control of each VTOL UAV is critical, and the designed fractional order controller for pitch-loop control guarantees the stable flight. Finally, the conclusion of this dissertation and suggestions for future research are presented.

(121 pages)

Public Abstract

Cyber-Physical Systems with Multi-Unmanned Aerial Vehicle-
Based Cooperative Source Seeking and Contour Mapping

by

Jinlu Han, Doctor of Philosophy
Utah State University, 2014

Major Professor: Dr. YangQuan Chen
Department: Electrical and Computer Engineering

This dissertation presents the design, simulation, and execution of multi-unmanned aerial vehicles (UAV)-based cooperative source seeking and contour mapping with cyber-physical systems (CPS). Both fixed-wing UAVs and vertical takeoff and landing (VTOL) UAVs are developed as the flight platforms. Compared with single UAV, multi-UAV formation with advanced cooperative control strategies has more advantages for radiative source detection, especially in urgent tasks, for example, detecting nuclear radiation before deploying the salvage. A contour mapping algorithm for the nuclear radiation is proposed, and practical predefined waypoint-based formation flights are realized. Next, four scenarios are developed for multi-UAV-based cooperative source seeking and contour mapping of radiative signal fields. The fixed wing UAVs are more suitable for widespread detection, while VTOL UAVs are better for accurate detection. The flight control of each VTOL UAV is very critical, and the designed fractional order controller for pitch-loop control guarantees the stable flight. The conclusion of this dissertation and suggestions for future research are presented in the end.

This work is dedicated to
my parents, Mr. Xifeng Han and Mrs. Shifeng Zhao, my wife, Yue Zhang,
and everyone who has helped me to grow and improve.

Acknowledgments

First of all, I would like to thank my Ph.D. advisor, Dr. YangQuan Chen, for providing me the opportunity to work in Center for Self-Organizing and Intelligent Systems (CSOIS) on AggieAir UAV projects. Dr. Chen's continuous pursuit for research excellence deeply impresses me, his rigorous research attitude encourages me, and his professional guidance brings me to a new level of research. Without his advising, I could not make current achievements.

Many thanks to my committee members for not only teaching me the academic knowledge, but also for giving me many instructions about my dissertation. I want to thank Utah Water Research Laboratory (UWRL) and Dr. Mac McKee for providing funding for my research, and encouraging me when I met with some problems. Thanks go to Dr. David Geller for teaching me navigation theories, Dr. Donald Cripps for giving me good suggestions about my research, Dr. Koushik Chakraborty for supporting my research interest and encouragement, and Dr. Todd Moon for providing much help for my dissertation and defense. Also thanks go to Mary Lee Anderson (ECE department graduate advisor), to Tricia Brandenburg (ECE department secretary), and to Kathy Phippen (ECE department business manager), for their professional advice and help when I encountered problems.

I appreciate all the colleagues in the AggieAir group I have worked with. I would like to thank Dr. Haiyang Chao for his guidance and sharing his research experience. Thanks go to Long Di for working together on multi-UAV formation flights, and helping me to proof papers for publication. Many thanks go to Austin Jensen for sharing his simulation experience to me and generous help when I encountered problems. Thanks go to Calvin Coopmans for his assistance on my UAV projects and research, and Nathan Hoffer for helping me to improve my presentation performance. Thanks go to Dr. Huifang Dou for supporting me to focus on my research topic, Dr. Jacob Gunther for teaching me further knowledge of signal processing, Dr. Chet Lo for helping me better understand stochastic processing, Dr. Sheng Hu for showing me how to make a 72-inch UAV, Dr. Ying Luo for

his help on pitch-loop control, Dr. Yan Li for helping me to settle down when I came to Utah State University (USU) and sharing his publication experience, Dr. Hongguang Sun for telling his research experience, Dr. Yaojin Xu for helping on simulation of multi-UAV source seeking, Michal Podhradsky for helping on flight preparations, Daniel Robinson for securing the flights as the safety pilot, Dr. Dali Chen for telling me interesting research about image processing, Dr. Hadi Malek for sharing experience about writing proposal, Dr. Sara Dadras for discussing fractional order control (FOC), Dr. Christophe Tricaud for discussing distributed control, Dr. Rajnikant Sharma for talking about multi-UAV research, and Dr. Rees Fullmer for sharing his optimal control experience. I would like to thank my other colleagues and friends for their help, including Corentin Chron, Tobias Fromm, Aaron Dennis, Daniel Stuart, Jun Pan, Dr. Igor Podlubny, Dr. Deshun Yin, Dr. Xuefeng Zhang, Dr. Aiming Ge, Dr. Kecai Cao, Dr. Changpin Li, Dr. Dingjin Huang, Dr. Kexue Li, Dr. Zhuang Jiao, Dr. Caibin Zheng, Dr. Chun Yin, Dr. Peng Guo, Yu Shang, Zhuo Li, Shuai Hu, Bo Li, Dr. Yongcan Cao, Dr. Yiding Han, Swathi Gorthi, Pooja Kavathekar, David Cornelio, Roque Lora, Yi Luo, Yunshu Liu, Ziang Wang, Xuan Xie, Dr. Chengjin Chu, Lin Zhang, etc.

A great deal of gratitude also goes to my parents for their constant love, concern, toleration, and understanding to support me through all my Ph.D. study life. I would like to thank my wife for her love, support, sacrifice, and understanding to help me face the busy research and colorful life.

Jinlu Han

Contents

List of Tables

List of Figures

Acronyms

ADC	Analog-to-Digital Converter
AHRS	Attitude Heading Reference System
AP	Autopilot
ARX	Auto-Regressive Exogenous
CPS	Cyber-Physical Systems
CSOIS	Center for Self-Organizing and Intelligent Systems
DAC	Digital-to-Analog Converter
DCM	Direction Cosine Matrix
DoM	Degree of Measurement
EPP	Expanded Polypropylene
ESC	Electronic Speed Control
FBW	Fly-By-Wire
FO	Fractional Order
FOPTD	First Order Plus Time Delay
GCS	Ground Control Station
GIS	Geographic Information System
GPS	Global Position System
I^2C	Inter-Integrated Circuit
IMU	Inertial Measurement Unit
IOPID	Integer Order Proportional-Integral-Derivative
LCD	Liquid-Crystal Display
MEMS	Micro Electro-Mechanical Systems
MZN	Modified Ziegler-Nichols
NSF	National Science Foundation
P2P	Point to Point
P2MP	Point to Multi-Point

PI	Proportional-Integral
PID	Proportional-Integral-Derivative
PPM	Pulse-Position Modulation
PWM	Pulse Width Modulation
RC	Remote Controlled
SD	Secure Digital
SPI	Serial Peripheral Interface
SPSA	Simultaneous Perturbation Stochastic Approximation
TWOG	Tiny Without GPS
UART	Universal Asynchronous Receiver/Transmitter
UAS	Unmanned Aerial System
UAV	Unmanned Aerial Vehicle
USB	Universal Serial Bus
USU	Utah State University
UWRL	Utah Water Research Lab
VTOL	Vertical Takeoff and Landing

Chapter 1

Introduction

1.1 Dissertation Roadmap

This dissertation focuses on how to design, simulate, and implement the multi-unmanned aerial vehicle (UAV) based cooperative source seeking and contour mapping with cyber-physical systems (CPS). CPS with UAVs could be taken as mobile sensors, and are widely used for personal remote sensing (PRS) in various applications, such as precision agriculture, vegetation mapping, and river monitoring. It is more useful to send the UAVs for urgent tasks before deploying the salvage; for example, radiative source seeking, especially for nuclear radiation detection. Compared to single UAV, multi-UAV formations could accomplish the task in cooperative flights, and save a lot of time. Equipped with proper sensors, the multi-UAV formations are able to execute the contour mapping besides source seeking by implementing the pre-designed control strategies, which can give the panoramic with radiative levels provided. Fixed-wing UAVs are more suitable to detect the radiative source at a wide range over the potential field, while the vertical takeoff and landing (V-TOL) UAVs, are good at accurate detecting. The fractional order controller can guarantee a more stable flight by comparison with other controllers, which is able to perform a better formation flight for source seeking and contour mapping.

1.1.1 Cyber-Physical Systems

CPS are attracting increasing attention, and will be used in more and more areas. In Wikipedia, the definition of CPS is "A cyber-physical system (CPS) is a system of collaborating computational elements controlling physical entities. Today, a precursor generation of CPS can be found in areas as diverse as aerospace, automotive, chemical processes, civil infrastructure, energy, healthcare, manufacturing, transportation, entertainment, and con-

sumer appliances. This generation is often referred to as embedded systems. In embedded systems the emphasis tends to be more on the computational elements, and less on an intense link between the computational and physical elements" [1].

Besides physical input and output, CPS also include the interaction as a network, and the current computing ability and networking technologies are the adequate foundations which can limit the function of CPS. As said by Lee [2] "Cyber-Physical Systems (CPS) are integrations of computation and physical processes. Embedded computers and networks monitor and control the physical processes, usually with feedback loops where physical processes affect computations and vice versa. The economic and societal potential of such systems is vastly greater than what has been realized, and major investments are being made worldwide to develop the technology. There are considerable challenges, particularly because the physical components of such systems introduce safety and reliability requirements qualitatively different from those in general-purpose computing. Moreover, physical components are qualitatively different from object-oriented software components. Standard abstractions based on method calls and threads do not work."

Figure 1.1 [3] in LIM Laboratory demonstrates CPS architecture for daily life.

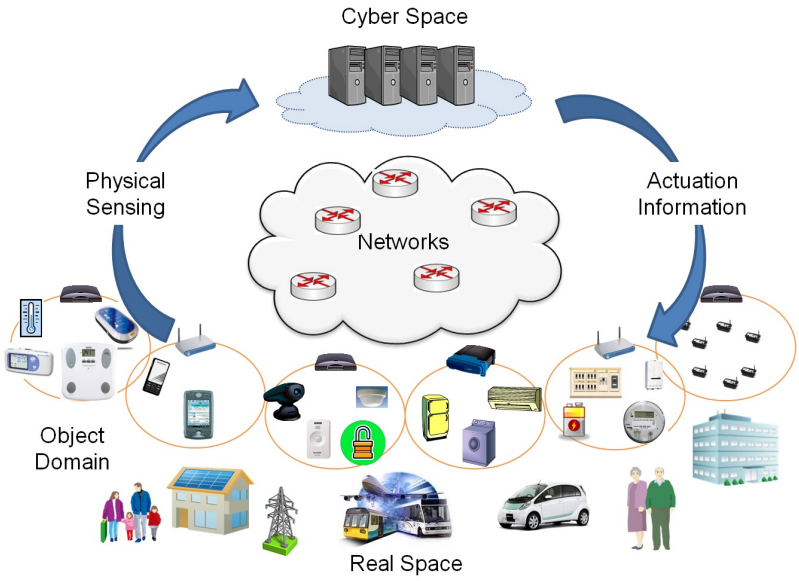

Fig. 1.1: An example for CPS architecture.

Right now, CPS are already used in many areas, for example:

- River detection,
- Wireless sensor network monitoring,
- Precision agriculture,
- Medical system,
- Firefighting.

The potential applications of CPS will be broadened [1] in various areas, and some examples are shown below.

- Collision avoidance: Figure 1.2 [4] and Figure 1.3 [5] describe the selected applications for obstacle collision avoidance and mutual collision avoidance.

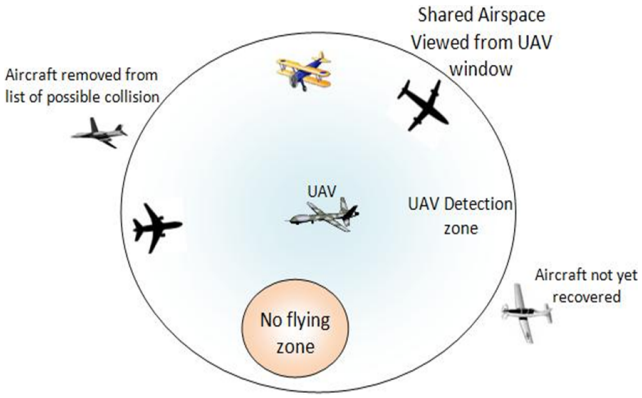

Fig. 1.2: UAV collision avoidance.

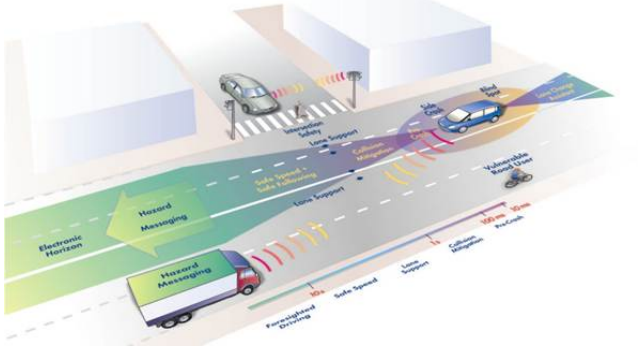

Fig. 1.3: Vehicle collision avoidance.

- Precision: In some applications, such as the personal safety and precise manufacturing, the precision is the essential requirement. Figure 1.4 [6] and Figure 1.5 [7] show the selected applications for robotic surgery and nano-level manufacturing.

- Coordination: The traffic control is becoming more and more important because of the increasing traffic in land, air, and water. Figure 1.6 [8] and Figure 1.7 [9] demonstrate the selected applications for optimal traffic light control and air traffic control.

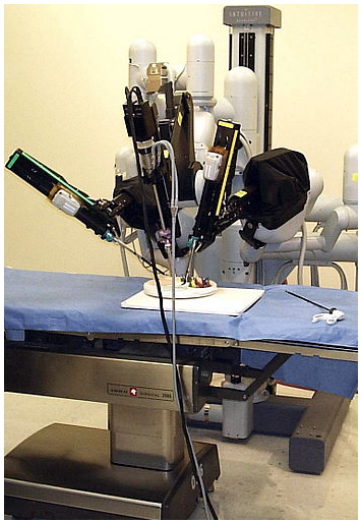

Fig. 1.4: Robotic surgery.

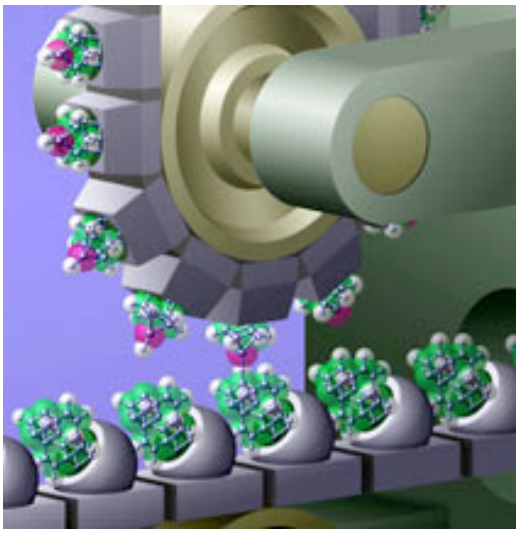

Fig. 1.5: Nanomanufacturing.

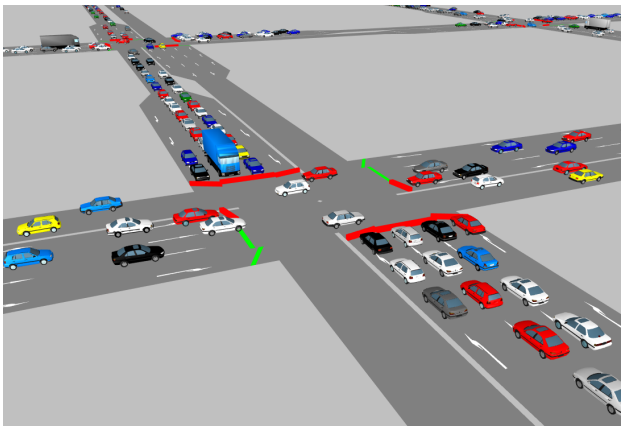

Fig. 1.6: Optical traffic control.

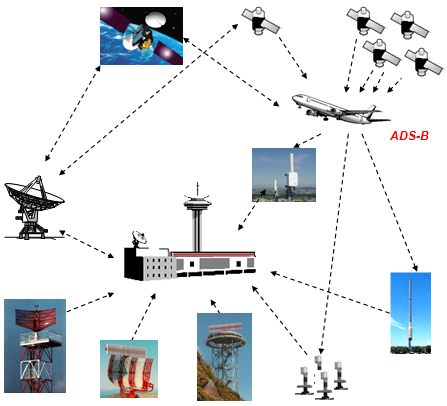

Fig. 1.7: Air traffic control.

- Efficiency: Alarm system is able to protect the safety of each family as well as the industrial products away from fire, and remote controlled haptic systems could give the professional operations to the injured persons thousands of miles away. Figure 1.8 [10] and Figure 1.9 [11] illustrate the selected applications for alarm system and haptic interaction.

- Expansion of human capabilities: Robotics have the ability to carry the people to the places far away, and also are able to deliver the products instead of using real people. Monitoring systems facilitate people's daily life by providing all kinds of real-time information. Figure 1.10 [12] and Figure 1.11 [13] show the selected applications for delivery and health care monitoring.

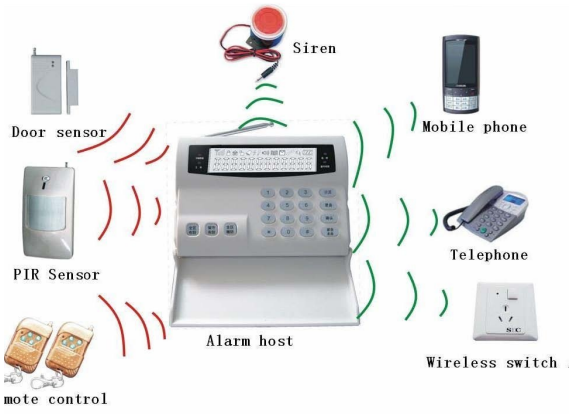

Fig. 1.8: Home alarm system.

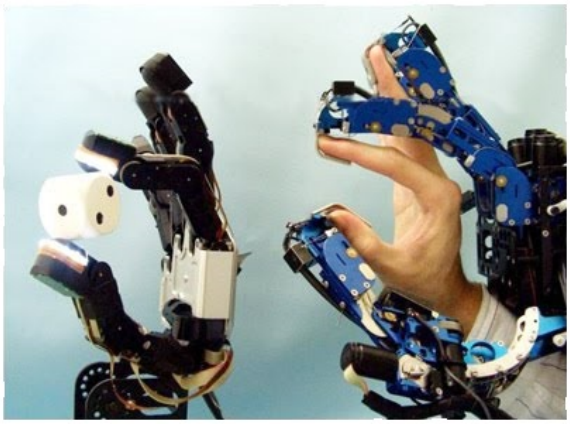

Fig. 1.9: Haptic robotic arm.

Fig. 1.10: Amazon prime air.

Fig. 1.11: Health monitoring system.

- Dangerous operation: Some areas are difficult for people to access, and a plenty of operations are very dangerous or harmful to people's health. Figure 1.12 [14] and Figure 1.13 [15] describe the selected applications for search, rescue, and radiative source detection.

- Exploration of the inaccessible environments: Figure 1.14 [16] and Figure 1.15 [17] show the selected applications for deep-sea exploration and space exploration, which help to explore the inaccessible environments.

The National Science Foundation (NSF) illustrates CPS as:

> "Cyber-physical systems (CPS) are engineered systems that are built from and depend upon the synergy of computational and physical components. Emerging CPS will be coordinated, distributed, and connected, and must be robust and responsive. The CPS of tomorrow will need to far exceed the systems of today in capability, adaptability, resiliency, safety, security, and usability. Examples of the many CPS application areas include the smart electric grid, smart transportation, smart buildings, smart medical technologies, next-generation air traffic management, and advanced manufacturing. CPS will transform the way people interact with engineered systems, just as the Internet transformed the way people interact with information. However, these goals cannot be achieved without rigorous systems engineering" [18].

Fig. 1.12: UAV for search and rescue.

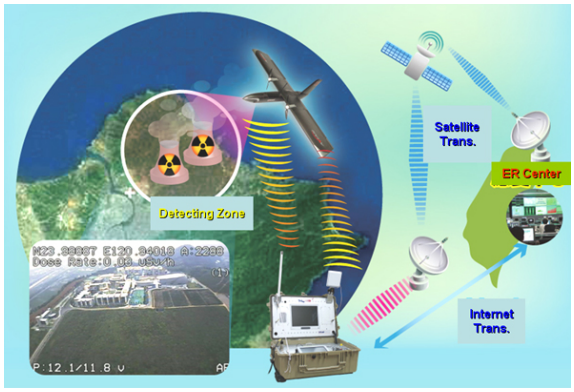

Fig. 1.13: Radiation detection.

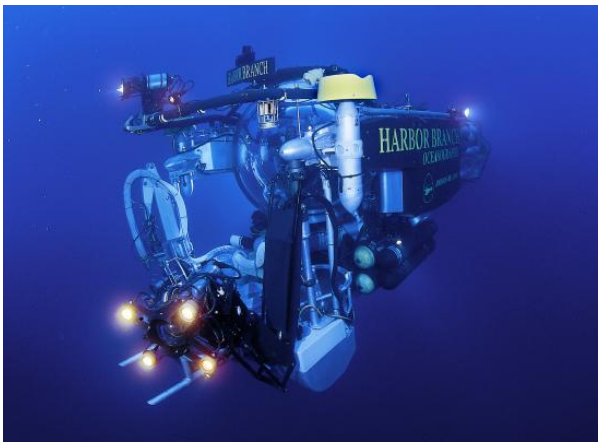

Fig. 1.14: Deep-sea explorer.

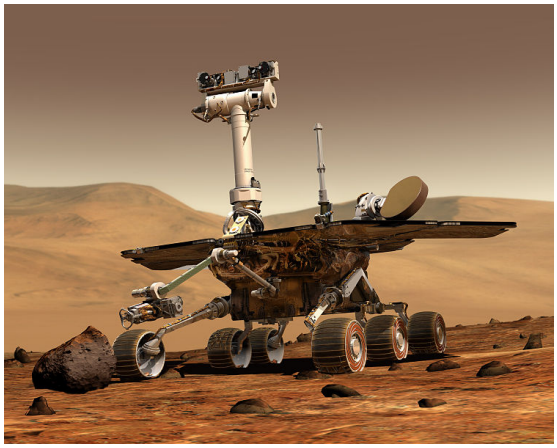

Fig. 1.15: Space explorer.

The concept of CPS is more related with "robotics," "vehicles," "network," and according to the author's best understanding, the definition can be described as "Cyber-physical systems (CPS) are composed of interacted (mostly networked) actuators (including robotics, manned and unmanned vehicles), use the equipped on sensors to detect the rich physical world, interact the detected information, calculate, then deploy the actuators to cooperatively execute the actions to control the physical entities."

This dissertation presents the challenges in designing such systems, considers the question of whether today's technology for actuators and sensors could provide adequate foundations for CPS, considers the advantages by utilizing CPS, examines the current computing and networking status, and chooses the appropriate methods: UAVs with CPS approach for the task (detecting and contour mapping of radiative signal fields).

1.1.2 UAVs with CPS Approach

UAVs are being used more and more in civilian applications and have attracted increasing attention in research. UAVs, especially low-cost UAVs, are becoming a new, potentially significant service product known as UAV-based personal remote sensing (PRS). On one hand, UAV research is becoming a notable area with the growing number of papers focused on system modeling, navigation, flight control, path planning, etc. On the other hand, with the rapid development of electronics and wireless communication technology, civilian remote

sensing becomes practical by installing inexpensive sensors on UAVs to measure and collect concerned real-time parameters, such as temperature, humidity, and image. Therefore, UAVs are being used as PRS in many different areas, such as water management, forest fire detection, wetland monitoring, and crop identification. Compared with satellite remote sensing, UAVs can provide equivalent or higher resolution imagery, and relevant parameters in more affordable ways [19].

There are many types of fixed-wing UAVs, and VTOL UAVs developed for AggieAir, which are used for various applications and research. Figure 1.16 [20] and Figure 1.17 [20] capture the flying AggieAir Minion and AggieAir hexorotor VTOL UAV separately.

There are many applications for the fixed-wing UAVs, and some examples are shown in the following:

- Wetland detection (Figure 1.18 [21]),
- Precision agriculture (Figure 1.19 [22]),
- Detection for Bear River Migratory Bird Refuge (MBR) (Figure 1.20 [23]),
- Fish tracking (Figure 1.21 [24]).

Fig. 1.16: AggieAir-Minion.

Fig. 1.17: AggieAir-VTOL (hexorotor).

Fig. 1.18: AggieAir for wetland.

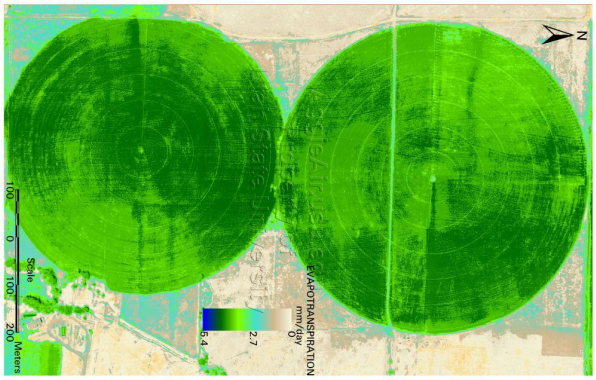

Fig. 1.19: AggieAir for agriculture.

Fig. 1.20: AggieAir for bird refuge.

Fig. 1.21: AggieAir for fish tracking.

Fixed-wing UAVs are popular for tasks with long endurance [25] and high altitude. In contrast to fixed-wing UAVs, VTOL UAVs have particular advantages, such as hovering capability and no space restriction for takeoff and landing, which are beneficial for applications, such as search and surveillance, static image capturing, and crop identification.

Compared with fixed-wing UAVs, VTOL UAVs are more suitable to be used in smaller area with more accurate detection. The applications of VTOL UAVs include the following aspects:

- High quality photos and videos (Figure 1.22 [26]),
- Water monitoring (Figure 1.23 [27]),

- Powerline inspection (Figure 1.24 [28]),
- Dam inspection (Figure 1.25 [29]).

Multi-UAV in a cooperative formation [30] can provide more robust and safety compared with single UAV, and save the time to fulfill different application requirements [31], which is very important for time urgent task, such as rescue, and radiative signal detection. Moreover, multi-UAV in decentralized formations can communicate with each other, share the information, and implement intelligent control algorithms to achieve many kinds of challenging missions.

This dissertation focuses on multi-UAV-based cooperative source seeking and contour mapping with CPS approach, especially for the radiative source.

Fig. 1.22: High quality photo capturing.

Fig. 1.23: Algae growth.

Fig. 1.24: Powerline inspection.

Fig. 1.25: Dam inspection.

1.1.3 Challenges for Multi-UAV-Based Cooperative Source Seeking and Contour Mapping

The challenges for the source seeking and contour mapping by using multi-UAV are listed below.

- Fast deployment: When the source leakage happens, the detecting action needs to be deployed fast to protect personal safety and property.
- Low cost: After leakage happens, the source seeking and contour mapping should be carried out immediately. It is also important to execute the regular detections above the fields to monitor if any radiation leakage happens, so low cost is an necessary demand.
- Detecting ability: With the installed sensors, the multi-UAV should be able to achieve the source seeking and contour mapping within a short period to time.
- Large area sensing: If the radiative source is mobile, and the ability to fly across a large area is a must to track the location of the source.
- Small area tracking: The detecting actuators should be able to hover or backward to keep tracking the mobile source with better precision.
- Easy manipulation: The operation for the task ought to be as simple as possible, and as easy as possible.
- Important information: The global positioning system (GPS) information based image maybe needed during the mission.

1.2 Research Motivations

The research motivation for the multi-UAV-based source seeking and contour mapping could be divided into several aspects, and stated in the following.

1.2.1 UAVs Design for Source Seeking and Contour Mapping

It is very important to monitor and detect the radiative source even it is a moving source. When something happens to cause it running in the abnormal situation, the detection has to be implemented as soon as possible to monitor the progress and evaluate the radiative impact to the environment and to the safety of the residents nearby. It is more challenging for the mobile source situation, because the actuators have to be able to continuously seek the source which is keeping moving.

The UAVs are chosen as the executors to implement the source seeking and contour mapping due to many reasons, such as low-cost design, simple operation, high-speed movement, no topography restriction, large area detection (fixed-wing UAV), small area detection and tracking (VTOL UAV), and GPS-based image acquirement.

The design of multi-UAV cooperative formations for source seeking and contour mapping is classified into three aspects: hardware, software, and control algorithms.

Because of the advantages of the fixed-wing UAVs and VTOL UAVs, heterogeneous flights (fixed-wing UAVs + VTOL UAVs) could enhance the abilities of both types of UAVs, and achieve better performance for a variety of tasks.

1.2.2 Low-Cost Multi-UAV formations for Contour Mapping of Nuclear Radiation Fields

Radiative source detection, especially the nuclear radiation detection is extremely dangerous, and the source seeking and contour mapping have to be executed before deploying the salvage. Since the nuclear radiation would bring great harm to people's safety, man operated vehicles could not get close to the nuclear radiation polluted field. The unmanned vehicle is the only way to explore and detect the field; considering the building and the ground have big possibility to block the unmanned ground vehicle, the UAV is the best option to implement the task.

Low-cost UAVs are becoming more and more popular in both research and practical applications, and multi-UAV system with advanced cooperative control algorithms has advantages over single UAV system, especially in time urgent tasks.

The way for executing the multi-UAV formation to seek the source depends on the purpose of the task along with the situation of the source. When nuclear radiation happens, scientific analysis could be implemented to the polluted fields, for example, by providing the contour mapping of specified level of the nuclear radiation. Scenarios should be considered in advance before the detection, which could be divided into two situations.

(1) Radiation level detecting on specified waypoints: In this scenario, the multi-UAV would fly in formations to cooperatively detect the level of radiation on specified waypoints (3D), monitor the radiation level on every point, and transmit back the data for analysis.

(2) Contour mapping of specified radiation level: This scenario could map the contour of predefined radiation level for the multi-UAV cooperative formations while keeping seeking the source. This contour mapping is able to give an visual understanding of the zone polluted by the nuclear radiation, which can provide tremendous help for the salvage.

Various experimental formation flights could imitate types of nuclear radiation detections.

1.2.3 Multi-UAV formations for Cooperative Source Seeking and Contour Mapping of Radiative Signal Fields

The radiative source could be a wide range of spatially distributed source, such as light spread, thermal energy, and acoustic signal dissemination. The situations for the radiative source and targeted fields may also differ from case to case. Consequently, various scenarios to detect the radiative source should be explored according to the status of the source and the purpose of the detection.

There are many factors need to be considered for the practical formation flights, such as the following.

- UAV speed limit during flight: There are maximum speed for both fixed-wing UAVs and VTOL UAVs, and minimum speed for fixed-wing UAVs while executing the cruise flight with altitude maintained.

- Minimum distances: During UAVs formation flights, the minimum distances among each other should be taken into account, especially when fixed-wing UAVs are used to execute the mission above relatively smaller fields.

- Effective distances: The distances for effective communication between UAVs and ground control station (GCS) should be considered in case accident happens.

- Minimum radius: When the UAVs circle in round, the minimum radius is an important factor to be considered for making the flight plan, which could not make fixed-wing UAVs turn too sharply.

- Envimental impact. For example, the wind gust could cause UAVs to crash.

For the multi-UAV cooperative source seeking and contour mapping, the communication between the UAVs and GCS are the fundamental of the task, and the communication between each UAV known as decentralized communication could bring more robust to the formation flight. So some scenarios should be considered including these following situations.

- Sensor noise: There is noise for every sensor, which is used to detect the radiative source. Because the sensors are equipped on UAVs for contour mapping, the sensor noise may affect the flight path somewhat, so the control algorithms should be able to handle the noise and maintain good formation.

- Moving source situation: For the moving source, the radiative source maybe installed on moving vehicles which makes the source seeking more urgent because the moving radiative source has a big potential threat to the public safety and would bring severe impact if it is not detected.

- Communication lost: If one or more UAVs lost the communication with GCS, they could still accomplish the mission by communicating with other UAVs while keeping the formation shape.

1.2.4 Pitch-Loop Control of a VTOL UAV

Fixed-wing UAVs and VTOL UAVs have their own advantages, and are suitable for different detection tasks. If fixed-wing UAVs and VTOL UAVs could collaboratively work in heterogeneous formation flight, in which fixed-wing would be sent to execute the wide range seeking and contour mapping, then the VTOL UAVs could explore the interested locations with more accurate information provided. Attitude control is the fundamental tuning step for VTOL UAVs, and has significant impact on the flight. Various control strategies should be compared in the following aspects.

- Wind gust disturbance: Wind gust is one of the main disturbance for small UAVs, which can deteriorate the performance of the UAVs or even make them crash. So the capability to handle certain level of wind gust is one criterion for the controller design.

- Controller robustness: The selected controller should have good robustness compared with other selected controllers. When the payload of an UAV is changed, which could be taken as the system gain varies, the controller should be able to handle the system gain variations.

- Fast response: When some situation is detected, the UAVs have to drop or climb the altitude, or change the attitude quickly. So the ability for fast response is essential for the control of UAVs.

All the three factors should be considered during the controller design to make sure the good control of the UAVs. Only if every UAV has good performance, the multi-UAV formation flight has the good foundation to fly well.

1.3 Dissertation Contributions

The major contributions of this dissertation include the following aspects:

- Built and tested the low-cost fixed-wing UAVs (48 inch),
- Built and tested the VTOL UAVs,
- Practical multi-UAV formation flights,
- Simulated multi-UAV contour mapping of nuclear radiation fields, and executed experimental formation flights,
- Proposed four scenarios for cooperative source seeking and contour mapping of diffusive signal fields by formations of multiple UAVs,
- Implemented the designed fractional order PI controller to VTOL UAV flight control.

1.4 Dissertation Organization

The dissertation is organized as the following. Chapter 1 introduces the research motivations and dissertation contributions. Chapter 2 describes the hardware, software, and control structure for the developed fixed-wing UAV and VOTL UAV platforms. In Chapter 3, two scenarios are presented for low-cost multi-UAV based nuclear radiation detection, with both simulated results and experimental flight data illustrated. Chapter 4 is dedicated to four scenarios designed for cooperative source seeking and contour mapping of radiative signal fields by multi-UAV formations with practical flight situation considered. In Chapter 5, the fractional order PI controller is designed and implemented for the pitch-loop control of a VTOL UAV, and the advantages is demonstrated by comparing with other controllers. Chapter 6 concludes this dissertation and proposes suggestions for future research.

Chapter 2

Fixed-Wing UAS and VTOL UAS

2.1 Introduction

This chapter focuses on the design of the unmanned aerial system (UAS). Compared to the traditional aircraft or satellite-based equipments or ground-based devices, small UAS, including UAV with equipped sensors, has many advantages in real-time and practical applications. UAS is able to detect a wide range of areas in a small period of time with acquired large amount of data for many civilian applications. Also, small UAS is easy to make, fast to setup, and cheap to maintain. There is already many UAS applications in civilian environment, such as vegetation mapping, river applications, and precision agriculture. UAS enables to replace the human pilots in tedious or dangerous tasks, especially for the radiative field.

Motivated by the advantages of UAS, AggieAir UAS (a remote sensing-based small low-cost UAS for scientific applications) is developed step to step at Center for Self-Organizing and Intelligent Systems (CSOIS) and Utah Water Research Laboratory (UWRL) in Utah State University. There are both fixed-wing UAVs and VTOL UAVs in AggieAir UAS. Fixed-wing UAVs are suitable for wide range and long endurance applications, and VTOL UAVs are more used for small area, static capturing, search and rescue because of the hovering ability, and no space restriction for takeoff and landing.

This chapter presents the designed two types of UAVs within various types of AggieAir UAVs: 48-inch fixed-wing UAVs and quadrotor VTOL UAVs. First, the overview of a fixed-wing UAS with single 48-inch UAV is introduced. After that, the hardware of the UAS is explained in details followed by the structure of the software. In the following, an investigation of the current VTOL UAV platforms are compared and demonstrated with classifications. Finally, the hardware and software of designed VTOL UAS are illustrated.

2.2 Fixed-Wing UAS

2.2.1 Fixed-Wing UAS Hardware

Figure 2.1 demonstrates the hardware of 48-inch fixed-wing UAS, which can be classified into four parts.

Control Part

Autopilot is used to run the algorithms, and give the commands to the actuator (motor+2 servos). GCS is the interface between operator and UAVs by sending out command while receiving the status of the UAVs.

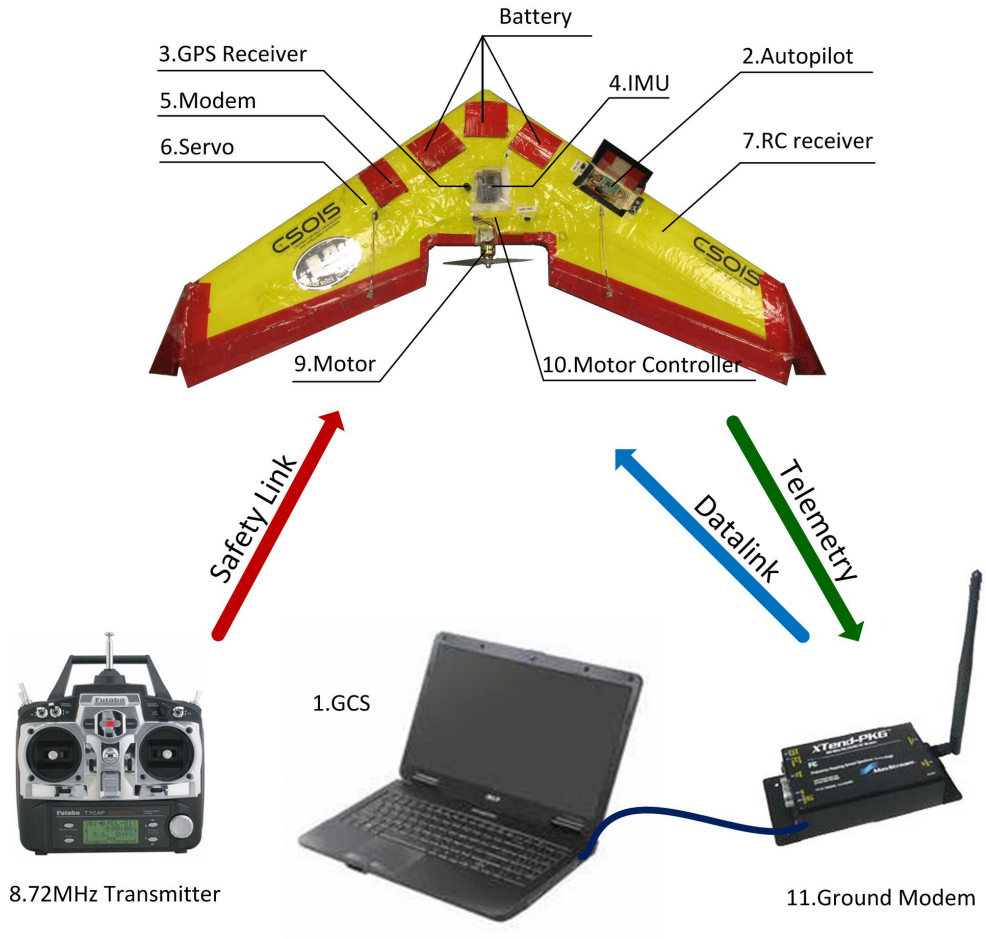

Fig. 2.1: Fixed-wing UAS with single UAV.

Navigation Part

Inertial measurement unit (IMU) and GPS can help the UAVs get the information about attitude change and accurate current status.

Communication Part

Remote controlled (RC) receiver and RC transmitter provide more secure by safety link. Onboard modem and ground modem are responsible for the communication between the UAVs and the GCS.

Actuators

Left and right servo cooperate to control the movement of the elevon (combination of elevator and aileron). The motor together with propeller provides propulsion for the UAV by receiving the control signal from motor controller.

The detailed explanation about the components of fixed-wing UAV is demonstrated in the following.

- GCS: The users not only can monitor the status of the UAVs in detailed information including battery, throttle, attitude, mode, ground speed, the current stage in flight plan, etc., but also can send the command to the autopilot through modem during flight.
- Autopilot: Paparazzi tiny without GPS (TWOG) board based on LPC2148 MCU could receive the information from RC receiver, modem, GPS, IMU, run algorithms, and give the command to the actuator (motor+2 servos) while sending back the telemetry to the GCS via modem.
- GPS receiver: Ublox GPS receiver which has 50 satellite tracking channels and updates at 4 Hz, is integrated with Ardu IMU, and passes the data to autopilot through Ardu IMU.

- IMU: Ardu IMU can run attitude heading reference system (AHRS) code, and the open-source direction cosine matrix (DCM) complementary filter makes it more competitive among low-cost IMUs.
- Onboard modem: Digi 9XTend modem is used for receiving and transmitting information for autopilot.
- Servo: Left servo and right servo cooperate to control the movement of the elevons.
- RC receiver: Castle Creations Berg 4L receiver is used because it is small, light, and reliable.
- RC transmitter: Futaba T7CAP has 10-model memory, a large LCD screen with adjustable contrast along with digital trims.
- Motor: AXI 2212/20 is a light weight brushless DC motor which can work with propeller to provide enough propulsion for the UAV.
- Motor controller: Motor controller receives the command from autopilot via inter-integrated circuit (I^2C) bus, and sends out the signal to the motor.
- Ground modem: Digi 9XTend modem has a universal asynchronous receiver/transmitter (UART) connecting to the GCS while communicating with onboard modem.

When hardware is correctly mounted in the suitable position of the airframe, and all connections among them are soldered, tuning is the next procedure. The tuning process should be done in Manual, Auto1, and Auto2 modes step-by-step, and then stable autonomous flight can be realized.

Paparazzi is an open-source hardware and software project, for the purpose to set up the exceptionally powerful and versatile UAV system. Paparazzi has the technical community for users to post questions, and give solutions by the best. The project covers the airborne software and hardware, which includes from voltage regulators designs to Kalman Filtering code. The project also contains the ground hardware and software, which have been test

verified and ever-expanding array updated. The interface of ground control software is highly user-friend. The software of the UAV-based system could be divided into two groups.

2.2.2 Fixed-Wing UAS Software

Autopilot Software

The paparazzi autopilot software contains autopilot (AP) process and fly-by-wire (F-BW) process. Figure 2.2 [32] shows the two processes of autopilot software.

GCS Software

The users could execute a variety of flights according to different tasks by using the GCS software.

2.3 VTOL UAS

VTOL is an acronym for vertical take-off and landing aircraft. This classification includes fixed-wing aircraft that can hover, take off and land vertically as well as helicopters and other aircrafts with powered rotors, for example, tiltrotor aircrafts. VTOL UAVs have many extensive applications because they are able to be operated from diverse airfields, be independent of launching and landing restrictions, and hovering at specified altitude, etc.

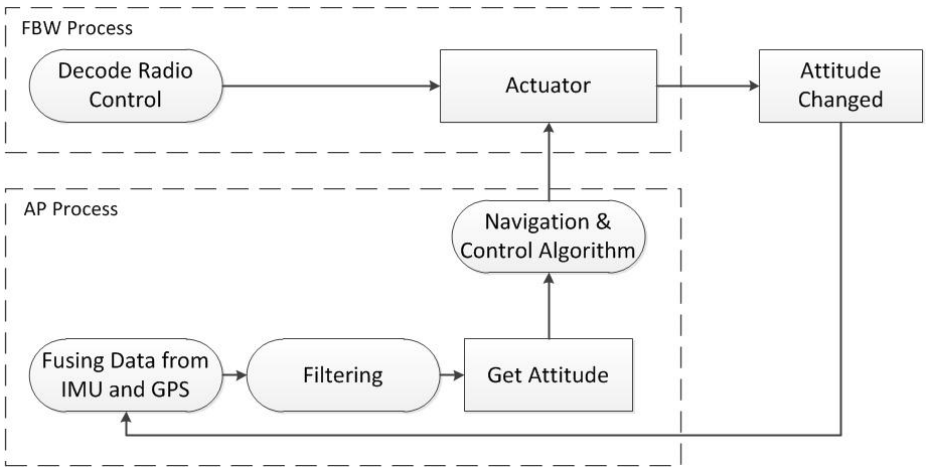

Fig. 2.2: Autopilot software.

Some typical applications for VTOL UAVs are searching and rescuing, acquisition of aero-images, transportation and so on. There are various projects with various platforms worldwide. Figure 2.3 [33], and Figure 2.4 [34] show the large size VTOL Platforms. Figure 2.5 [35] describes the VTOL platform with full model provided. Figure 2.6 [36] illustrates the tiny size VTOL UAV. Figure 2.7 [37], and Figure 2.8 [38] demonstrate the commercial VTOL products. Figure 2.9 [39] shows the high accuracy sensor-based VTOL navigation and Figure 2.10 [40] captures the VTOL formations.

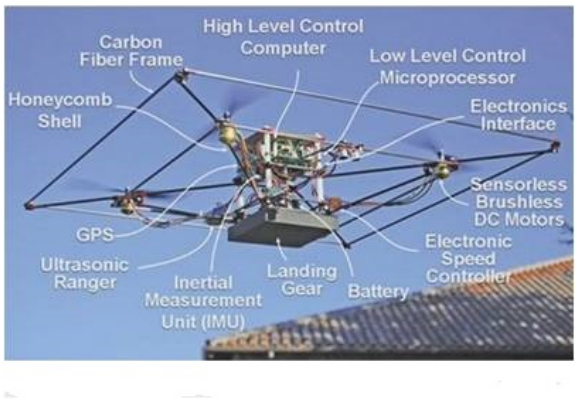

Fig. 2.3: VTOL projects in STARMAC.

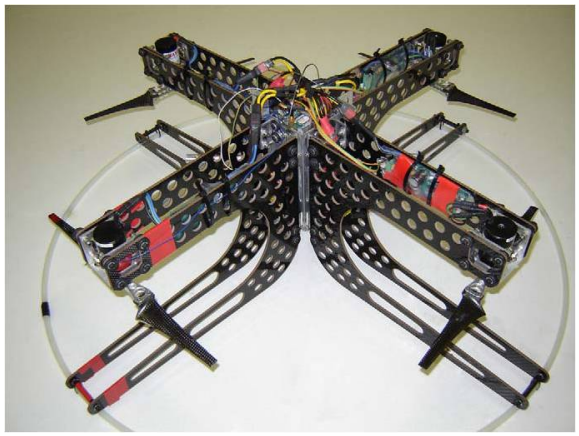

Fig. 2.4: VTOL projects in CSIRO ICT.

Fig. 2.5: VTOL projects in EPFL.

Fig. 2.6: VTOL projects in Mesicopter.

Fig. 2.7: VTOL projects in Microdrones.

Fig. 2.8: ARDrone VTOL.

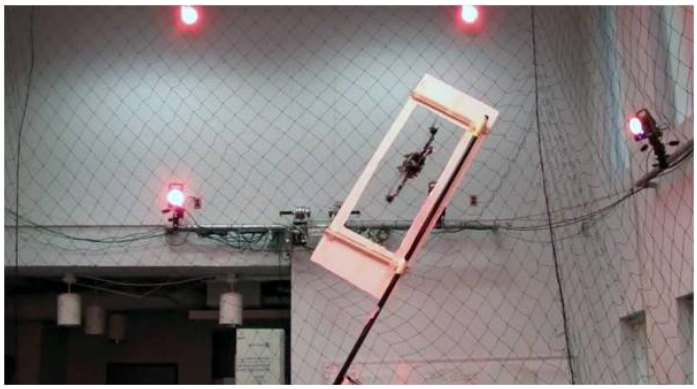

Fig. 2.9: VTOL projects in GRASP.

Fig. 2.10: VTOL projects in ACL.

Two types of AggieAir VTOL UAV platforms are demonstrated in the following. Figure 2.11 demonstrates the quadrotor UAV platform and Figure 2.12 shows the octorotor UAV platform. Compared to quadrotor VTOL UAV, octorotor VTOL UAV could carry more payload for certain applications. Ocorotor VTOL UAV also has more robustness because of various options for motors combinations.

Table 2.1 illustrates the specification of the AggieAir octorotor UAV platform, which is demonstrated in Figure 2.12.

Table 2.1: Octorotor VTOL UAV specification.

Frame Weight	504 g
Autopilot Weight	150 g
8 Motors Weight	633.6 g
8 brushless Controllers Weight	66.4 g
Camera Weight	350 g
Propeller Radius	5 inch
Mounted Round Plate Radius	3.5 inch
Rotor to Frame Center	15 inch

Fig. 2.11: Booz quadrotor VTOL UAV

Fig. 2.12: Booz octorotor VTOL UAV

2.3.1 VTOL UAS Hardware

Figure 2.13 shows the structure of Booz VTOL UAS platform.

Booz VTOL UAV is powered by a LiPo battery which is tightly fixed to the bottom of the center round plane. The center round plane is composed of three boards, controller board, IMU board, and GPS board, which are mounted in the center and eight motor controllers mounted at the edge. The main component of controller board is LPC2148, ARM7TDMI-S CPU with 512 kB flash, 10-bit analog-to-digital converter (ADC), and digital-to-analog converter (DAC) in LQFP64 package. Motor controllers are connected to LPC2148 via I^2C bus and generate pulse width modulation (PWM) to control the separate brushless direct current (BLDC) motor.

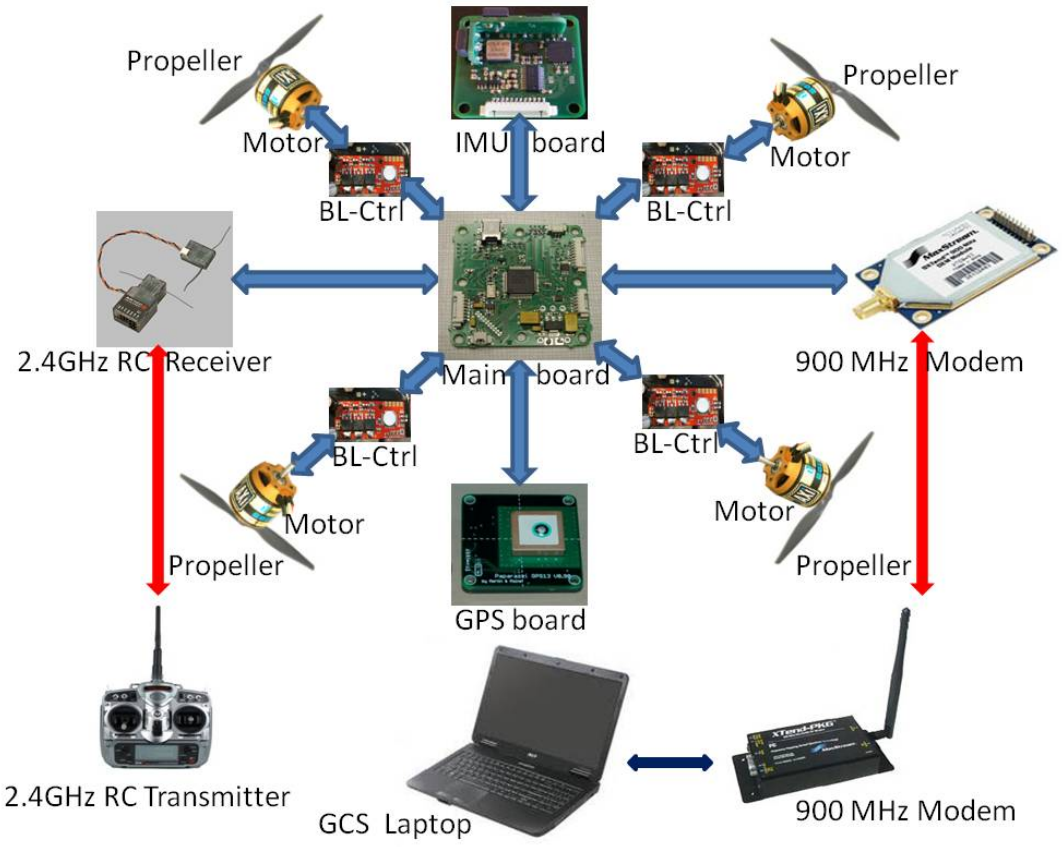

Fig. 2.13: VTOL UAS structure.

A pressure sensor is mounted on the controller board to measure the altitude information more exactly than the GPS altitude information. The IMU board provides acceleration, angular rates and magnetic information by accelerometer, gyro sensor, and magnetometer separately. GPS board receives data from satellites and sends the data to LPC2148. Camera is mounted to the bottom to capture the image and stores the images in 8 G volume secure digital (SD) card.

Figure 2.14 shows the relationship between the rotation and the movement [41].

In flight, position information is acquired from GPS and barometer could be used for more accurate altitude. Triaxial accelerations, triaxial gyro, and triaxial magnetometer are provided by the IMU (3DM-GX3), and all the information is used to calculate the current position and attitude, and compared with the set points. Guidance control is applied during the waypoints flight and stabilization control should be guaranteed during all the flight. Autopilot generates PWM control signal to the electronic speed control (ESC) in order to control the BLDC motor.

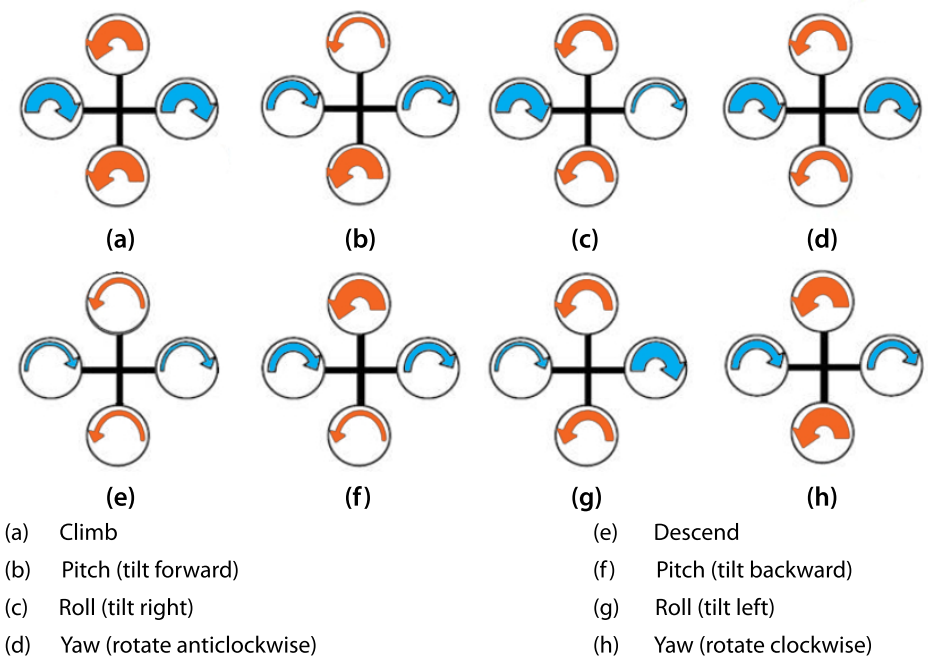

Fig. 2.14: Quadrotor rotation control.

There are two control strategies for the VTOL UAS: manual control (controller still works for stabilization) and autonomous control. A pair of 900 MHz modems are used for the data link communication. GCS is used to monitor the status of VTOL UAV, adjust the tuning parameters, change the flight plan, etc. GCS sends the control commands to the autopilot system, meanwhile, the autopilot system sends back the status of the VTOL UAV including current battery voltage, throttle percentage, GPS data, attitude information, etc. The safety pilot should take over the control for the VTOL UAV, and land it if any accident happens.

The details for the hardware are introduced as follows.

Autopilot

Figure 2.15 [42] is the Booz main board, which contains the following parts:

- Power supply,
- Micro-controller (LPC2148),
- Barometer,
- Universal serial bus (USB) connector.

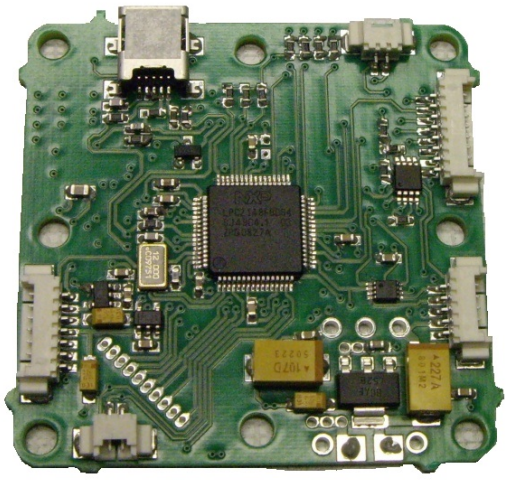

Fig. 2.15: Booz main board.

Newer version autopilot for AggieAir VTOL UAV is Lia board. Figure 2.16 [43] shows Lia board, built based on the 72 MHz 64-pin STM32 processor, which is the same as Lisa/M. There are 8 PWM outputs for ESCs and Motors, 3 UART interfaces, 1 CAN bus, 1 serial peripheral interface (SPI) bus, 2 I^2C bus, 1 micro USB, and 4 status LEDs.

IMU

Three types of IMUs have been used for flight tests.

(1) Booz IMU: Figure 2.17 describes the Booz IMU board, which contains three boards: main IMU board, YZ board, and XZ board.

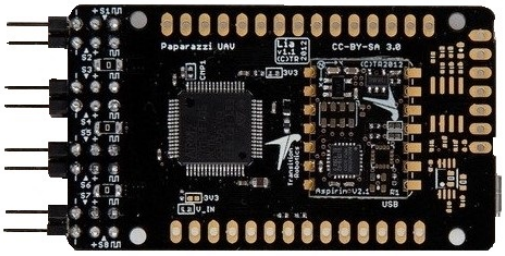

Fig. 2.16: Lia board.

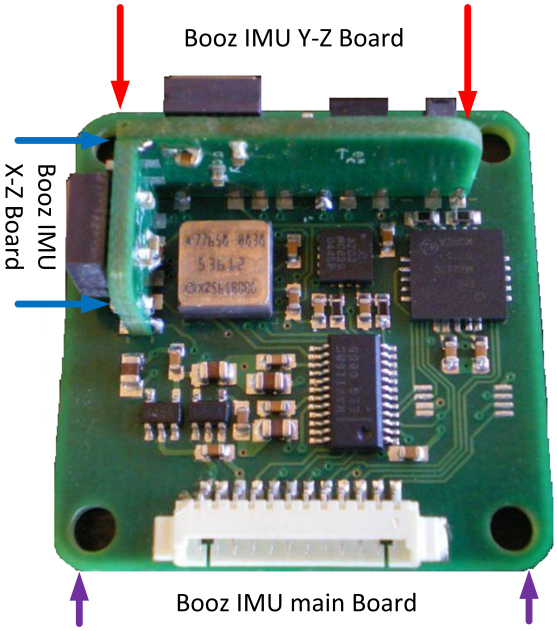

Fig. 2.17: Booz IMU.

- On main IMU board, the main components are:
  - 22 pin ADC chip (MAX1168),
  - Magnetometer (MS2100),
  - Gyroscope (ADXRS610),
  - Accelerometer (ADXL320).
- On YZ board, the main components are:
  - SMT magnetometer sensor,
  - Gyroscope (ADXRS610),
  - Accelerometer (ADXL320).
- On XZ board, the main component is only gyroscope (ADXRS610).

(2) Aspirin IMU: Figure 2.18 [43] shows Aspirin IMU, which is a full 10-degree of measurement (DoM) could be mounted on Lia board. On Aspirin IMU, there are triaxial accelerometer and triaxial gyroscope InvenSense MPU-6000, triaxial magnetometer Honeywell HMC5883, and barometer MS5611-01BA03. Voltage regulators LP2992 and I^2C EEPROM are also included.

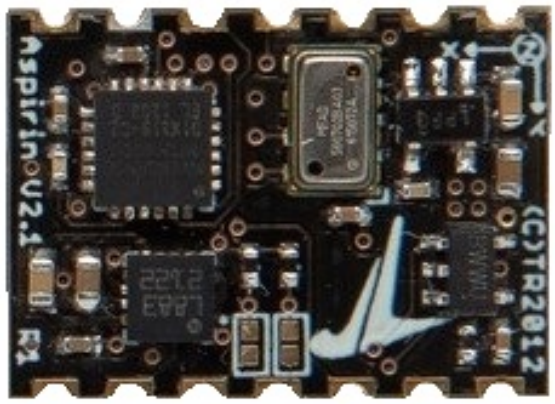

Fig. 2.18: Aspirin IMU.

(3) 3DM-GX3: Figure 2.19 [44] shows 3DM-GX3-25, which is a high-performance miniature AHRS, utilizing micro electro-mechanical systems (MEMS) sensor technology. It includes the fully calibrated triaxial magnetometer, triaxial accelerometer, triaxial gyro, temperature sensors, and an on-board processor. The processor is used to run the sophisticated sensor fusion algorithm to output the inertial measurements, static and dynamic orientation.

GPS Board

Figure 2.20 [45] demonstrates Ublox LEA-5H-0-007, which is chosen as the GPS board, a versatile product with high performance, small size, low cost, and multiple connectivity options. The LEA-5 module series are widely used in automotive, consumer, and industrial applications.

Fig. 2.19: 3DM GX3.

Fig. 2.20: LEA-5 GPS.

Modem

The Digi 9XTend Modems work on 900 MHz band (can also work on 2.4 GHz) under supply voltage from 2.8 V to 5.5 V, and provide data rate at 9.6 Kbps or 115.2 Kbps. Figure 2.21 [46] shows the modem installed on UAV, and Figure 2.22 [47] illustrates the modem connected with GCS.

Motor

Figure 2.23 [48] shows AXI 2217/20 gold line motor, which is powered from 2-4 cells li-poly batteries, has the maximum efficiency at 82%, maximum efficiency current at 8-14 A, and weight is around 70 g with cable.

Fig. 2.21: 9XTend modem on UAV.

Fig. 2.22: GCS 9XTend modem.

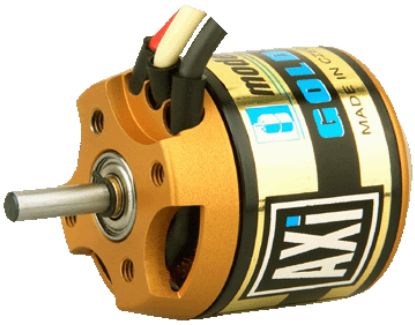

Fig. 2.23: AXI motor.

Transmitter and Receiver

Figure 2.24 [49] shows the Spektrum DX7 transmitter, which works on 2.4 GHz, and has 20-model memory, 5-point throttle curve, 3 flight modes plus hold. The receiver for DX7 is AR7000 (shown in Figure 2.25 [49]), which includes a main receiver and a smaller satellite receiver connected by a 6-inch lead.

Motor Controller

Figure 2.26 shows the motor controller for VTOL UAV, which is 20 mm * 43 mm, with six 60 A MosFets, and has three usable connectors:

Fig. 2.24: Transmitter: Spektrum DX7.

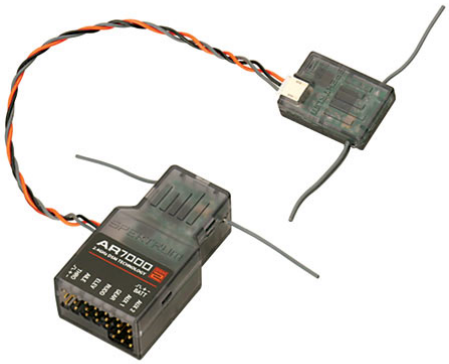

Fig. 2.25: Receiver: Spektrum AR7000.

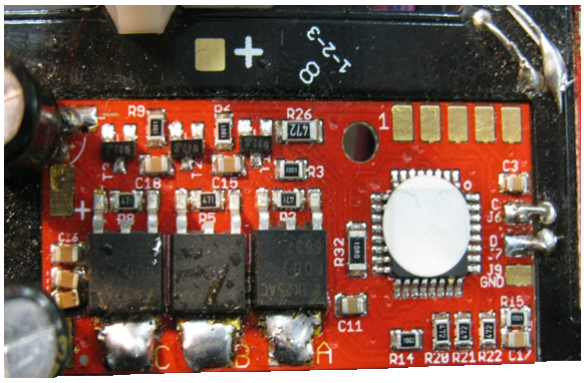

Fig. 2.26: Motor controller.

- I^2C (the way we used),
- PPM (standard input),
- Asynchron serial connector (for control or debugging).

This motor controller is previously used for Mikrokopter project.

BLDC Motor Introduction

Figure 2.27 [50] shows the section of a BLDC motor, and every component inside the motor.

Figure 2.28 [50] shows a 3-phase power stage, utilizing six power transistors with independent switching for the 3-phase BLDC motor. Two motor phases are supplied concurrently, when the third phase is not powered, which contributes to six possible combination applied to the BLDC motor.

The BLDC motor is driven by rectangular voltage strokes related with the rotor position. The rotor magnet generates the rotor flux, and together with the generated stator

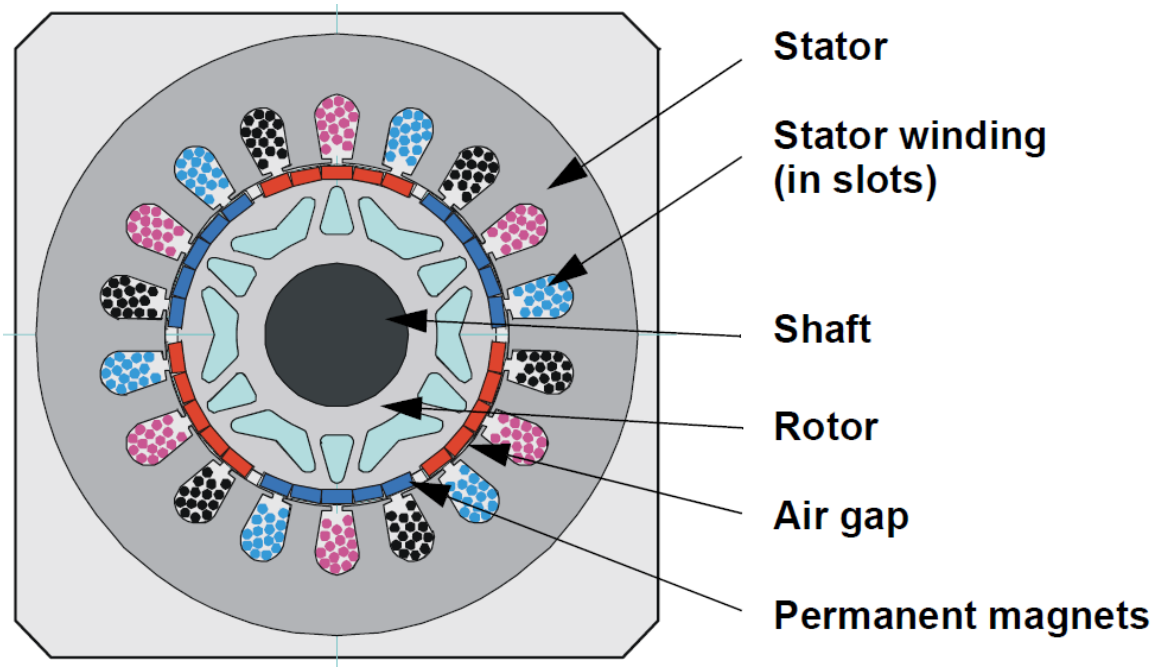

Fig. 2.27: Cross section of a BLDC motor.

flux to determine the torque, and thus the speed of the motor. Figure 2.29 [50] shows that the voltage strokes applied onto the 3-phase BLDC motor.

2.3.2 VTOL UAS Software

The software of the VTOL system is based on the Paparazzi UAV project. For the GCS software part, segment applications are provided, such as plotter, settings, and replay function.

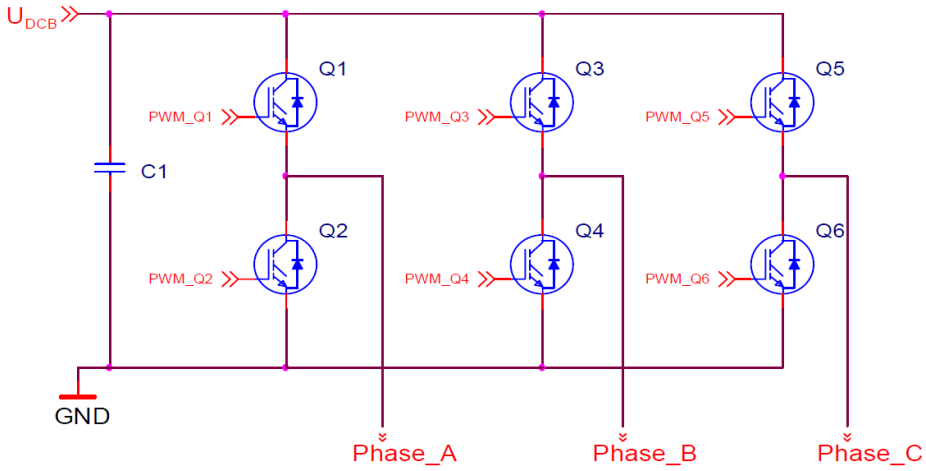

Fig. 2.28: 3-phase BLDC power stage.

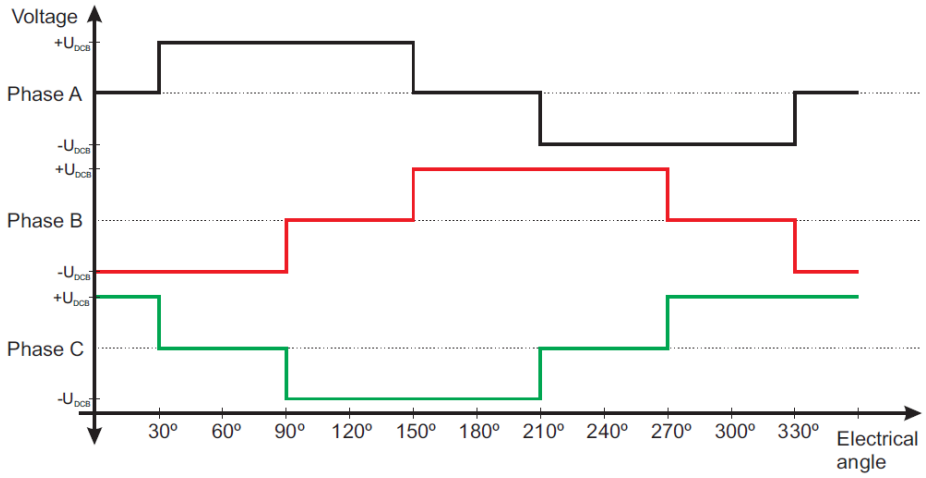

Fig. 2.29: Voltage onto 3-phase BLDC motor.

By the telemetry and datalink, the well developed code could realize the attitude stabilization, both vertical guidance and horizontal guidance, and make the VTOL UAVs to fly in automatic navigation according to the specified flight plans.

MotoCalc Software

Figure 2.30 [51] demonstrates MotoCalc, which is a software to predict the performance of an electric model aircraft power system by considering the characteristics of the battery, gearbox, motor, propeller, speed control, etc. Many options are provided, such as the number of cells, diameter of the propeller, and pitch angle of the propeller. MotoCalc can predict the current, voltage, power, lift, drag, thrust, RPM, throttle, run time, stall speed, rate of climb, motor temperature, motor and electrical efficiency, propeller overall efficiency, etc.

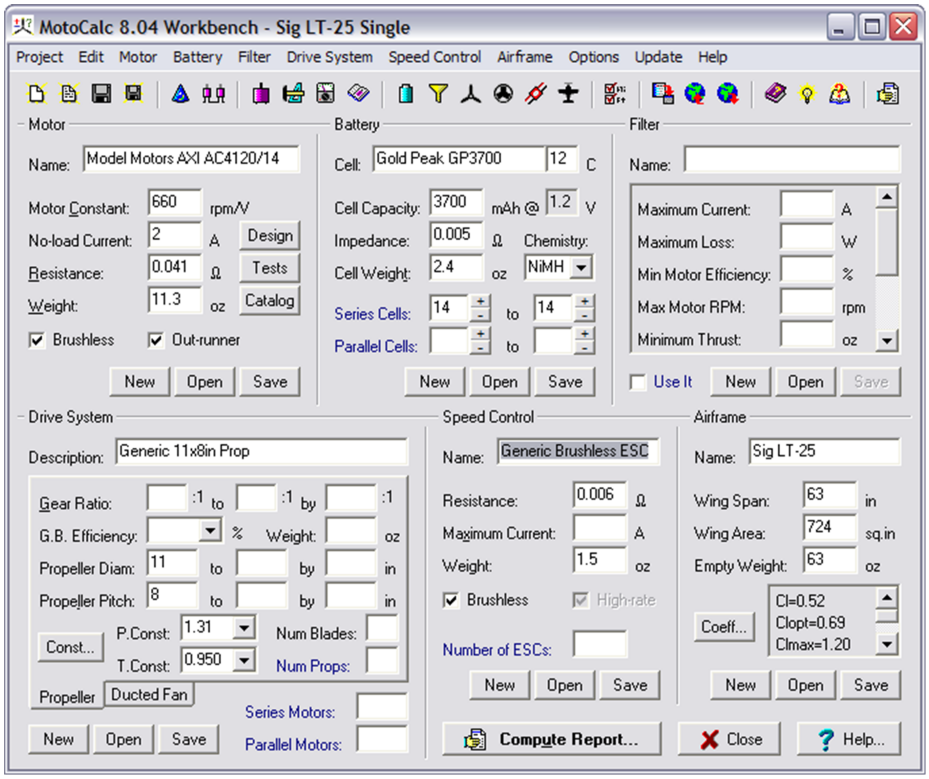

Fig. 2.30: MotoCalc.

2.4 Chapter Summary

This chapter introduces the design for both fixed-wing UAS and VTOL UAS. First, the big picture of fixed-wing UAS is demonstrated, then the detailed hardware and software are illustrated. Next, the famous VTOL UAV platforms worldwide are listed. In the end, the big picture of designed VTOL UAS, hardware, and software are also explained in details.

Chapter 3

Low-Cost Multi-UAV Formations for Contour Mapping of Nuclear Radiation Fields

3.1 Introduction

Low-cost UAVs [52] are becoming more and more popular in both research and practical applications leading to a new, potentially significant service product known as PRS [25]. On one hand, UAV research is becoming a notable area with the growing number of papers focused on system modeling, navigation, flight control, path planning, etc. On the other hand, with the rapid development of electronics and wireless communication technology, civilian remote sensing becomes a reality by installing inexpensive sensors on UAVs to measure and collect concerned real-time parameters, such as temperature, humidity, and image. Therefore, UAVs are being used as PRS for applications in many different areas, such as water management, forest fire detection, wetland monitoring, and crop identification. Compared with satellite remote sensing, UAVs can provide equivalent or higher resolution imagery, and relevant parameters in more affordable ways [19].

Compared with single UAV, the cooperative UAV system can perform with more safety and efficiency [53]. It could reduce the time for tasks, lower the demand of payload capacity for one UAV, and operate in a distributed manner which increases the redundancy and robustness of the entire system [54]. Moreover, multiple UAVs can share information with each other via wireless communication [55], so some advanced and optimal algorithms can be implemented for interesting applications, for example, gradient searching [56]. Therefore, multi-UAV system with advanced cooperative control algorithms can offer advantages over single UAV system, especially in time urgent tasks; for example, detecting nuclear radiation before deploying the salvage.

These advantages of UAVs are obvious especially in situations where the people's safety may be jeopardized, such as pollutant diffusion, gas leakage, and forest fire [57]. In March 2011, an earthquake happened in Japan and the subsequent tsunami caused serious crisis due to the nuclear radiation leakage. It is extremely dangerous to carry out the salvage, and difficult to detect the level of radiation around nuclear plant. However, if UAVs equipped with radiation detection instruments could be sent there, the radiation data with high precision can be collected nearby. Some corporations and institutes, such as Honeywell and Virginia Tech, have started the related research already [58, 59]. Furthermore, if multiple UAVs in specified formation can conduct the radiation contour mapping in 3D space, which is quite important for analyzing the safety factor around the damaged nuclear plant, it would be significantly helpful to take appropriate actions at the beginning to avoid going worse.

The main task of the chapter is to detect the level of nuclear radiation timely and efficiently using multiple low-cost UAVs. The contribution of this work is that two different scenarios of radiation detection tasks are explored. The scenario of contour mapping is demonstrated through simulation, and the other scenario of waypoint detecting is validated by the experimental flight test.

The main content of this chapter is organized as follows. The first section presents the scenarios for nuclear radiation detection with simulation results. The next section introduces our low-cost UAV platform. The following section explains the formation flight architecture and enumerates the standard flight test routine. Then, preliminary experimental flight results are demonstrated. The final section concludes this chapter and points out the future work.

3.2 Scenarios for Nuclear Radiation Detection

In order to cater for the increasing energy requirement while trying to reduce the level of the pollution, nuclear reactors are continuously constructed and put into use all over the world. The nuclear radiation level is always an important parameter which has to be measured. Figure 3.1 [60] shows the nuclear leakage in Japan.

Fig. 3.1: Nuclear leakage.

The nuclear leakage has posed a huge challenge to ensure the security of the nuclear power plant. Therefore, when an accident of nuclear radiation happens, the level of the nuclear radiation needs to be monitored continuously in order to deploy the salvage. Moreover, the radiation detection plays an important role in detecting and monitoring the transportation of radiological material in urban environments.

Based on such conditions, low-cost UAVs equipped with detecting sensors are suitable for those tasks. In this chapter, the following two scenarios for nuclear radiation detection are considered.

3.2.1 Level of Nuclear Radiation Detecting with Predefined Waypoints

In this scenario, the objective is to detect the radiation level of some important spots distributed around the power plant. Actually, this can be considered as the problem of trajectory planning and tracking. Assuming that the UAVs fly at a constant altitude, we can formulate this as follows. Suppose that $(x_i, y_i), i = 1, 2, \cdots, m$ are the required waypoints to be monitored. Devise the navigation controller as $u_i = u(t_i, x_i, y_i)$ that for the instants $t_i, i = 1, 2, \cdots, m, (x(t_i), y(t_i)) = (x_i, y_i)$. In order to make the trajectory of UAVs

more smooth and steady, extra points between predefined points could be interpolated, or the technique of trajectory planning can be utilized to generate the route which is able to achieve better performance. Experimental predefined waypoints formation flights have been implemented, both the process and results in details will be illustrated in the following section.

3.2.2 Contour Mapping of Nuclear Radiation

When the indication for the level of the nuclear radiation is available, it is necessary to draw the contour of the same level of radiation to master the trend of the radiation and make corresponding decisions. We can formulate this scenario as follows: $\rho(x, y) : R^2 \to R^+$ is defined as the level of nuclear radiation at position (x, y), and ρ_0 is the desired level of radiation to be detected. The navigation controller of UAVs is devised as $u = u(t, \rho, \rho_0)$ that there exists some $t_0, \rho(x(t), y(t)) = \rho_0$, for $t \geq t_0$. In this scenario, the objective is to detect and track the specified level of nuclear radiation, therefore, it is more difficult to develop the navigation controller. Only a few results have been published until now [61–63]. Figure 3.2 demonstrates the Matlab simulation platform, which has included the developed controller [64].

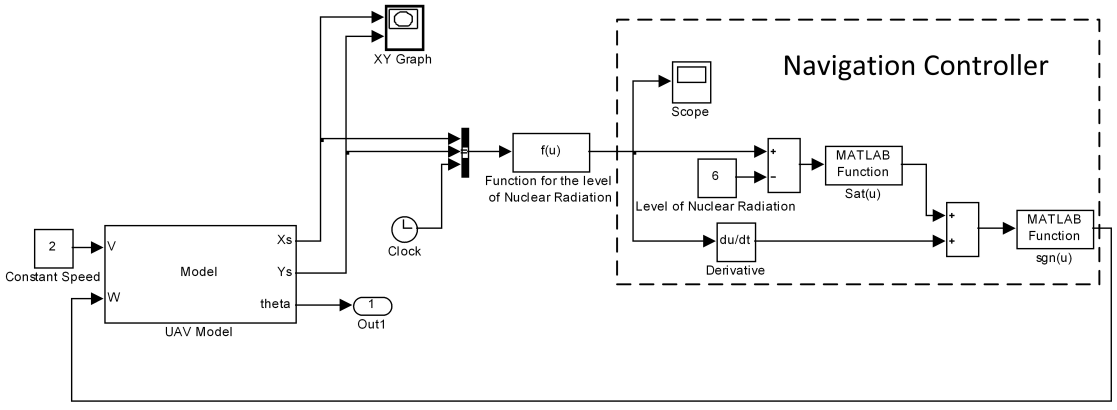

Fig. 3.2: Contour mapping simulation of the nuclear radiation.

The following simplified UAV model with nonholonomic constraints is chosen. For simplicity, we also consider the flight is at a constant altitude,

$$\begin{cases} \dot{x} = v\cos\theta, \\ \dot{y} = v\sin\theta, \\ \dot{z} = 0, \\ \dot{\theta} = \omega. \end{cases} \tag{3.1}$$

We apply the following controller:

$$\omega = \mathrm{sgn}(\dot{\rho} + \chi(\rho - \rho_0)), \tag{3.2}$$

where sgn is the sign function and χ is the saturation function defined as

$$\chi(x) = \begin{cases} kx & |x| \leq \delta, \\ \mathrm{sgn}(x) \cdot k\delta & |x| > \delta, \end{cases} \tag{3.3}$$

and the speed is set as a constant value. The block $f(u)$ is the function indicating the level of nuclear radiation set as

$$12 - 0.1X_s^2 - 0.2Y_s^2 = 6, \tag{3.4}$$

which is related with position in X-axis X_s, and position in Y-axis Y_s. Next, the desired level of nuclear radiation is compared, and then the sliding mode controller is used to make sure that the UAV always tracks the desired level of nuclear radiation. The altitude is constant in our simulation.

Figure 3.3 illustrates the simulation result, and Figure 3.4 shows the whole contouring process with given time.

It can be seen that, the desired level of nuclear radiation is tracked properly by using the sliding mode controller within a short time moving from the initial position to keep tracking the desired level of radiation. Since in the real world, the level of radiation is also

related with vertical distance, consequently, flying two or more UAVs at different altitude to trace different desired levels of radiation could save significant amount of time. Tracing with two UAVs at different altitudes is also simulated, and the results are demonstrated in Figure 3.5.

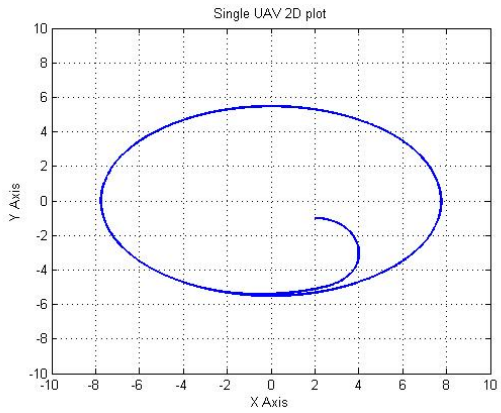

Fig. 3.3: Single UAV 2D contouring.

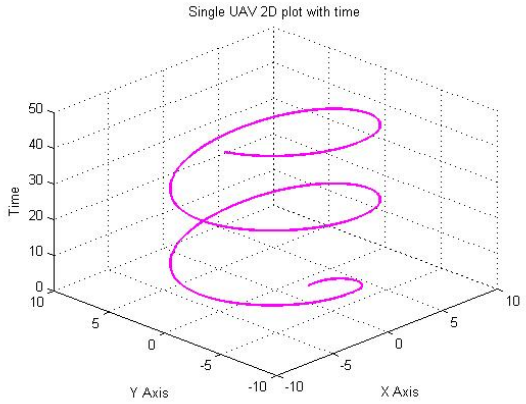

Fig. 3.4: Single UAV contouring with time.

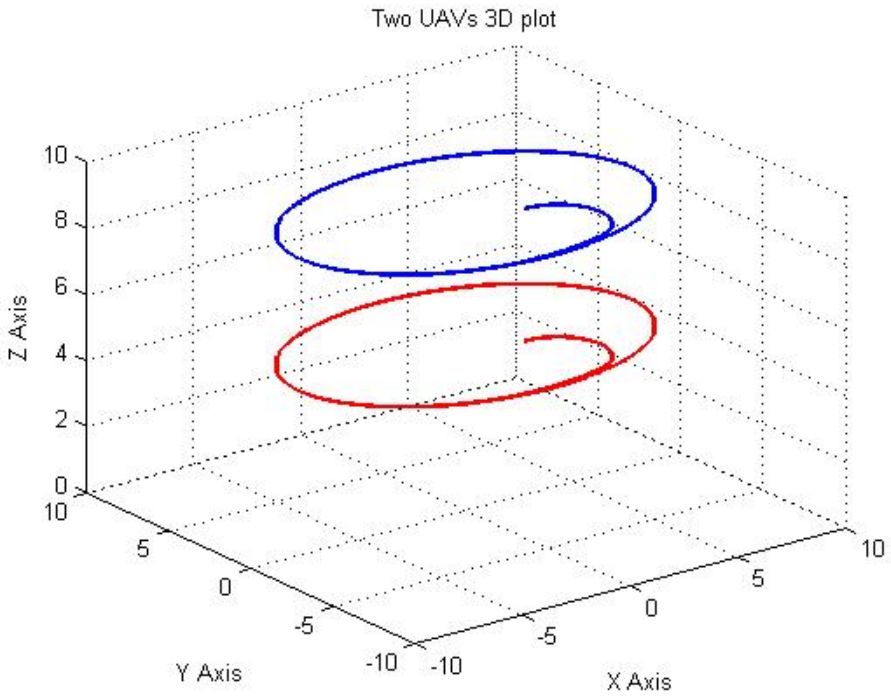

Fig. 3.5: Two UAVs 3D contouring.

In order to save time for the salvage, two or more UAVs could be sent for cooperative detecting and tracking the levels of nuclear radiation. The cooperative contour mapping simulation is shown using the developed controller [65]:

$$u = k \sum_{i=1}^{N} D_i(x, y)\, e(\theta_0 + \frac{2\pi}{N}(i-1)), \quad N \geq 3, \tag{3.5}$$

where k is the gain factor which could be time-varying, $D_i(x, y)$ is the measurement of radiation level from ith UAV, $e(\phi) = \begin{bmatrix} \cos\phi \\ \sin\phi \end{bmatrix}$, θ_0 is the initial deflection angle, and N is the number of UAVs.

The level of the nuclear radiation is assumed as

$$D(x, y) = 10e^{-\frac{(x-8)^2+(y-5)^2}{600}}. \tag{3.6}$$

Figure 3.6 gives the simulation result for 4-UAV cooperative contour mapping.

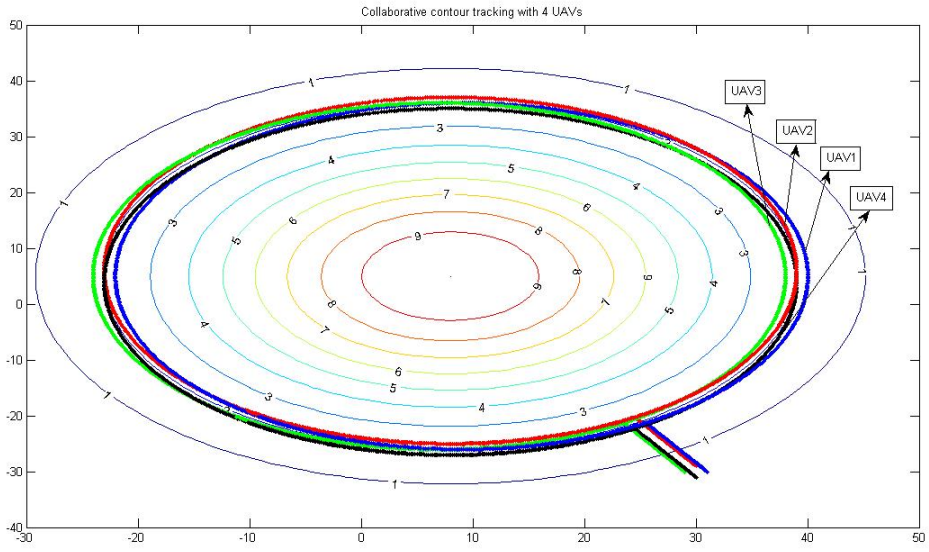

Fig. 3.6: Multi-UAV collaborative contour mapping.

3.3 Low-Cost UAV Platforms for Personal Remote Sensing

Multiple UAVs have great superiority in measuring the nuclear radiation, and the study of the PRS UAV platform is promisingly attractive. Many research projects related with UAV have been carried out in CSOIS, such as multi-spectral remote sensing by AggieAir [25], data fusion for attitude estimation [66], and fractional order controller design [67]. Numerous durable autonomous flight tests have been achieved based on the low-cost platform [52], which proved the dependability of our UAV platforms. A series of actual formation flight tests have already been achieved in CSOIS with many lessons and experience gained. Moreover, every low-cost UAV has the ability to carry payload around 1.6 lb. Therefore, a variety of potential sensors could be installed for different applications, including radiation detecting sensor [68].

There are many advantages of our low-cost UAV platform due to the features shown in the following.

- Safety: The expanded polypropylene (EPP) foam and electrical power make it more safe for the UAVs.

- Small size and light weight: The wingspans of the UAVs are about 48 inches (122 cm), and the total weight of the system is only 3.3 lb (1.5 kg).

- Flexibility: The foam frame makes the replacement of any electronics easy, and it is also convenient to install additional electronics.

- Open-source: Both Paparazzi hardware and software are open-source, so new functions are able to be implemented by modifying the existing code and equipping new sensors.

- Low cost with high endurance: The total cost of the upgrade from RC aircraft to low-cost autonomous fixed-wing UAV is around 500 dollars [52]. Powered by 3 Li-Polymer 2000 mAh/11.1 V batteries, our UAV has flied over 70 minutes with cruise speed at around 15 m/s.

3.4 Formation Flight Architecture and Standard Flight Routine

3.4.1 Formation Flight Architecture

Figure 3.7 describes the formation flight architecture. The formation controller receives the information from every UAV via the GCS, and compares the information with the set-point, then sends out the commands for each UAV to track the formation flight route [30].

3.4.2 Standard Flight Routine

Experimental formation flight test is achieved by cooperating each single UAV, so every single UAV needs to be tuned well for autonomous navigation before formation flight. Otherwise, it is difficult for the operator to adjust the formation control parameters with the existence of uncertainties from single UAV. At least one safety-pilot is needed to observe the status of each single UAV, and the safety-pilot needs to instantly take control if any unanticipated situation happens during the formation flight. More safety-pilots are needed during the three UAVs formation flight. Figure 3.8 demonstrates the UAV platform used in this chapter, and multi-UAV standard flight test routine is enumerated below.

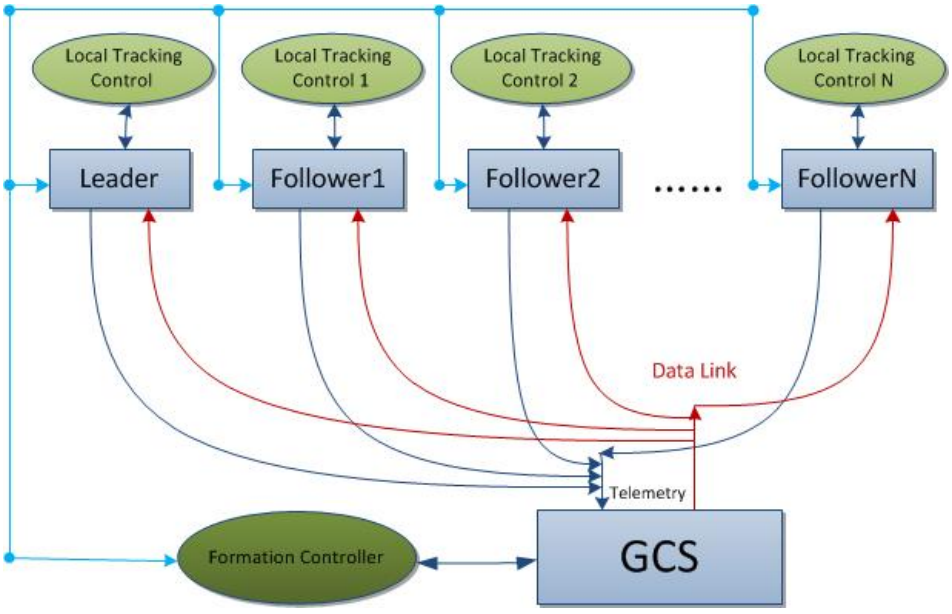

Fig. 3.7: Centralized control architecture.

Fig. 3.8: UAVs platforms.

(1) Launch the leader UAV and follower UAVs continuously using bungee. Keep all the UAVs participate in the formation flight standby by circling in their own fly zones and maintain different altitudes.

(2) The leader UAV needs to switch to formation mode first with manual switch by GCS operator and begins flying towards the designated routine, and usually it starts with a circling waypoint. When the leader reaches the updated altitude and performs steadily, the follower UAVs can switch to formation mode and adjust the original altitudes until they start tracking the leader's altitude and flight path.

(3) When the entire fleet is in the formation mode and the followers perform reasonable tracking performance, the leader can switch to the waypoint routine. The follower UAVs should be guided to follow the transition. When all the UAVs are flying straightly, the GCS operator can tune the position and speed proportional control gains designed in the formation controller, so that their latitudinal, longitudinal differences converge to be the desired ones specified in the flight plan. Besides, the GCS operator also needs to adjust the altitude proportional gain so their altitude differences stay close to the expected value.

(4) The waypoint routine is usually planned similar to the shape of an outdoor running track with flexible distance (usually 1600 m for 9 waypoints). When UAVs approach the turning waypoints, the leader UAV who usually flies higher than the followers might drop some altitude so their intervals could get really close. The safety pilot should always watch the UAV that is in charge and divert its flight path when necessary. The GCS operator should make sure the traffic collision avoidance (TCA) function is activated, spread the fleet horizontally when three or more are flying due to flight altitude limitations, and reserve sufficient spaces between each UAV.

(5) If entire UAV fleet maintains satisfactory formation shape and tracking performance in either straight line or turning, the tuning process can be stopped and other formation scenarios related to the practical applications can be carried out. Otherwise, any single UAV that behaves inefficiently or the data link between ground control station and UAVs needs to be inspected. Additionally, the wind condition also plays a critical role in the turning process, so the decision needs to be analyzed accordingly.

(6) For other formation scenarios, in order to avoid collision, the UAVs usually switch back to individual mode and fly back to their allocated flight zone. Then the leader first switches back to the new formation flight plans and the follower UAVs track the updates similar to what has been described. When the mission for formation flight is accomplished, the followers should first consecutively switch back to single mode and fly towards their fly zone, then prepare for landings. After all the followers have landed, the leader can follow the same procedure to land. In this way, collisions and crashes can be maximally prevented.

3.5 Experimental Flight Test Results for Proof-of-Concept

Good preparation is necessary for successful flight, which includes checking weather forecast, charging batteries, inspecting tools and devices according to checklist, etc. The flight test results shown in this chapter were taken in Cache Junction, UT. Figure 3.9 [69] shows the author and Long Di preparing leader UAV take-off [69].

Fig. 3.9: Leader UAV take-off.

Figure 3.10 shows the multi-UAV communication topology. The ground station communicates with multiple UAVs via modems. The topology has been changed from point to point (P2P) to point to multi-point (P2MP), and the transmission delay is reduced while the flight data is increased, which is extremely important for centralized control structure and helps improve the flight performance.

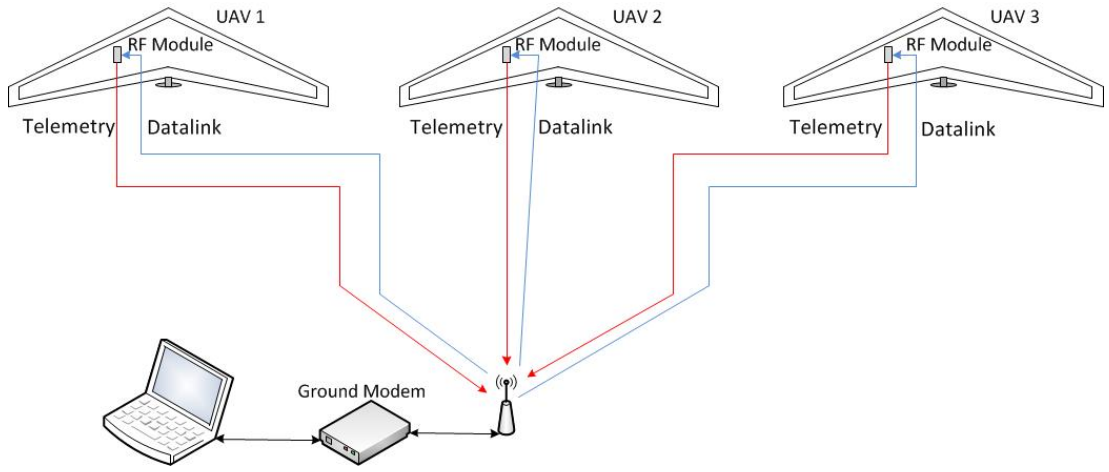

Fig. 3.10: Multi-UAV communication topology.

Because of the complexity of the formation flight, flight plan needs to be simulated before every real flight in order to get the GCS operator familiar with the cooperation among the GCS operator and the satety autopilots, as well as decrease the unnecessary incorrect operation. The GCS operator could monitor the entire formation flight status in GCS. Furthermore, because of the "replay" function in Paparazzi, the whole multi-UAV flight test can be replayed. Figure 3.11 shows the replay for the executed leader-follower formation flight.

It can be seen that 2-UAV waypoint formation flight is achieved successfully by Dimon (leader, in yellow color), and Phoenix (follower, in red color). Figure 3.12, Figure 3.13, and Figure 3.14 show the results of the three types of real waypoint formation flights, respectively.

Circling formation shown in Figure 3.12 is a general action during flight test, and it is usually carried out while tuning parameters, turning directions, beginning or ending of formation flights, etc.

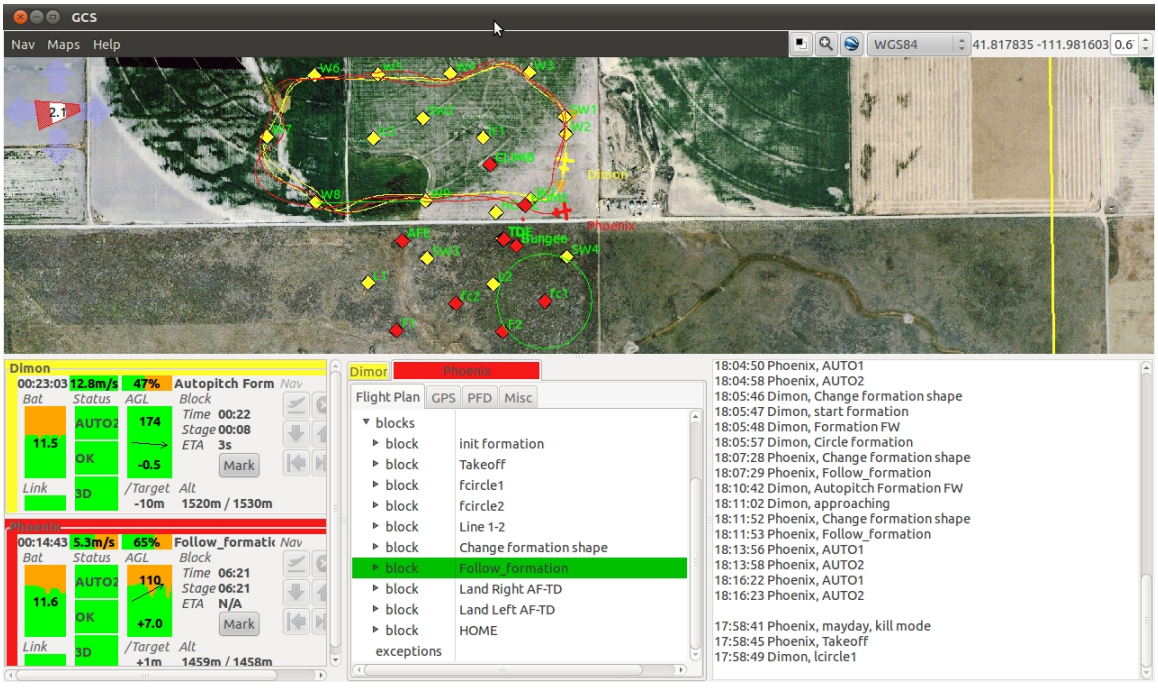

Fig. 3.11: Formation flight overview in GCS.

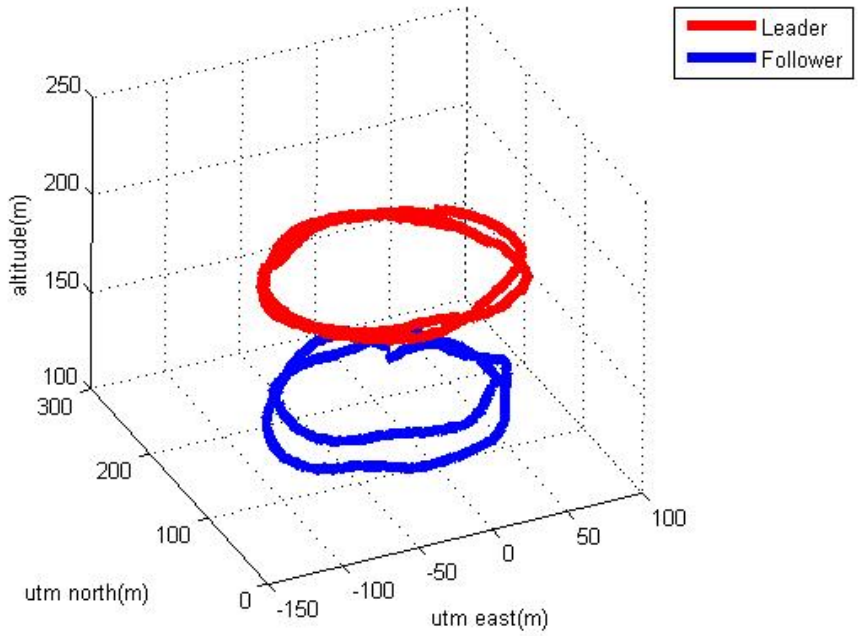

Fig. 3.12: Circle formation flight.

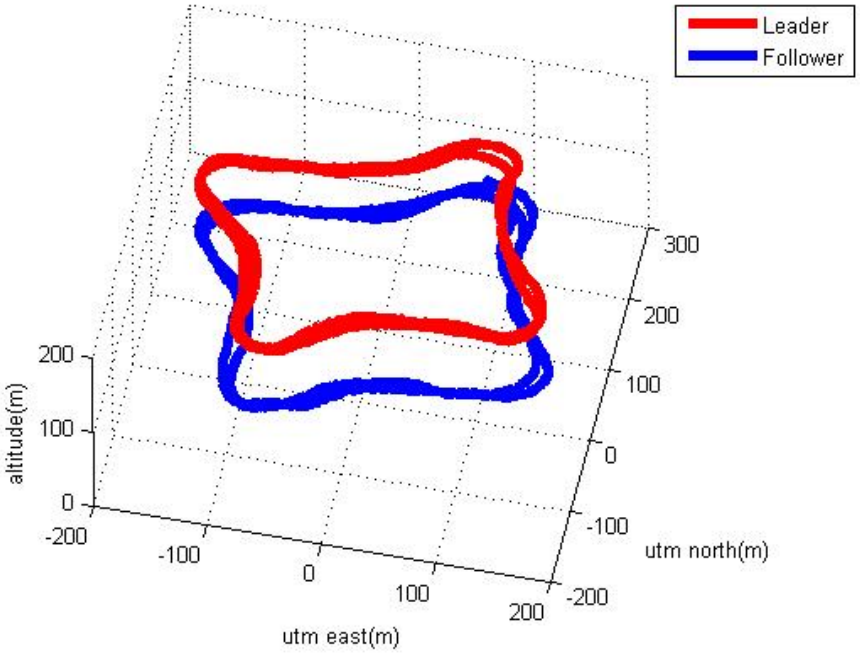

Fig. 3.13: Square formation flight.

During the square formation flight shown in Figure 3.13, the follower closely tracks the leader's trajectory and maintains the desired altitude within the 350 m (east)× 350 m (north)× 200 m (altitude) zone.

Figure 3.14 demonstrates a stable multi-point formation tracking within a bigger space which is approaching the practical.

D-tect systems [68] makes the famous D-tect products for radiation detection. Among all the D-tect products, MiniRad-V is suitable to be installed on the UAVs. The MiniRad-V could do self-calibration to natural background radiation, has the ability to be used in high-RF environments, and can keep high sensitivity while implementing mobile radiation detection.

Figure 3.15 [68] shows the MiniRad-V radiation detector.

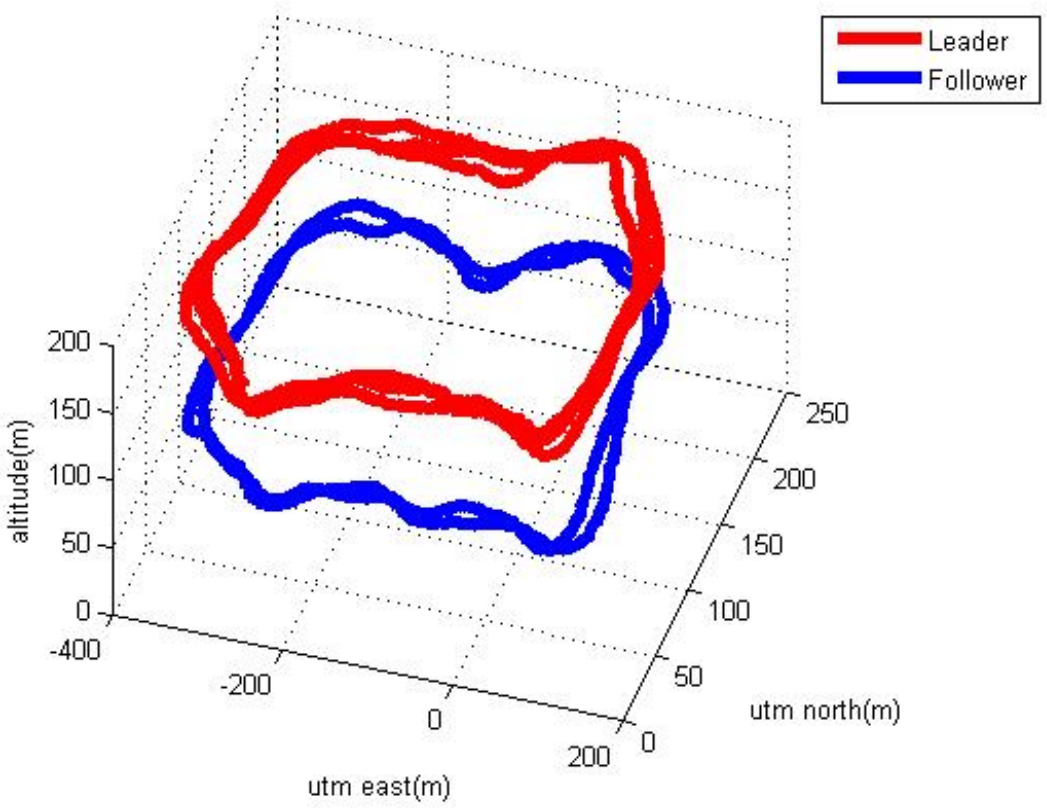

Fig. 3.14: Multi-point formation flight.

Table 3.1 [68] illustrates the specifications for MiniRad-V.

Waypoint formation flight is very important for real application, especially for detecting the level of nuclear radiation and other dangerous scenarios. During these tasks, first of all, the targets are selected and set in the GCS, then a flight plan containing all the required waypoints is designed by adding other necessary points to confine the route of the UAVs. Then the UAVs with the specified sensors, or cameras are sent out to collect the data, transmit the information back and display the data on the GCS. The high-resolution images can be stored in onboard memory card or transmitted back by wireless devices in real-time communication [25]. Based on the acquired accurate data, salvage can be carried out at earliest convenience and maximally save people's life and property.

Table 3.1: MiniRad-V specification.

Detector	0.5" d x 1.5 CsI(Na) with PMT
Energy Range	30 keV - 3 MeV
Power	12V DC
Response Time	<1 Second
Dimensions	4.7" x 3.1" x 1.7"
Weight	1.2 lbs
Environment	Driving rain, -10°F - 122°F

Fig. 3.15: MiniRad-V radiation detector.

3.6 Chapter Summary

In this chapter, using multi-UAV formation flight to detect the nuclear radiation has been discussed in both the cases of nuclear reactor normal running and radiation leakage. This approach is particularly suitable for the time urgent detection task when the radiation leakage is found. First of all, two scenarios are designed for nuclear radiation detection using multiple low-cost UAVs, then contour mapping of the nuclear radiation is simulated. Afterwards, developed UAV system and experimental formation flight are introduced. Finally, the result of the practical formation flight tests that imitate the nuclear detection mission is shown.

Chapter 4

Multi-UAV Formations for Cooperative Source Seeking and Contour Mapping of Radiative Signal Fields

4.1 Introduction

The radiative signal can be a spatially distributed source; for example, thermal energy spread, acoustic signal transmissions, light propagation, chemicals dissemination, electromagnetic radiation, and even radiation leakage. As an interesting research topic, source seeking has attracted increasing attentions. Extremum seeking method is used to tune the forward velocity for source seeking without position measurements [70]. The stability of source seeking scheme is analyzed by tuning only the angular velocity while keeping the forward velocity constant [71], and the continuing paper [72] talks about the application of this source seeking method. A sliding mode controller is designed for gradient climbing and source seeking [73]. Groups of vehicles are considered as a sensor network, and a control strategy is presented to guarantee the mobile sensor network to achieve gradient climbing in an unknown environment [74]. In practical situations, the radiative sources may be moving instead of being stationary, and the moving source cases are also studied in some publications. The costs and benefits are analyzed and evaluated to detect a moving radioactive source by using a network, and the source is constricted to move along a single path [75]. A control scheme is proposed to combine with state estimation and a moving source detection method by utilizing a sensor network [76]. The Bayesian methods are implemented for sensor networks by detecting the moving point source with constant speed, and compares the consequences with different radiation levels [77]. The model for biochemical dispersion from a moving source is derived with two possible situations considered, and then a statistical signal processing algorithm is developed to detect the moving source, and estimate the

diffusion parameters [78]. A control strategy is introduced to tune the angular velocities of a nonholonomic vehicle for the moving scalar signal source, and it proves the local exponential convergence of the scheme [79]. The extremum seeking method is used to navigate a modeled underwater vehicle for moving source seeking [80]. Controllers are designed to drive the mobile robots for randomly switching source seeking by extending the simultaneous perturbation stochastic approximation (SPSA) algorithm [81]. The convergence of the controllers is guaranteed for the stochastic source field.

Because of the rapid development of UAV technologies, stable flight control for a single UAV has been strengthened [67, 82]. Based on single UAV stable flights, experimental multi-UAV formation flights are also achieved [30]. Cooperative multi-UAV formations could extend the capabilities of a single UAV, and accomplish the task in less time with higher efficiency and more robustness. Using multi-UAV formations for source seeking has been investigated in many papers. Cooperative UAV formation is demonstrated to track the moving targets by using the developed guidance algorithms with both software simulation and hardware for application provided [83]. Two scenarios are presented for nuclear radiation detection by multi-UAV formation flights: one simulated contour mapping of the radiation field, and the other one studied nuclear radiation level detection on predefined waypoints [31]. A method is introduced to estimate the gradient by a leader UAV based on the detected data from all the UAVs in formation, and then both the guidance law and the heading rate controller are designed for the leader UAV. Afterwards heading rate controllers are applied to each follower UAV to circle around the leader UAV for the cooperative source seeking [84]. A cooperative Kalman Filter is introduced to combine measurements from mobile sensor platforms for the unknown gradient estimation. The UAV formation is driven by a steering control algorithm to track the level curves of the scalar area [85]. Under the fractional order potential fields, the UAV formations are used to track the radio transmitters which are implanted to the fish, and the Kalman Filter is utilized to estimate the location of the transmitters [86]. A leader-followers formation is presented to seek a moving source with a least-squares scheme, and it generates the guidance

law for the leader UAV based on the estimations of both the source gradient and source moving velocity [87]. The preliminary work of this chapter is presented [88], in which we show the control strategies for source seeking and contour mapping of a stationary diffusive signal field and provide the simulation results for validation.

In this chapter, multi-UAV formations are used to achieve cooperative source seeking and contour mapping of radiative signal fields [89]. Source seeking and contour mapping can help people to recognize the radiative signal fields. The decision-makers could evaluate the situation based on the acquired contour mapping, and then deploy the appropriate salvage or corresponding actions within least amount of time. The four scenarios which are the main contributions of this chapter are illustrated step by step to detect, locate the radiative signal fields and perform contour mapping. First, an existing controller is adopted with saturation considering the practical flight speed limit, and it is applied to a linear UAV model simplified from the nonholonomic model for source seeking and locating. Then the controller is modified to steer the specified signal level contour mapping with the moving source situation covered. Next, a method used for multi-vehicle consensus is simplified and utilized to stabilize the formation flights for detecting the radiative field. At last, these two methods in above two steps are combined to realize the cooperative contour mapping of the radiative signal fields by multi-UAV formations.

This chapter first presents the radiative source seeking and locating driven by the improved controller. Next section illustrates the signal level contour mapping for both stationary and moving source using the modified controller. Then this chapter applies a control strategy once used in multi-agent consensus problem to stabilize the multi-UAV formations for detecting the radiative signal fields. In the following, the contour mapping controller and formation controller cooperatively control the multi-UAV formation to achieve the contour mapping. The section in the end concludes this chapter.

4.2 Source Seeking and Locating of Radiative Signal Fields

The source seeking problem usually considers the nonholonomic model [65], which is shown as

$$\begin{cases} \dot{x} = v\cos\theta, \\ \dot{y} = v\sin\theta, \\ \dot{\theta} = \omega, \end{cases} \tag{4.1}$$

where (x, y) denotes the position, v represents the linear velocity, θ means the orientation, and ω is the angular velocity. In order to get rid of the nonholonomic constraint, feedback linearization could be used to simplify the model,

$$\begin{cases} x_i = x + L\cos\theta, \\ y_i = y + L\sin\theta. \end{cases} \tag{4.2}$$

Suppose that there is a point at position (x_i, y_i) which is off the center of the vehicle (x, y) with distance L and orientation θ. If v and ω in Equation (4.1) are defined as functions of v_{ix}, v_{iy}, L, and θ properly, the kinematic model for (x_i, y_i) in Equation (4.2) could be linearized as

$$\begin{cases} \dot{x}_i = v_{ix}, \\ \dot{y}_i = v_{iy}, \end{cases} \tag{4.3}$$

where (x_i, y_i) is the position of the ith UAV, and (v_{ix}, v_{iy}) is the velocity of the ith UAV which is considered as control input in this chapter with restriction within (-20m/s, +20m/s).

All the UAVs are assumed to fly at constant altitudes denoted as $\dot{z}_i = 0$, where z_i is the altitude of the ith UAV, and in order to avoid the collision, each UAV should stay at different altitude.

In this chapter, the radiative signal model is defined as

$$D(x, y) = 10e^{-\frac{(x-100)^2+(y-90)^2}{80000}}, \tag{4.4}$$

which is a Gaussian signal. The range of the field is restricted within a square from $-400m$ to $600m$ in X axis and from $-400m$ to $600m$ in Y axis in simulation.

Figure 4.1 gives the simulation model, which could be used for all of the four scenarios in this chapter by only adjusting some parameters.

The developed controller [65] is adopted to the linearized model in Equation (4.3) with saturation, and defined as

$$u = Sat[k \sum_{i=1}^{N} D_i(x,y)\, e(\theta_0 + \frac{2\pi}{N}(i-1))], \quad N \geq 3, \tag{4.5}$$

where $\begin{bmatrix} v_{ix} \\ v_{iy} \end{bmatrix} = u$, $Sat[]$ is the saturation to restrict the velocity considering the practical situation, k is the gain which is set to 30 in this scenario, $D_i(x,y)$ is the detected radiative

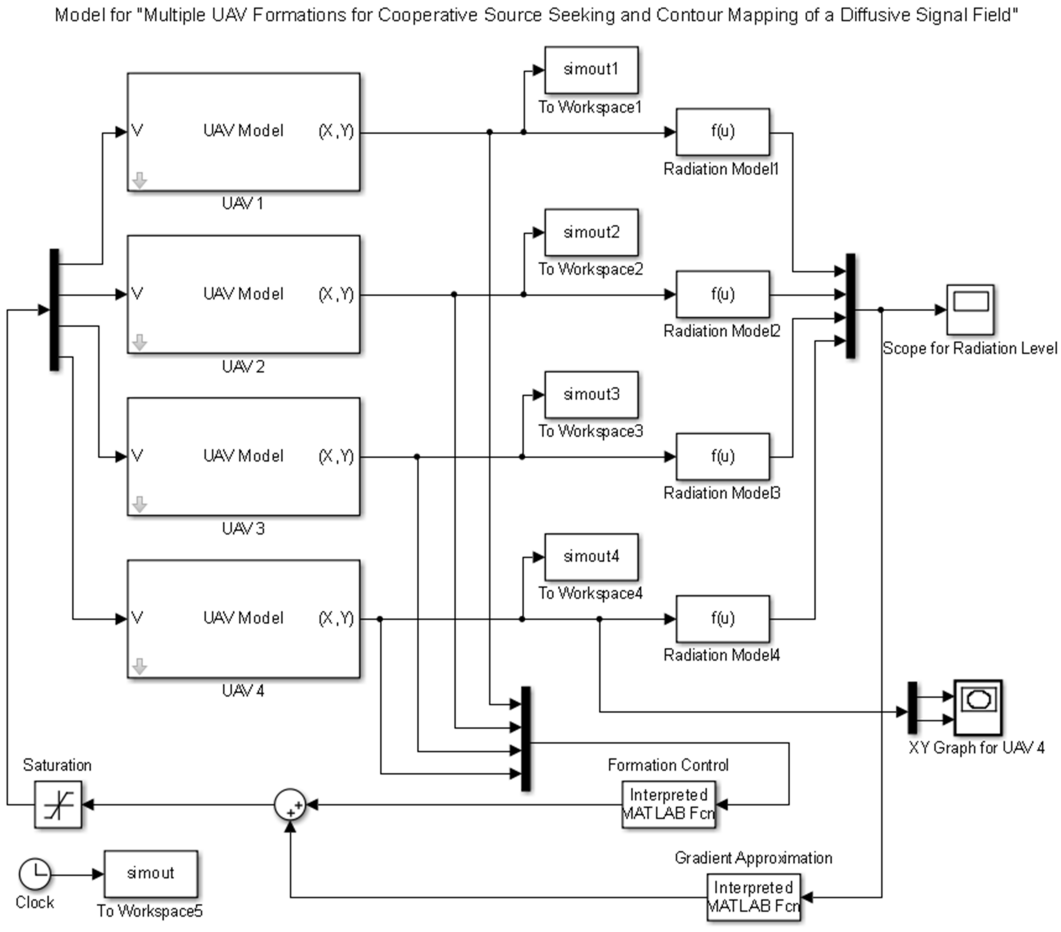

Fig. 4.1: Multi-UAV formation for cooperative source seeking and contour mapping.

signal level from the sensor installed on the ith UAV, $e(\phi) = \begin{bmatrix} \cos\phi \\ \sin\phi \end{bmatrix}$, θ_0 is the initial deflection angle which is set to 0 degrees, and N is the number of multiple UAVs in formation, which is set to 4 in this chapter.

This controller guarantees the 4-UAV formation to detect the gradient of the radiative signal, and achieve source seeking and locating. Figure 4.2 demonstrates the process beginning from the initial positions.

The actions of each UAV during source seeking are plotted in X axis and Y axis. Figure 4.3 and Figure 4.4 demonstrate the actions separately.

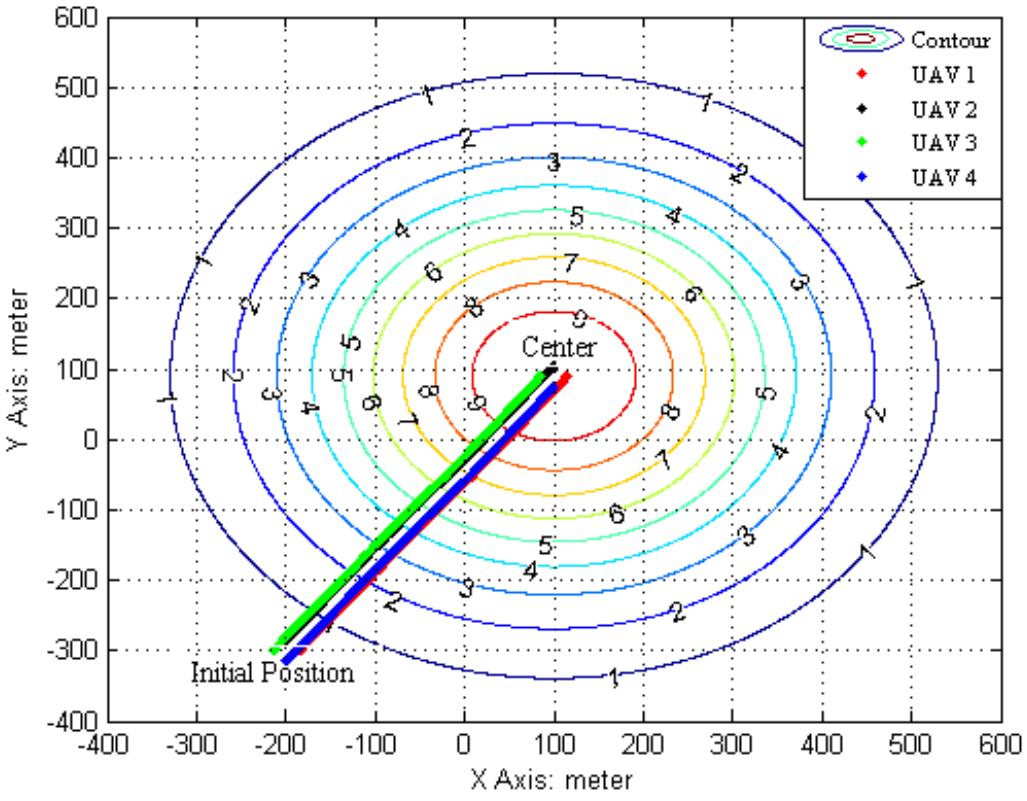

Fig. 4.2: UAV formation for radiative source seeking and locating.

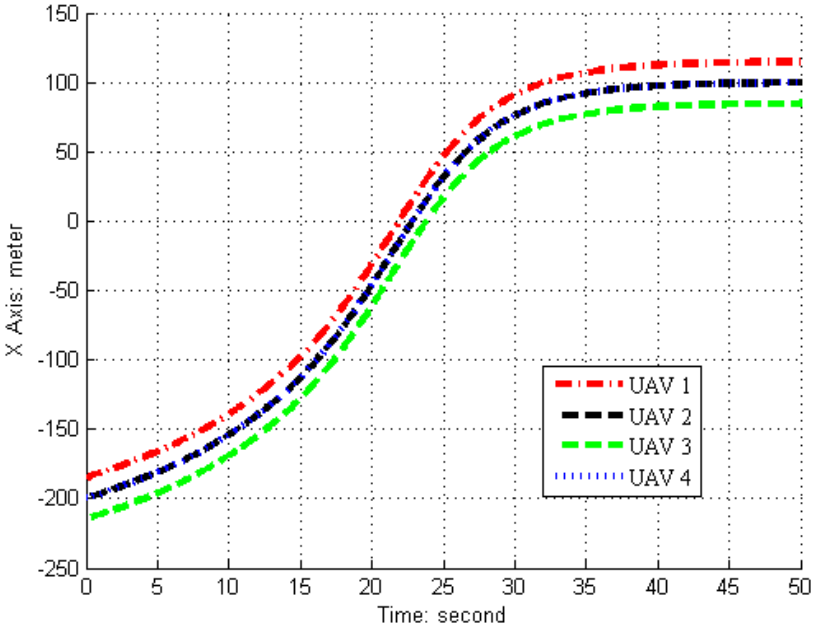

Fig. 4.3: X axis plot for each UAV action in source seeking.

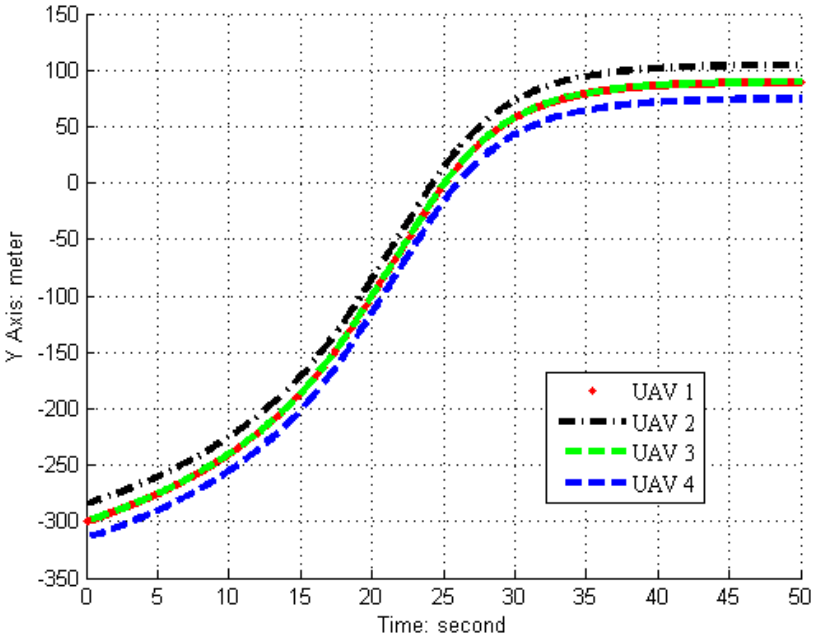

Fig. 4.4: Y axis plot for each UAV action in source seeking.

According to the X-axis plot and Y-axis plot, it can be seen that the four UAVs fly towards the gradient direction of the source signal in a circular formation. The center of the 4-UAV formation is set at (-200m, -300m) originally. After 50s, the 4-UAV formation achieves the source seeking, and successfully locates the radiative source at position (100m, 90m).

k is an important factor for the controller, which should be properly adjusted. Because when k is set to a bigger value, the output of u will reach the saturation limit at 20m/s, and affect the path of the formation while shortening the time to locate the source. Figure 4.5 demonstrates the UAVs reach the saturation limit during source seeking and locating process with $k = 80$.

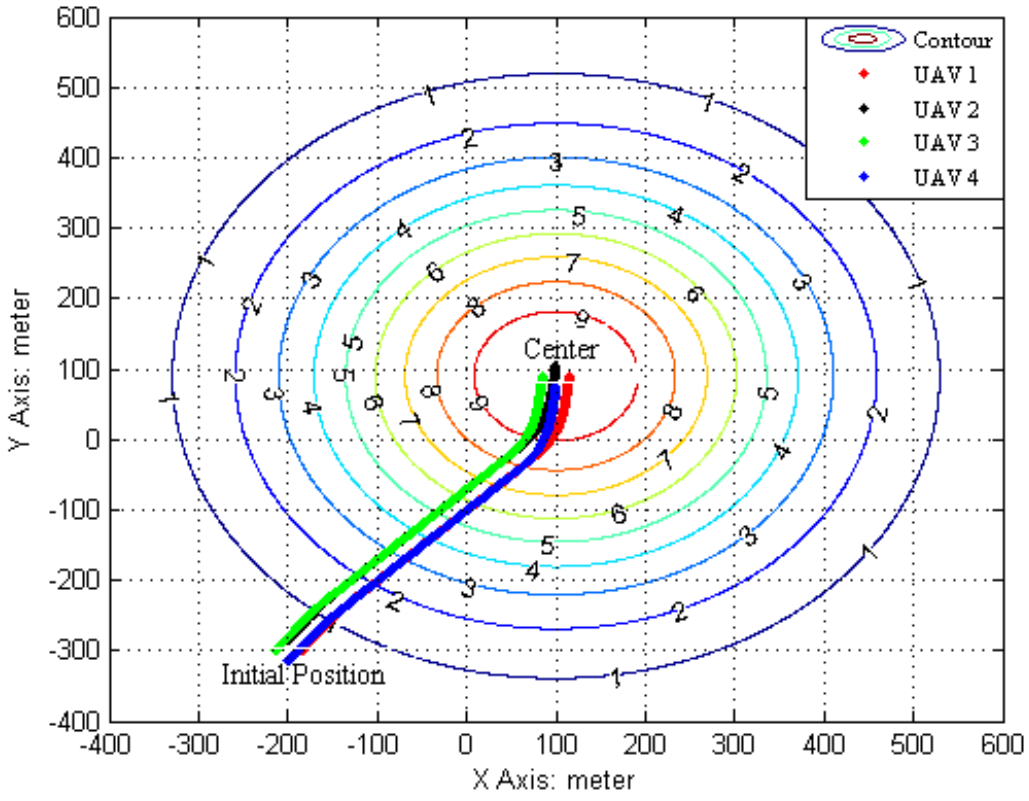

Fig. 4.5: UAV formation for source seeking when k=80.

From Figure 4.6, it can be seen that the 4-UAV formation locates the radiative source after $20s$.

4.3 Contour Mapping of Radiative Signal Fields

4.3.1 Stationary Source Contour Mapping

In this scenario, the introduced controller [65] is modified for contour mapping of specified radiative signal fields. The modified controller could detect the gradient level of the radiative source, and when the 4-UAV formation reaches the desired radiative level, the direction of the formation will be rotated to the orthogonal direction. Consequently, the 4-UAV formation is able to track the specified radiative signal level, and achieves the contour mapping. The radiation level at the center of the N UAV formation is denoted as $D_{mean}(x, y)$, which is calculated by Equation (4.6),

$$D_{mean}(x, y) = \frac{\sum_{i=1}^{N} D_i(x, y)}{N}, \quad N \geq 3. \tag{4.6}$$

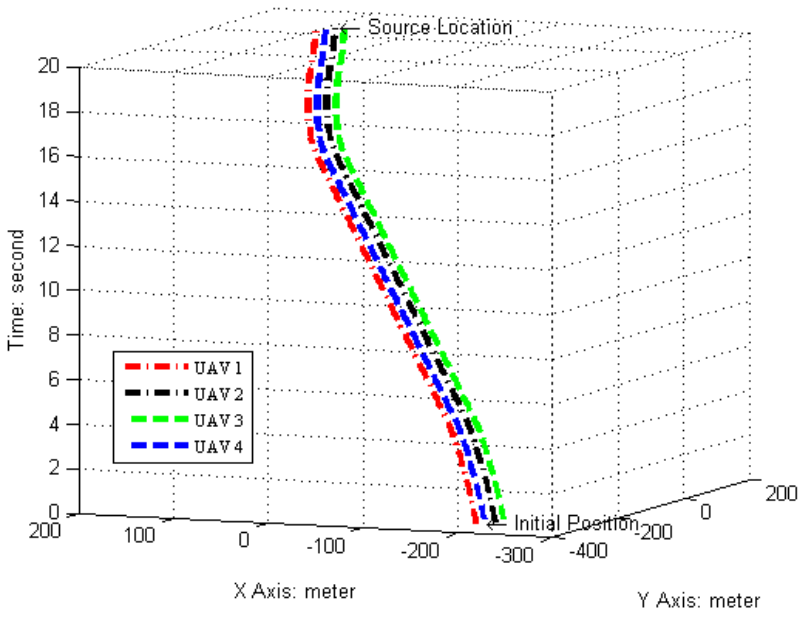

Fig. 4.6: 3D plot of UAV formation for source seeking when k=80.

The radiative signal level $D_s(x, y)$ could be pre-specified in the modified controller before executing the contour mapping, and when $D_s(x, y) \geq D_{mean}(x, y)$, the formation will rotate the flight heading to the orthogonal direction with process shown in Equation (4.7),

$$u = (\begin{bmatrix} 0 & -1 \\ 1 & 0 \end{bmatrix} u^{\mathrm{T}})^{\mathrm{T}}. \tag{4.7}$$

u is already defined in Equation (4.5), and u^{T} is the transpose of u. In the simulation for this scenario, the center of the 4-UAV formation is also set at (-200m, -300m) initially, the $D_s(x, y)$ is pre-specified to level 2, and $k = 30$. Figure 4.7 demonstrates the contour mapping progress.

The result shows that, the radiative signal with pre-specified level 2 is tracked properly by the stabilized 4-UAV formation, and the contour mapping is realized successfully.

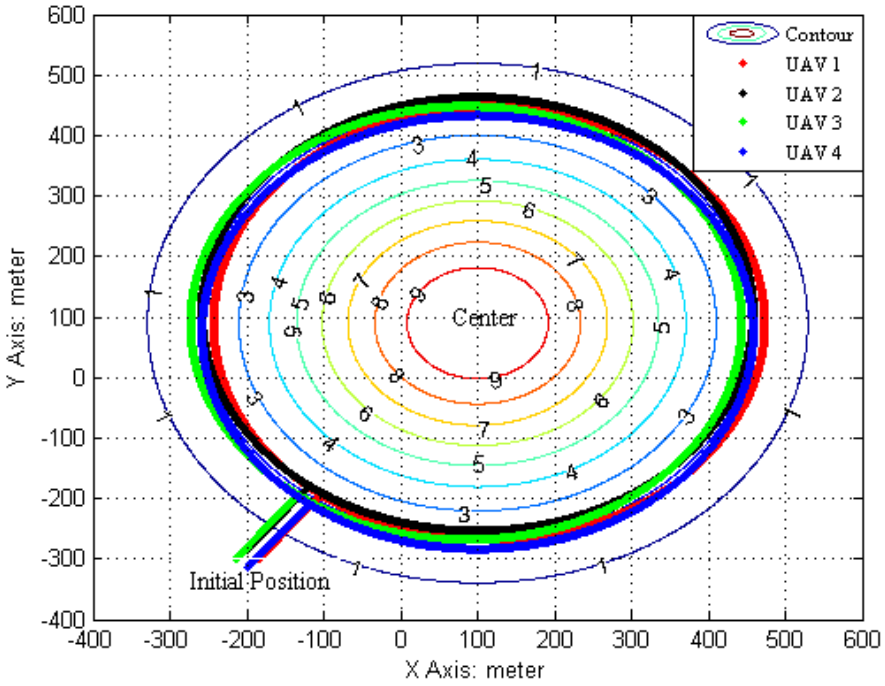

Fig. 4.7: UAV formation for contour mapping of specified radiative level.

In more realistic situation, there is some noise for the sensors installed on every UAV which are used to detect the radiation level. Therefore, a Gaussian noise is added for each sensor which is set as $\frac{1dBW}{9}$ in the simulation. Figure 4.8 describes the process with sensor noise.

4.3.2 Moving Source Contour Mapping

The model for the moving source is assumed as

$$\begin{cases} x_s = 100 - 0.8t, \\ y_s = 90 - 0.6t, \end{cases} \tag{4.8}$$

where (x_s, y_s) is the position of the source related with initial position $(100m, 90m)$ and t, t is the simulation time which is set to $980s$ in this simulation, and all the other parameters are set the same as stationary source situation. Figure 4.9 demonstrates the process of the moving source contour mapping by UAV formation.

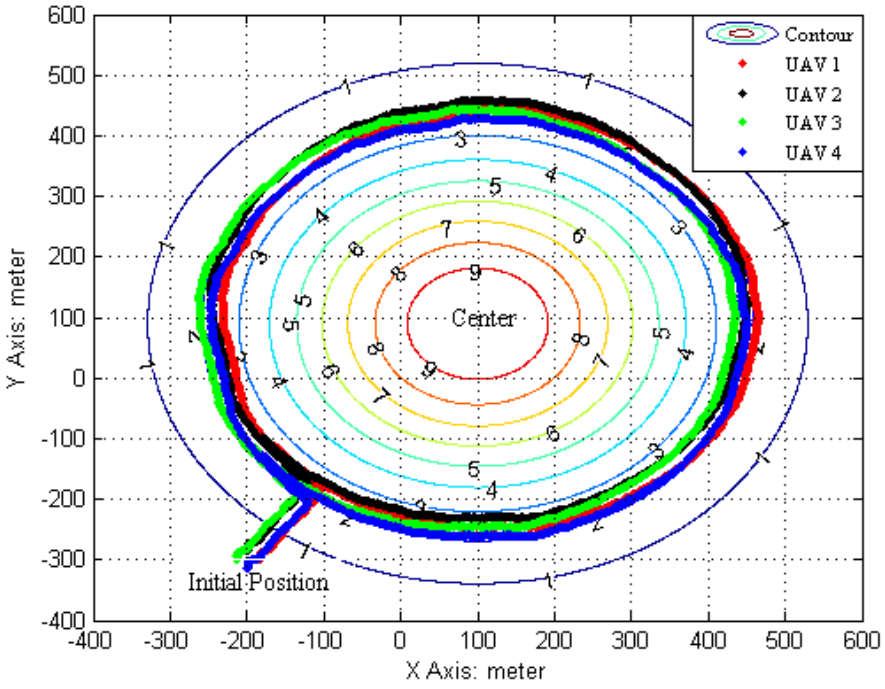

Fig. 4.8: Contour mapping of specified level with sensor noise.

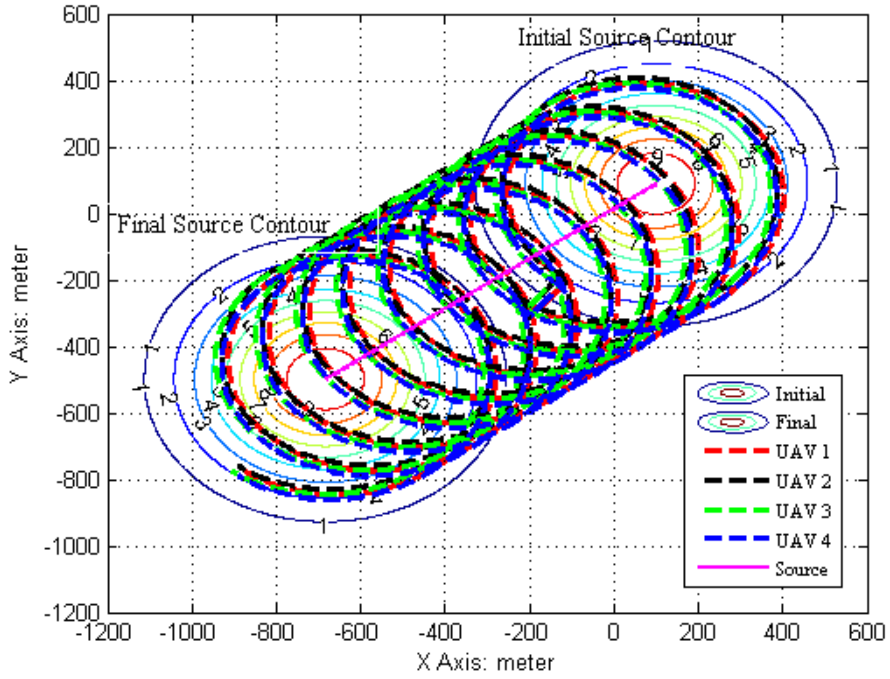

Fig. 4.9: UAV formation for contour mapping of moving radiative signal fields.

The plotted result shows that the radiative source moves from (100m, 90m) to (-684m, -498m) after 980s, and the 4-UAV formation properly achieves level 2 contour mapping of the moving radiative source during the process.

4.4 Decentralized Multi-UAV Formation for Radiative Signal Detection

In this scenario, the multiple UAVs (also use 4 UAVs as an example) are steered in decentralized formation to detect the radiative signal fields. Each UAV in decentralized formation could share information with other UAVs during flight. Consequently, this greatly enhances the robustness of the formation flight. In case the communication between the GCS and one of the UAVs is in bad status or even totally lost, the 4 UAVs could still stabilize the formation to detect the radiative level along the desired path.

Figure 4.10 illustrates the topology for the decentralized 4-UAV formation.

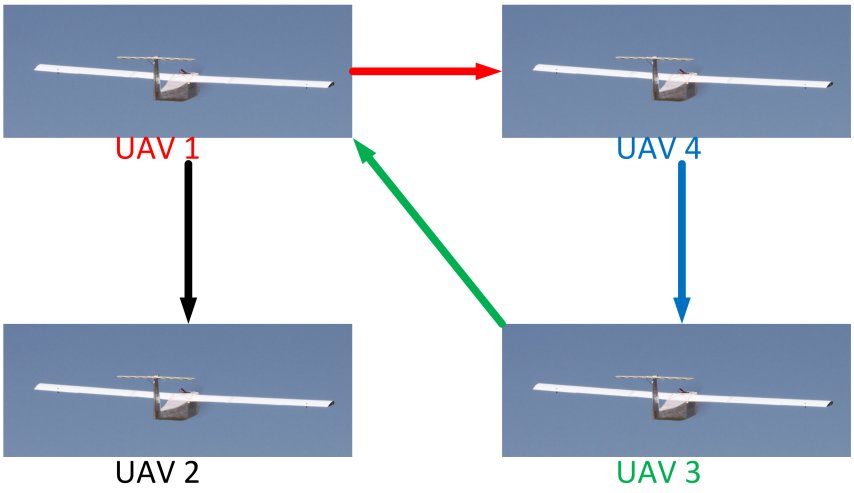

Fig. 4.10: Topology for four UAV decentralized formation.

A controller used for multi-UAV consensus problem [90] is simplified and then implemented to the model given in Equation (4.3) for stabilizing the decentralized formations during the detection. The simplified controller is defined as

$$\begin{cases} v_{xi} = Sat[-l(x_i - x_i^d) - \sum_{j=1}^{N} k_{ij}[(x_i - x_i^d) - (x_j - x_j^d)]], \\ v_{yi} = Sat[-l(y_i - y_i^d) - \sum_{j=1}^{N} k_{ij}[(y_i - y_i^d) - (y_j - y_j^d)]], \end{cases} \tag{4.9}$$

where Sat[] is the saturation, $l > 0$, (x_i, y_i) is the position of the ith UAV, (x_i^d, y_i^d) is the desired destination of the ith UAV, (x_j, y_j) and (x_j^d, y_j^d) follow the same definitions, and N is the number of UAVs set to 4. $k_{ij} > 0$ if the ith UAV can receive information from the jth UAV, otherwise $k_{ij} = 0$. According to the communication topology demonstrated in Figure 4.10, it can be found that only $k_{13} > 0$, $k_{21} > 0$, $k_{34} > 0$, $k_{41} > 0$, all the other k_{ij} are all equal to 0.

This scenario is designed to detect the radiative source level along certain path, for example, between a certain specified position and the source position. In this scenario, $l = 0.05$, $k_{ij} = 1$ for the k_{ij} which are not 0, the initial position for the center of 4-UAV formation is also set at (-200m, -300m), and the source position is still at (100m, 90m). In the simulation, the initial positions for UAV 1–UAV 4 are set at $(-185m, -300m)$,

$(-200m, -285m)$, $(-215m, -300m)$, $(-200m, -315m)$, respectively, and the positions for according destination are set at $(115m, 90m)$, $(100m, 105m)$, $(85m, 90m)$, $(100m, 75m)$. The gains l, and k_{ij} should be properly adjusted to achieve a stabilized formation. Figure 4.11 shows the detecting process, which could not be a straight line if the l and k_{ij} are not set within certain range.

The result shows that the formation controller can steer the 4 UAVs from pre-defined positions to approach the destinations with stabilized formation.

4.5 Cooperative Contour Mapping of Radiative Signal Fields

In this scenario, the modified contour mapping control strategy, and the decentralized formation controller are combined to steer the 4-UAV formation for cooperative contour mapping of the radiative signal fields. The formation controller could guarantee stabilized formation flight while the contour mapping controller could detect the gradient of the radiative signal, and they cooperatively drive the 4-UAV formation to execute contour mapping.

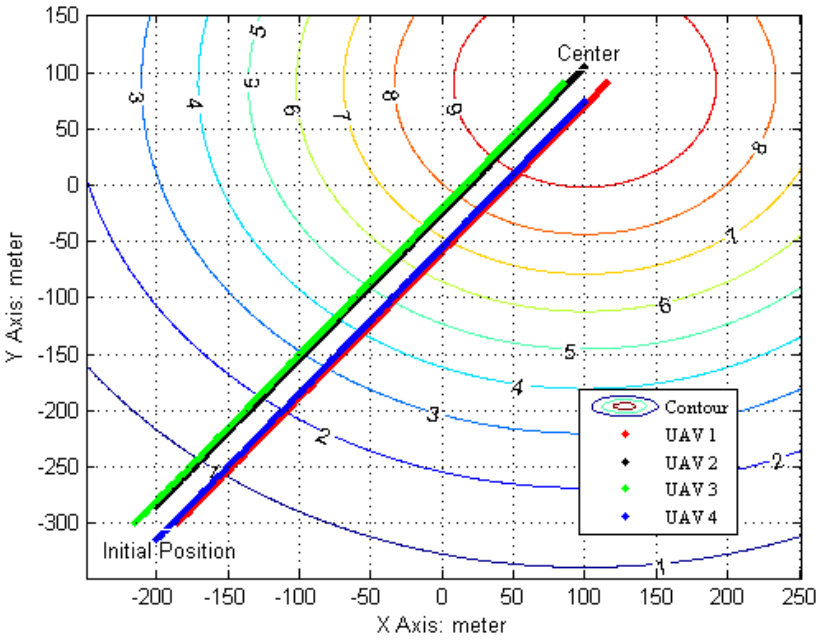

Fig. 4.11: UAV decentralized formation for radiative source detection.

After the combination, the 4-UAV formation could accomplish the contour mapping of the radiative signal with decreasing radius circular loop or square loop until the radiative source is located and reached.

In the scenario, the specified signal level for contour mapping is still set at 2, which is denoted as $D_s(x, y) = 2$. The initial positions of each UAV, the position of the source, and k, l, k_{ij} are all set to the same parameters as prior scenarios in this chapter. Because the physical limitation of fixed wing UAVs, there is a minimum radius for the circling formation flight, so when the 4 UAVs in formation reach the minimum flight radius, they will maintain the circling formation flight with the minimum radius for a while. Figure 4.12 shows the simulation result.

l could be adjusted to a smaller parameter if more area of the radiative signal fields is required to be covered with more accurate contour mapping provided. For example, if $l = 0.01$ instead of $l = 0.05$. Figure 4.13 describes the process with more area contour mapping provided. Figure 4.14 demonstrates the process of the 4-UAV formation with time.

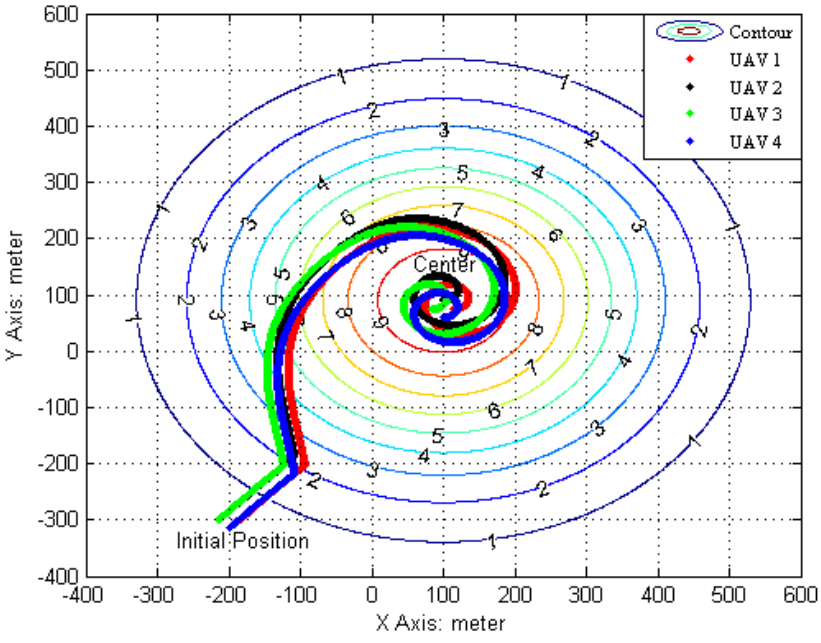

Fig. 4.12: UAV formation for cooperative source seeking and contour mapping.

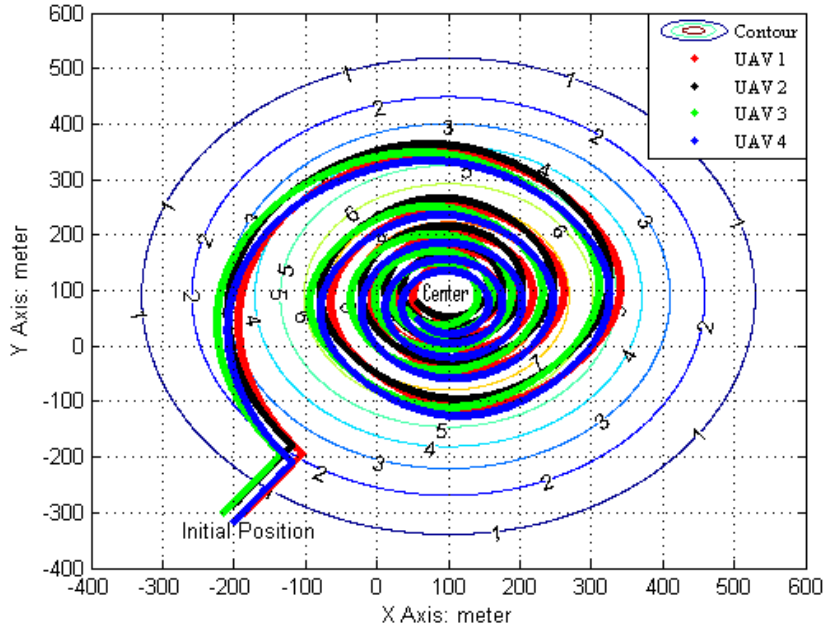

Fig. 4.13: Cooperative source seeking and contour mapping with l=0.01.

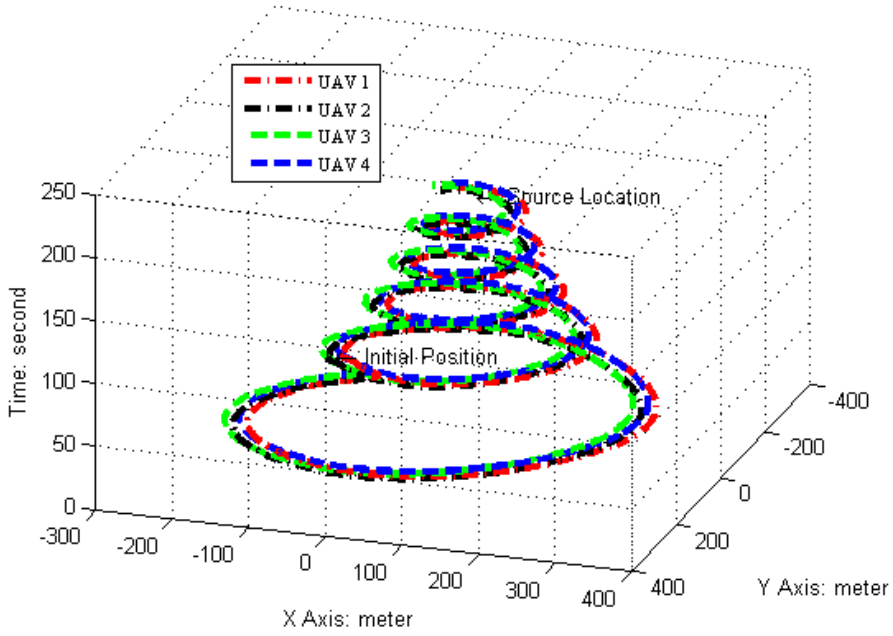

Fig. 4.14: Cooperative source seeking and contour mapping plot with time.

It is more safe for the multi-UAV formation to fly in square path instead of circular path. Because for the square formation flight path, the multiple UAVs could slightly adjust their positions to keep better formation in the practical situation. While for the circular formation flight path, the UAVs keep turning which is more likely to overshoot, and difficult to keep desired formation. This situation is also considered in this chapter, k could be adjusted to a bigger value if an approximate square flight path is needed for contour mapping. For example, if $k = 60$ instead of $k = 30$, the process is another result. Figure 4.15 demonstrates that the square formation flight path is executed instead of circular flight path.

Figure 4.16 shows the simulated process of the 4-UAV formation flight in square path from initial position.

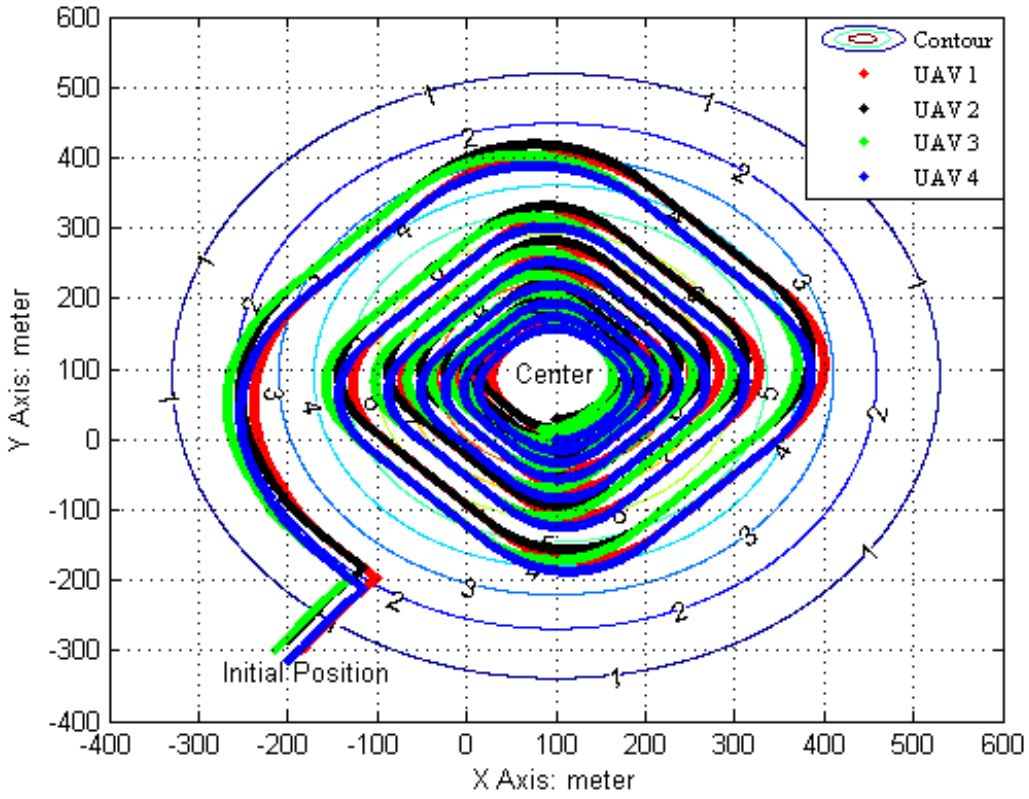

Fig. 4.15: Cooperative source seeking and contour mapping with l=0.01 and k=60.

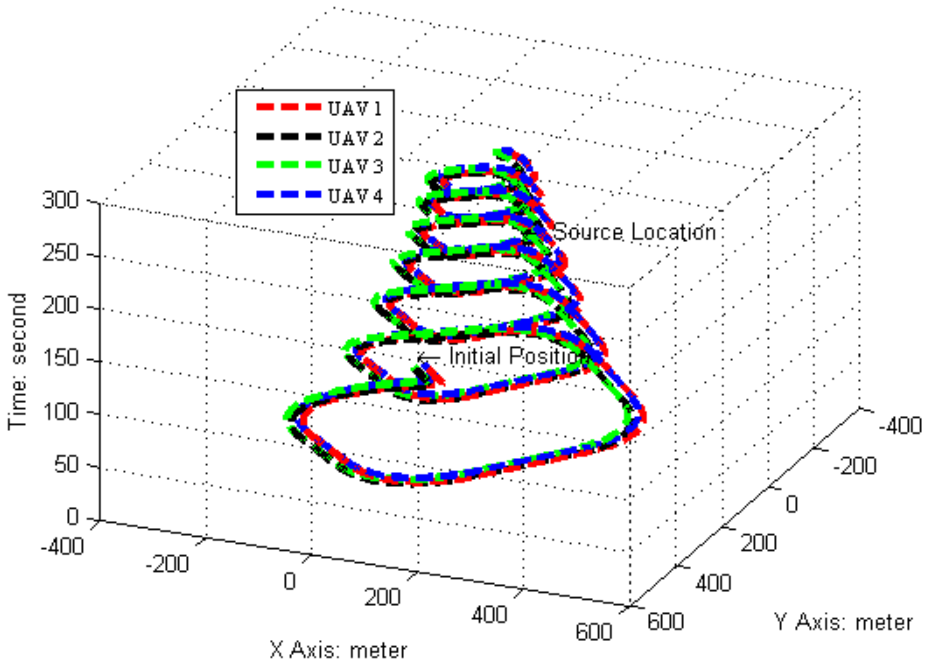

Fig. 4.16: Cooperative source seeking and contour mapping in square path.

4.6 Chapter Summary

This chapter is focused on multi-UAV formations for cooperative source seeking and contour mapping of radiative signal fields. Four scenarios are provided: the first scenario is 4-UAV formation based source seeking and locating with an adopted controller. In second scenario, the controller is modified for contour mapping under both stationary source and moving source conditions. The third scenario is the radiative signal level detection along certain path by 4-UAV decentralized formations. In the last scenario, the two control strategies illustrated in scenario 2 and 3 are combined to cooperatively control the multi-UAV formation for source seeking and contour mapping by flying in a decreasing radius circular or square loop. Those scenarios are simulated by considering practical flight situations, and verified by the simulation results.

Chapter 5
Pitch-Loop Control of a VTOL UAV Using Fractional Order Controller

5.1 Introduction

Compared with fixed-wing UAVs, which are mainly used for long endurance [25] flight and detections [31], VTOL UAVs have obvious advantages in the aspects of hovering capability, no space restriction for takeoff and landing, etc., which is more suitable for small area operation, static image capturing, search and rescue, etc. In addition, more and more research topics are focused on VTOL UAVs with a growing number of papers. Hancer et al. [91] illustrate a robust position controller with disturbance observer to compensate the disturbances including both the external wind and aerodynamic vibration for a tilt-wing VTOL. Two types of fractional order controllers are designed for altitude control and their effectiveness are verified by comparing with traditional PID controllers [92]. Garcia-Carrillo et al. [93] present the comparisons of three control schemes: nested saturations, backstepping, and sliding mode for stabilizing the position of a quadrotor using visual feedback. A formation control scheme is proposed to maintain the desired formation by tracking a linear reference velocity without linear-velocity measurement [94].

Pitch-loop control is a fundamental tuning step for VTOL UAV flight, and plays an important role in the attitude control performance. A VTOL UAV model for simulation is introduced by Bouabdallah and Siegwart [95], which also covers the entire dynamic control of the system. A mathematical model for a three-rotor VTOL UAV is proposed as well as the control strategy for attitude stabilization [96]. Tayebi and McGilvray [97] demonstrates that a quaternion-based feedback control strategy achieves exponential attitude stabilization by compensating the Coriolis and gyroscopic torques as well as the use of PD^2 feedback

structure.

Since fractional order control system design can improve the robustness and the control performance, a variety of fractional order controllers have been gradually applied to different applications. Monje et al. [98] cover fundamentals of fractional order control systems, illustrate the methods and tools for implementations, and analyze the real applications. A tutorial is given on fractional calculus applications which includes fractional order dynamic systems, fractional order PID, and examples to simulate fractional order systems [99]. Motion control is talked about, and fractional order modeling and control is compared with traditional velocity and position control methods [100]. Chao et al. [67] design a fractional controller on roll-channel for a small fixed-wing UAV, and demonstrate its advantages by experimental flight results. The preliminary work of this chapter [82], shows the validation of the fractional order controller for pitch-loop in the simulation platform.

This chapter first obtains a 7th order auto-regressive with exogenous input (ARX) model from our VTOL UAV simulation model using closed-loop identification method, and then converts it to a first-order plus time delay model for the pitch-loop. A fractional order [proportional-integral] (FO[PI]) [92] controller is designed based on the obtained VTOL UAV model. The designed FO[PI] controller is compared with an integer order proportional-integral-derivative (IOPID) controller and a modified Ziegler-Nichols (MZNs) PI controller. The results show that the proposed fractional order controller outperforms both the MZNs PI controller and the integer order PID controller in terms of gain variations and minimizing disturbance. At last, the identified ARX model for an AggieAir VTOL platform is provided based on the acquired flight data [101].

5.2 System Identification

In order to design a pitch-loop controller for VTOL UAV, it is critical to identify an accurate analytical model. Hoffer et al. [102] give a survey and categorization for the small low-cost UAV system identification. A traditional method for identification of a system is the open-loop analysis. However, several constraints prohibit the use of this method, such as small references and difficulties of stabilizing the VTOL UAV under open loop. So a

closed-loop system identification method is adopted instead since it is able to guarantee the pitch-loop stability of the original system. If the closed-loop system is not stabilized, a rough-tuned PID controller should be added to make it stabilized before identification. By following the procedure of system identification, the model can be identified under stable condition, and an accurate closed-loop model is acquired.

An ARX model is used in this chapter due to that the first order ARX model can facilitate the fractional order controller design. For pitch-loop ARX model, it can be defined as

$$\frac{\theta_p(z)}{\widehat{\theta}_p(z)} = \frac{b_0 + b_1 z^{-1} + \cdots + b_m z^{-m}}{a_0 + a_1 z^{-1} + \cdots + a_n z^{-n}}, \tag{5.1}$$

where $\theta_p(z)$ is the actual pitch angle and $\widehat{\theta}_p(z)$ is the desired pitch angle.

In order to implement the fractional order controllers and MZNs PI tuning rule, a first order plus time delay (FOPTD) model is derived and used based on the ARX model, which is defined as

$$G_p(s) = \frac{\theta_p(s)}{\widehat{\theta}_p(s)} = \frac{K}{Ts+1} e^{-Ls}. \tag{5.2}$$

The system identification part for the VTOL simulation model is based on the work by Bouabdallah and Siegwart [95]. Significant modifications have been made, so the simulation model can closely represent our experimental VTOL platform. This model includes the kinematics, energy equations, motion dynamics and rotor dynamics. The system control states and sensor measurements are composed of the following.

Control States

- Position: x, y, z;
- Ground Speed: V_x, V_y, V_z;
- Attitude: ϕ, θ, ψ;

- Angular Rate: p, q, r.

Sensor Measurements

- IMU: ϕ, θ, ψ;
- GPS and barometer: x, y, z;
- Ground Speed: V_x, V_y, V_z.

Throttles are represented in Equation (5.3), and pitch is calculated by Equation (5.7) [103],

$$U_1 = \sqrt{\dot{V_x}^2 + \dot{V_y}^2 + (g + \dot{V_z})^2}, \tag{5.3}$$

$$U_2 = \ddot{\phi}, \tag{5.4}$$

$$U_3 = \ddot{\theta}, \tag{5.5}$$

$$U_4 = \ddot{\psi}, \tag{5.6}$$

$$\theta = \arctan \frac{(\dot{V_x} \cos\psi + \dot{V_y} \sin\psi)}{g + \dot{V_z}}. \tag{5.7}$$

For pitch-loop identification, a sine function with magnitude between 0 and 2 at frequency $0.05Hz$ is used as the desired $\dot{V_y}$ while the desired $\dot{V_x}$ is set to 0, and desired yaw angle ψ is supposed to be 2 radians. After running the simulation for $20s$, the ARX model in Equation (5.23) is calculated as

$$G_{p1}(s) = \frac{Y_{p1}(s)}{U_{p1}(s)}, \tag{5.8}$$

where $Y_{p1}(s) = 0.3904s^7 - 456.6s^6 + 1.336 \times 10^5 s^5 + 1.114 \times 10^7 s^4 - 6.196 \times 10^9 s^3 + 4.239 \times 10^{11} s^2 - 3.19 \times 10^{14} s + 1.587 \times 10^{15}$, and $U_{p1}(s) = s^7 + 1225s^6 + 8.421 \times 10^5 s^5 + 2.25 \times 10^8 s^4 + 5.494 \times 10^{10} s^3 + 4.576 \times 10^{12} s^2 + 4.334 \times 10^{14} s + 6.485 \times 10^{14}$.

Figure 5.1 shows the comparison between the actual output and the output generated using the $7th$ order ARX model based on the desired pitch input. It can be observed that the $7th$ order ARX model is able to represent the actual pitch-loop properly.

The continuous time first order plus time delay (FOPTD) model is derived from the $7th$ order ARX model by using getfoptd function [104] and is shown as

$$G_{p2}(s) = \frac{2.447e^{-0.0818s}}{0.1282s + 1}. \tag{5.9}$$

In Figure 5.2, a step response is used to compare the 7th order ARX model and the derived FOPTD model. It shows that FOPTD model is able to approximate the $7th$ order ARX model.

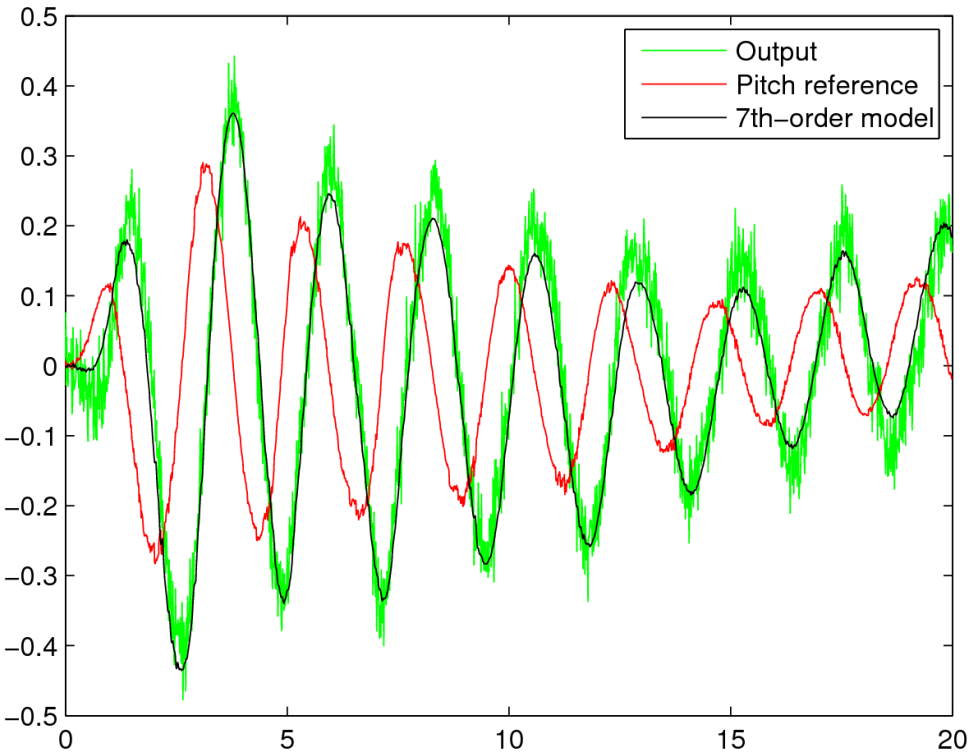

Fig. 5.1: 7th order ARX model.

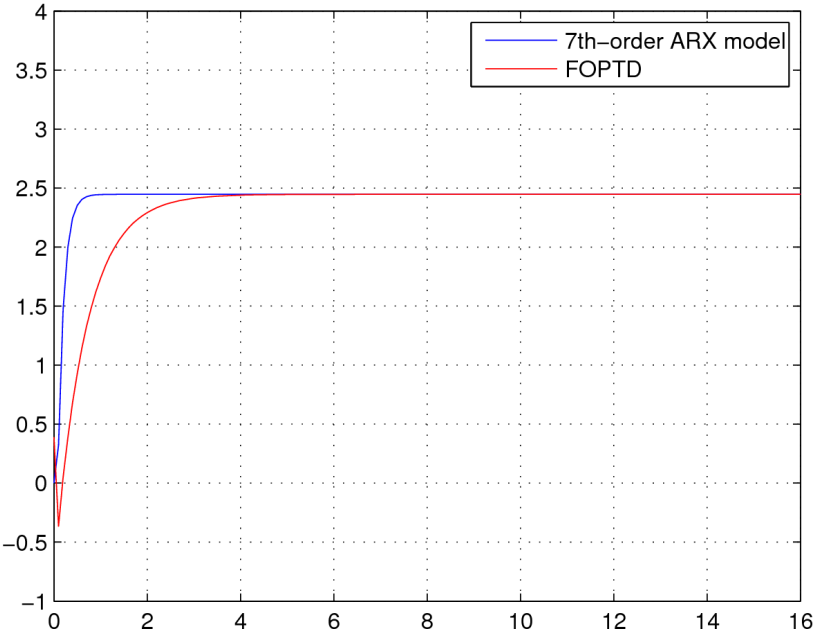

Fig. 5.2: FOPTD comparison with 7th order ARX model.

5.3 Controller Design Procedures

In this section, the design procedures of MZNs PI controller, integer order PID controller and FO[PI] controller are introduced in detail. They are all designed based on the FOPTD model which is obtained from the system identification for the pitch-loop of the VTOL UAV simulation model.

5.3.1 MZNs PI Controller Design

As a tuning rule that has been applied to many systems, the MZNs PI controller is shown as

$$C_{p1}(s) \quad = \quad K_{p1}(1 + \frac{1}{T_{p1}s}). \tag{5.10}$$

Based on Equation (5.10), the MZNs PI controller tuning rule follows three categories to get the desired controller [104].

(1) $L < 0.1T$ (Lag dominated)

$$K_{p1} = 0.3T/(KL), \quad T_{p1} = 8L;$$

(2) $0.1T < L < 2T$ (Balanced)

$$K_{p1} = 0.3T/(KL), \quad T_{p1} = 0.8T;$$

(3) $L > 2T$ (Delay dominated)

$$K_{p1} = 0.15/K, \quad T_{p1} = 0.4L.$$

According to the tuning rules, the MZNs PI controller is designed as

$$C_{p1}(s) \quad = \quad 0.1921(1 + \frac{9.7503}{s}). \tag{5.11}$$

The Bode plot of the open loop transfer function in Figure 5.3 demonstrates that the gain crossover frequency ω_c is $4.38 rad/sec$, and phase margin ϕ_m is 65°.

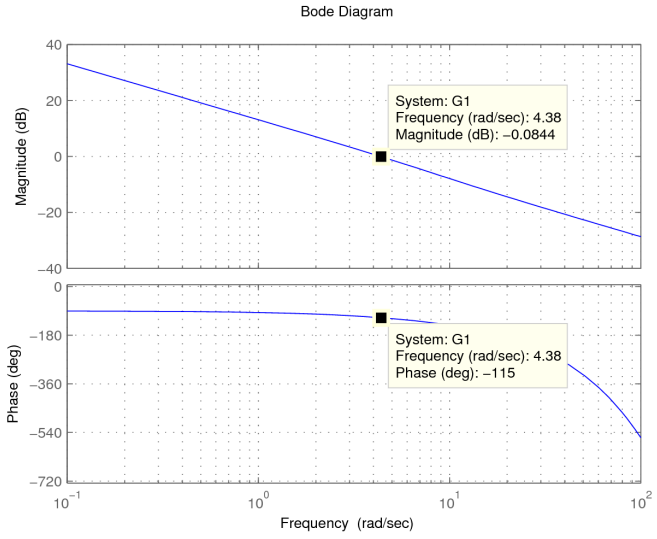

Fig. 5.3: Open-loop Bode plot with MZNs PI controller.

5.3.2 Preliminary on Fractional Order Calculus

The fractional order operators include Riemann-Liouville (RL) definition, Caputo definition and Grünwald-Letnikov definition. As one of the most famous definition, the RL fractional integral definition is shown as [105]

$$ {}_0D_t^{-\alpha} f(t) = \frac{1}{\Gamma(\alpha)} \int_0^t (t-\tau)^{\alpha-1} f(\tau) \mathrm{d}\tau, \tag{5.12} $$

where $0 < \alpha < 1$, $\Gamma(\cdot)$ is the Gamma function with the definition

$$ \Gamma(z) = \int_0^\infty e^{-t} t^{z-1} \mathrm{d}t, Re(z) > 0. \tag{5.13} $$

Under zero initial condition, the Laplace transform of the RL fractional operator could be derived as

$$ L[\ {}_0D_t^{-\alpha} f(t)] = \frac{1}{s^\alpha} F(s), \tag{5.14} $$

where $F(s)$ is the Laplace transform of $f(t)$.

The Caputo fractional integral definition [105] is shown as

$$ {}_0D_t^{-\alpha} f(t) = \frac{1}{\Gamma(\alpha)} \int_0^t \frac{f(\tau)}{(t-\tau)^{1-\alpha}} d\tau, \tag{5.15} $$

where $0 < \alpha < 1$, $\Gamma(\alpha)$ is also the Gamma function.

5.3.3 IOPID and FO[PI] Controllers Design

The designed IOPID and FO[PI] controllers are

$$ C_{p2}(s) = K_{p2} + \frac{1}{T_{p2} s} + D_{p2} s, \tag{5.16} $$

$$ C_{p3}(s) = (K_{p3} + \frac{1}{T_{p3} s})^\lambda, \tag{5.17} $$

where the fractional order $\lambda \in (0, 2)$.

The relationship between gain crossover frequency and phase margin is given in the following.

$$\mathrm{C_p(j\omega)G_p(j\omega)}|_{\omega=\omega_c} = \mathrm{e}^{-\mathrm{j}(\pi-\phi_m)}.$$

- Phase margin relationship

$$\mathrm{Arg[G(j\omega_c)]} = \mathrm{Arg[C_p(j\omega_c)G_p(j\omega_c)]} = -\pi + \phi_m \tag{5.18}$$

- Open-loop system gain relationship

$$|\mathrm{G(j\omega_c)}| = |\mathrm{C_p(j\omega_c)G_p(j\omega_c)}| = 1 \tag{5.19}$$

- The flat phase specification for more robust to both the gain variations and overshoot [67]

$$\frac{d(\mathrm{Arg(G(j\omega))})}{d\omega}|_{\omega=\omega_c} = 0. \tag{5.20}$$

According to the three specifications with certain crossover frequency $\omega_c = 4.38 rad/s$ and phase margin $\phi_m = 65^\circ$, IOPID and FO[PI] controllers are designed, and the equations are shown as

$$C_{p2}(s) = 0.1933 + \frac{2.0924}{s} + 0.0116s, \tag{5.21}$$

$$C_{p3}(s) = (0.645 + \frac{3.678}{s})^{1.45}, \tag{5.22}$$

where the fractional order $\lambda = 1.45$.

Figure 5.4 and Figure 5.5 show the open-loop Bode plots for the IOPID and FO[PI] controllers separately.

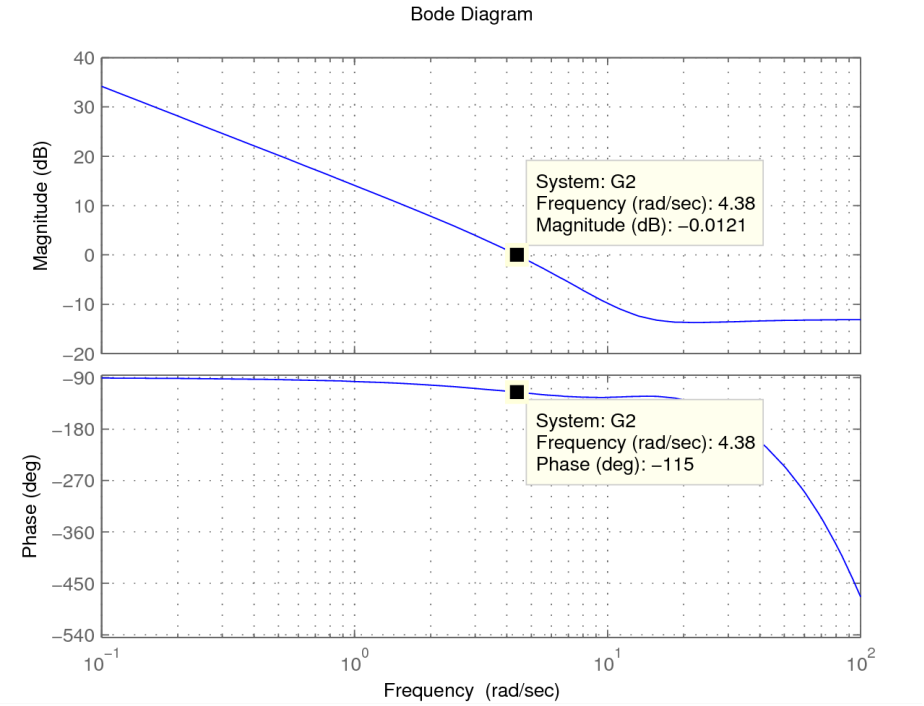

Fig. 5.4: Open-loop Bode plot with IOPID controller.

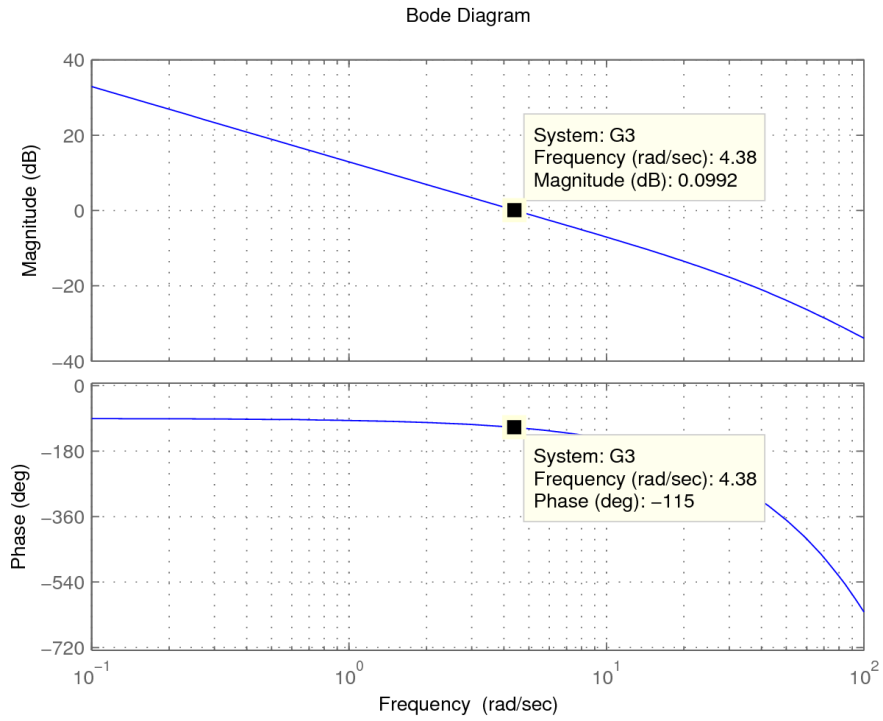

Fig. 5.5: Open-loop Bode plot with FO[PI] controller.

From the open-loop Bode plots, it can be observed that the gain crossover frequencies and phase margins of both designs meet the requirement and the phase is flat around the given gain crossover frequency.

5.4 Simulation Results

The step response with system gain variations ±20% is demonstrated for MZNs PI controller, IOPID controller and FO[PI] controller, respectively. Then they are compared under wind gust simulation to verify the capability of disturbance rejection.

5.4.1 System Gain Variation

One advantage of the flat phase around gain crossover frequency is that when the system gain varies, the controller is still able to control the system effectively.

Figure 5.6 demonstrates that when the system gain varies from 80% to 120%, the overshoot increases for MZNs PI controller.

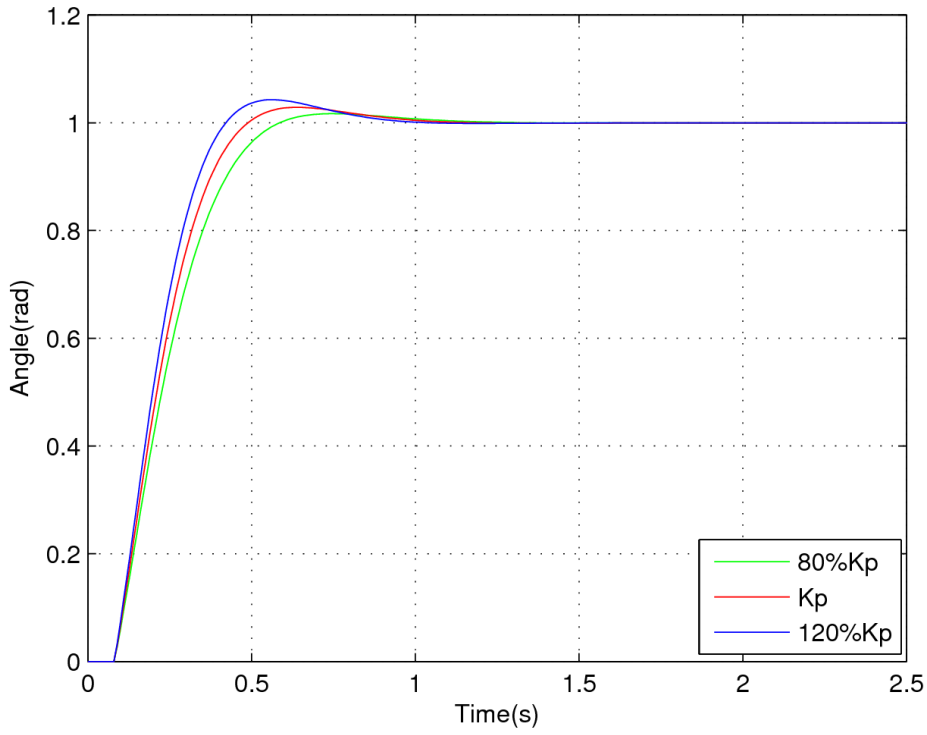

Fig. 5.6: MZNs PI controller with system gain variations ±20%.

Figure 5.7 illustrates the performance of the IOPID controller with system gain varies also from 80% to 120%. Figure 5.8 shows that overshoot maintains when the system gain changes for FO[PI] controller.

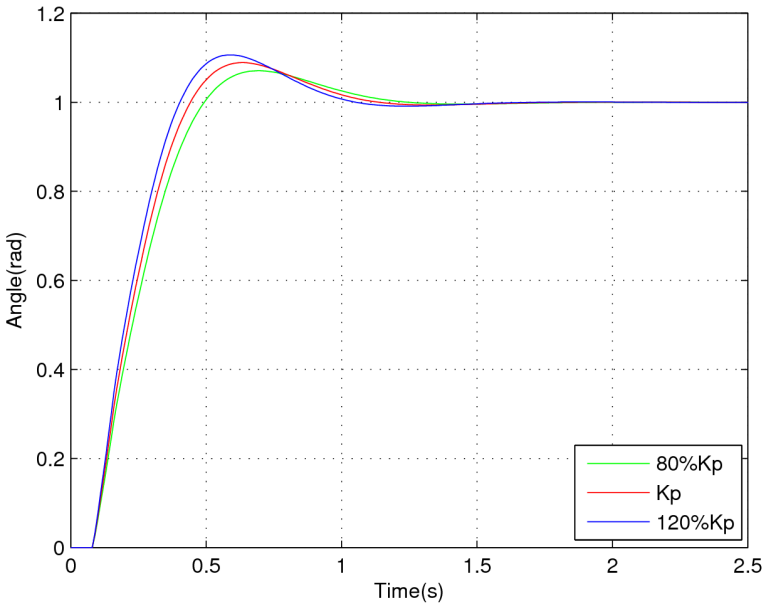

Fig. 5.7: IOPID controller with system gain variations ±20%.

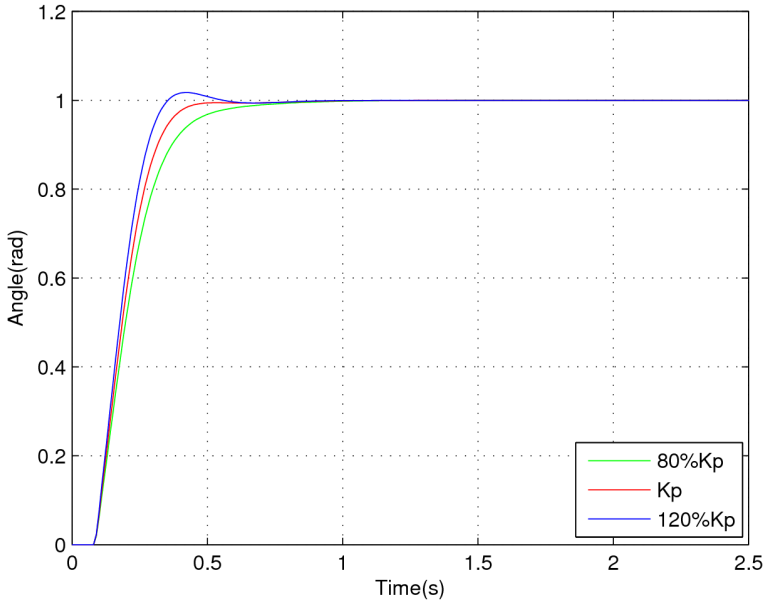

Fig. 5.8: FO[PI] controller with system gain variations ±20%.

From the comparison, it can be seen that, when the system gain varies from 80% to 120%, the FO[PI] controller has less overshoot also with less settling time.

5.4.2 Comparison of Step Response

From Figure 5.9, it can be observed that the FO[PI] controller has fastest responding speed, smallest overshoot and shortest settling time compared with MZNs PI and IOPID controllers.

5.4.3 Comparison of Wind Gust Response

Stabilization under wind gust condition is extremely important for VTOL UAV. If the controller can not handle properly, the performance of VTOL UAV will be deteriorated and it will even cause crash. Figure 5.10 demonstrates that when the wind gust is introduced, which arrives at $0.8m/s$ for $0.05s$, the FO[PI] controller has the shortest settling time compared with both MZNs PI controller and IOPID controller. And the overshoot is much smaller, which is also important for VTOL UAVs.

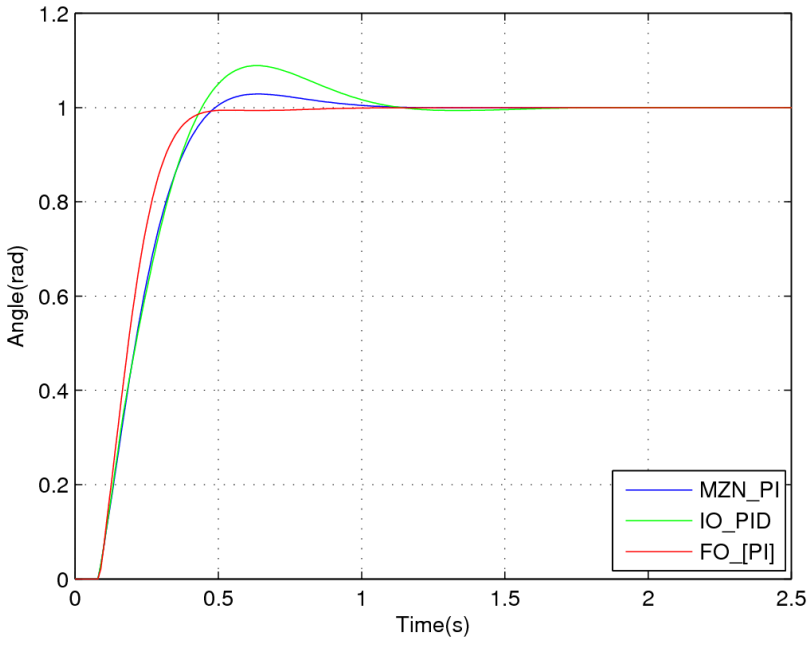

Fig. 5.9: Comparison of step response.

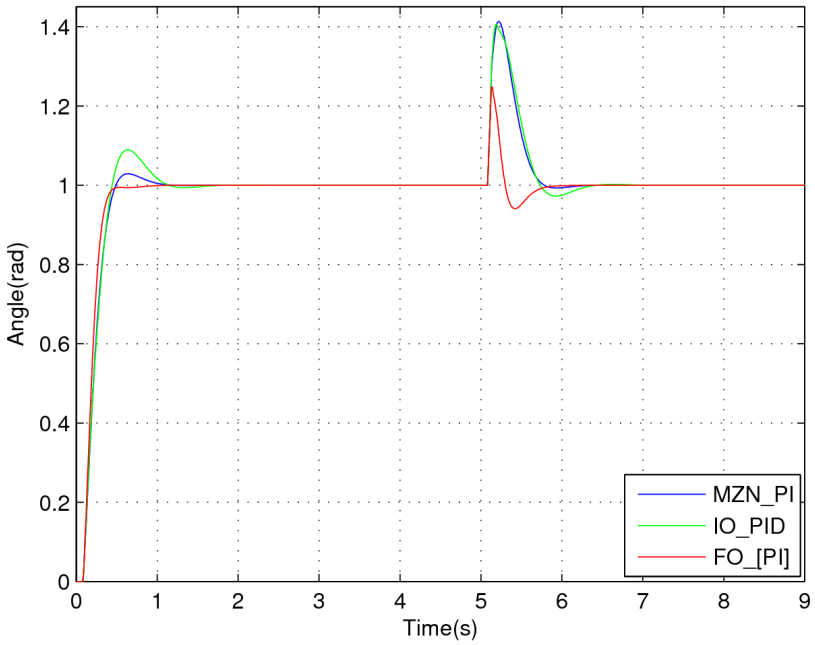

Fig. 5.10: Comparison of wind disturbance response.

5.5 ARX Model Identification Based on Practical Flight

Figure 5.11 shows one of AggieAir [106] small VTOL UAV platforms. Table 5.1 lists the specification.

Fig. 5.11: AggieAir quadrotor VTOL UAV platform.

Table 5.1: VTOL UAV specification.

Weight	4.5 lbs
Flight Time	Around 20 minutes
Flight Speed	< 5 m/s
Diagonal Distance	14.5 inch
GPS Accuracy	2 meters
IMU Accuracy	$\pm 2^{\circ}$
Operational Range	≤ 1 mile
Propeller Radius	6 inch

AggieAir VTOL UAVs use the open-source Paparazzi autopilot, consumer grade electronics and sensors, while maintaining excellent flight characteristics and reliability [107]. The avionics of such small low-cost UAVs consist of an Inertial Measurement Unit (IMU), which outputs attitude estimation, a GPS providing position information, pressure sensors for precise altitude estimation relative to a certain setpoint, a radio transmitter/receiver for telemetry remote control, and an autopilot unit which runs all control loops and stabilizes the attitude and altitude.

Several practical flights have accomplished using the designed AggieAir VTOL UAV platform which is shown in Figure 5.11. The safety pilot used the transmitter to send out the command to the AggieAir VTOL platform for pith up and down. The command is the reference for pitch angle, and the actual pitch angle can be measured by the IMU. The $7th$ order ARX model calculated from the pitch angle reference and actual pitch angle is shown as in Equation (5.23) as

$$G_{p1}(s) = \frac{Y_{preal}(s)}{U_{real}(s)}, \tag{5.23}$$

where $Y_{preal}(s) = 1.199s^7 + 573.2s^6 - 2.99 \times 10^5 s^5 + 9.737 \times 10^6 s^4 - 1.12 \times 10^{10} s^3 + 2.099 \times 10^{12} s^2 + 1.494 \times 10^{14} s + 3.807 \times 10^{15}$, and $U_{preal}(s) = s^7 + 1880s^6 + 8.486 \times 10^5 s^5 + 3.441 \times 10^8 s^4 + 5.234 \times 10^{10} s^3 + 6.106 \times 10^{12} s^2 + 1.887 \times 10^{14} s + 4.068 \times 10^{15}$.

The output of the $7th$ order ARX model is based on the pitch angle reference. Figure

5.12 demonstrates the result by plotting the pitch angle reference, the actual output, and the output of the $7th$ order ARX model.

From the result, it can be seen that the obtained $7th$ order ARX model can approximate the model of the AggieAir VTOL UAV platform properly.

The FOPTD model could be calculated according to the methods shown in the simulation part. Figure 5.13 illustrates the step response comparison between $7th$ order ARX model and FOPTD model.

The result demonstrates that the converted FOPTD model can approximate the $7th$ order ARX model. By following the same calculation method illustrated in the simulation part, MZNs PI controller, integer order PID controller, and FO[PI] controller could be designed, and be applied to experimental flight for validation.

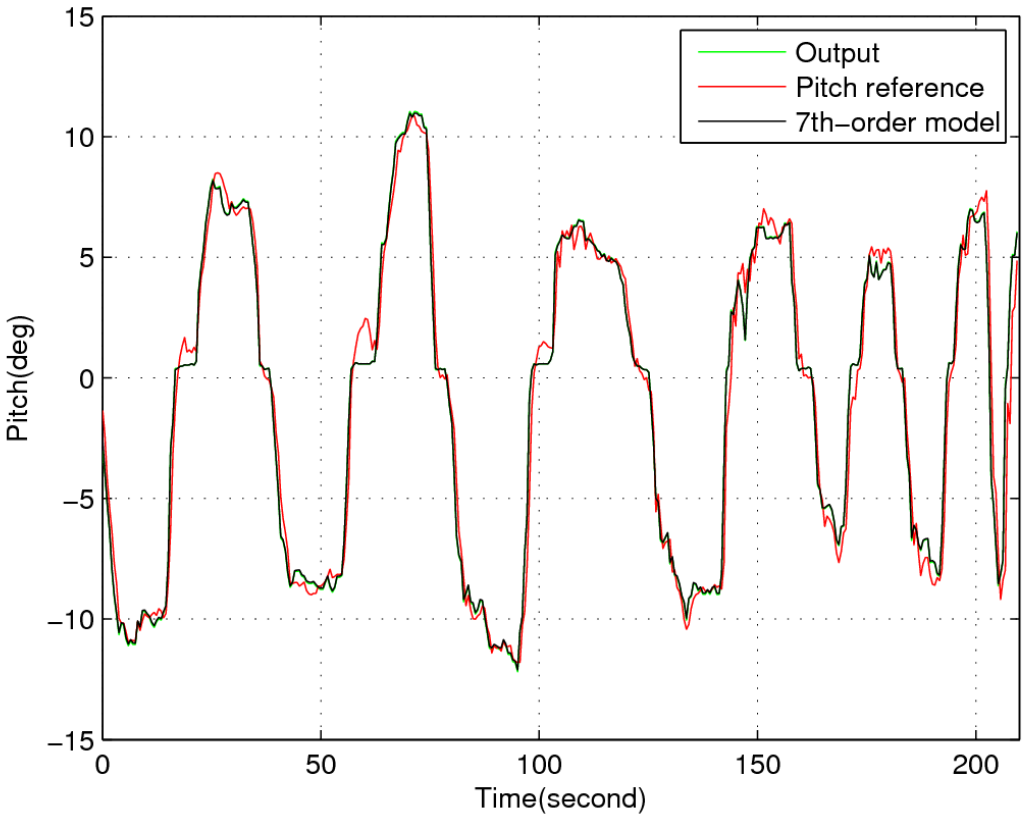

Fig. 5.12: 7th order, pitch angle reference, and actual output.

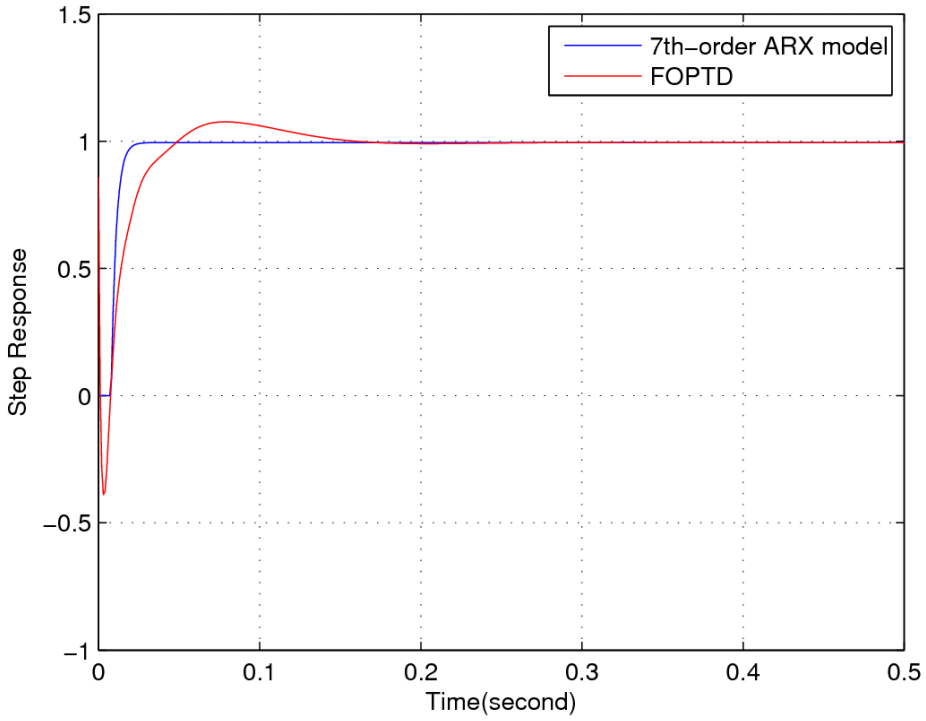

Fig. 5.13: Step response between 7th order ARX model and FOPTD model.

5.6 Chapter Summary

In this chapter, an ARX model for pitch-loop is first obtained using closed-loop identification from the VTOL UAV simulation model. Then a FOPTD model is converted from the $7th$ order ARX model. According to the FOPTD model, a MZNs PI controller is designed following the tuning rules, and both gain crossover frequency and phase margin of the open-loop transfer function are acquired. Based on the same gain crossover frequency and phase margin as well as three controller design specifications, an integer order PID controller and a FO[PI] controller are designed for comparisons under three situations: system gain variations, step response, and wind gust response. From the simulation results, it can be observed that the fractional order controller has less overshoot, shorter rising time, and is more robust compared with MZNs PI controller and IOPID controller. The ARX model for an AggieAir platform is acquired based on the practical flight data.

Chapter 6

Conclusions and Suggestions for Future Research

6.1 Conclusions

CPS are used in all kinds of areas, and bring great benefit to the world; people's lives have been greatly improved because of CPS. Some radiative sources are dangerous, especially in abnormal situation, so the source seeking and contour mapping of the radiative source is extremely important. This dissertation considers the huge advantages of CPS as well as the challenges, according to current technologies, chooses UAVs with CPS approach as the method for the source seeking and contour mapping task. The designed platforms including fixed-wing UAVs and VTOL UAVs are introduced in Chapter 2 with detailed system review, hardware design, and software setup. Chapter 3 considers two scenarios for nuclear radiation detection using multiple UAVs, of which contour mapping of the nuclear radiation is simulated. Then, for real applications, this chapter presents a low-cost UAV platform with built-in formation flight control architecture together with a formulated standard flight test routine. Three experimental formation flight scenarios that imitate the nuclear detection missions are prepared for contour mapping of nuclear radiation fields in 3D space. In Chapter 4, four scenarios are presented for cooperative source seeking and contour mapping of radiative signal fields by multi-UAV formations. A source seeking strategy is adopted with saturation, and then it is modified to achieve contour mapping of the signal fields with the moving source situation considered. A formation controller used for consensus problem is simplified and applied in one scenario to stabilize the multi-UAV formation flight during source detection. The contour mapping strategy and the formation control algorithm are combined to guarantee stable source seeking and contour mapping in both circular flight path and square flight path via multi-UAV formations. A fractional order strategy is designed to control the pitch-loop of a VTOL UAV in Chapter

5. First, an ARX model is acquired and converted to a FOPTD model. Next, based on the FOPTD model, a FO[PI] controller is designed. Then, an integer order PI controller based on the MZNs tuning rule and a general integer order PID controller are also designed for comparison following three design specifications. Simulation results have shown that the proposed fractional order controller outperforms both the MZNs PI controller and the integer order PID controller in terms of robustness and disturbance rejection. At last, ARX model-based system identification of VTOL UAV platform is achieved from experimental flight data.

6.2 Suggestions for Future Research

There are interesting challenges for the future work. Decentralized cognitive formation flight is the first future work which includes the inter-UAV communication, cognitive planning, and will contribute to more robust formation flight. Next, some of the scenarios presented in this dissertation for multi-UAV based cooperative source seeking and contour mapping should be validated by the practical flights. Furthermore, in order to utilize the advantages of different types of UAVs, the scenarios for heterogeneous flights including both the fixed-wing UAVs and VTOL UAVs should be created, and verified by the experimental flight tests.

6.2.1 Decentralized Cognitive Formation Flight

More robust and stabilized controller for formation flights is always the goal for accomplishing the source seeking missions. The decentralized cognitive formation flight could strengthen the robustness of the multi-UAV formation flight, and guarantee the success of the tasks. The general process for the decentralized cognitive formation flights can work in three stages.

Executing Command and Collecting Data

In the beginning, each UAV should be pre-programmed according to the situation. Every UAV will execute the flight plan after take off, and fly in the formation. The sensor

installed on each UAV begins to work, and collect data. The data can be radiation level, gas concentration, light brightness, image, etc.

Communicate with GCS and other UAVs

Each UAV will keep communicating with GCS and other UAVs for four aspects.

- Keep passing down the information to GCS: The passed down information not only contains collected data, but also includes the flight situation, such as position, speed, attitude, throttle, and power usage.

- Keep receiving the command from GCS: The GCS stores all the collected sensor data, and analyzes the next steps for the UAV formation, which may change the flight plan according to unexpected situation. So each UAV keeps receiving the command from GCS no matter the flight plan is changed or not. There may be some control loop tunings needed for better formation.

- Keep sending out the signal to other UAVs: Each UAV should continuously send out the signal to other UAVs including position, speed, attitude, throttle, collected data, etc., especially when the flight situation is abnormal or the UAV begins to detect certain source level.

- Keep receiving the signal from other UAVs: Continuous receiving the signal from other UAVs would help the UAV to be aware of the formation working situation. Each UAV may change the flight plan if abnormal situation warning received, and should send the notification to GCS.

During the whole process, the multi-UAV formation is decentralized and cognitive. Each UAV should communicate with each other as well as the GCS, and be able to accomplish individual computing, diagnosing, optimizing, and planning. The GCS should be powerful enough to analyze all the information, compute, and design the optimized flight plan to guidance the actions of the formation flight.

Safe Flight

Each UAV should have the pre-programmed plan to meet with some unexpected situation, such as running out of power, loosing communication with GCS or other UAVs, etc. The UAV should have the precaution for all the emergencies, and achieve the safe landing as well as sending out the warning to GCS and other communicated UAVs.

6.2.2 Heterogeneous Flights

The heterogeneous flights will maximize the advantages of both fixed-wing and VTOL UAVs for various purposes and tasks with a better performance. The advantages of fixed-wing UAVs and VTOL UAVs are classified below.

Advantage of Fixed-Wing UAVs

- Long flight time, which makes fixed-wing UAVs eligible for long distance tasks;
- Fast speed, which is good for tracking missions and can save the time;
- High power efficiency, which would improve the flight performance;
- Big payload, which extends the functionality of fixed-wing UAVs;
- Capability to high altitude, which enlarge the range for activities.

Advantage of VTOL UAVs

- Hovering ability, which is good for more precise detecting, and image capturing;
- No space restriction for takeoff and landing, which is able to fly the VTOL UAVs everywhere, such as in small areas, indoor, and even in tough fields;
- Speed changes quickly, which can make the VTOL UAVs more agile for actions including moving avoid the obstacles;
- Altitude maneuverability, which brings great flexibility to drop or climb;

- Small size, which is easy to carry and put into box;
- More safety with multi-rotors, which will enhance the fly safety by changing rotor running strategies (for hex-rotor, octo-rotor, etc.).

Heterogeneous flights combine the advantages of both the fixed-wing UAVs and VTOL UAVs, according to various tasks, execute the corresponding scenarios. For example, in a source seeking task, one or more fixed-wing UAVs (the number of UAVs depends on time requirement and the size of the field) will be sent out for source seeking at the beginning. When the sources are located, the VTOL UAVs would be dispatched for accurate contour mapping or images capturing, etc.

The future research will consider more tasks for practical heterogeneous flights.

6.2.3 Extremum Seeking Control for Source Seeking

Extremum seeking control has already been applied to CPS, including tuning PID parameters in a control system, minimizing the power in the industry, maximizing the yield of crops, etc. Extremum seeking control has already been achieved for source seeking, and some work has been explored for moving targets tracking by multi-vehicle formations. The difficulty of the multi-UAV-based extremum seeking control for source seeking lies on that the shape of the multi-UAV-formation needs to be maintained while tracking a diffusive source by using extremum seeming control.

There are three methods for multi-UAV-based extremum seeking control design.

- Gradient-based extremum seeking control,
- Perturbation-based extremum seeking control,
- Numerical optimization-based extremum seeking control.

In the future work, the obstacle avoidance should be taken into account during the multi-UAV extremum seeking control for source seeking, and some control algorithms would be applied to the formation control to guarantee the task.

References

[1] Wikipedia, 2013, "Cyber-physical system." [Online]. Available: http://en.wikipedia.org/wiki/Cyber-physical_system

[2] E. A. Lee, "Cyber physical systems: Design challenges," technical report, 2008. [Online]. Available: http://www.eecs.berkeley.edu/Pubs/TechRpts/2008/EECS-2008-8.html

[3] LIM Laboratory, 2013, "Cyber physical systems (cps)." [Online]. Available: http://www.jaist.ac.jp/is/labs/lim-lab/research.php

[4] B. M. Albaker and N. A. Rahim, "A conceptual framework and a review of conflict sensing, detection, awareness and escape maneuvering methods for UAVs," in *Aeronautics and Astronautics*, M. Mulder, Ed. InTech, 2011, pp. 953–978.

[5] K. Bür, "Vehicular ad hoc networks," 2013. [Online]. Available: http://www.eit.lth.se/index.php?uhpuid=dhs.kbr&hpuid=741

[6] Cyber-physical systems virtual organization, 2013, "National workshops on medical cyber-physical systems," 2013. [Online]. Available: http://cps-vo.org/group/Medical%20CPS

[7] E. Drexler, "High-throughput nanomanufacturing," 2013. [Online]. Available: http://metamodern.com/2009/02/27/high-throughput-nanomanufacturing/

[8] COGA group at TU Berlin, 2013, "Screenshot of a traffic simulation (ptv)." [Online]. Available: http://www3.math.tu-berlin.de/coga/projects/traffic/advest/

[9] B. Olivier, G. Pierre, H. Nicolas, L. Peter, O. Lo̍c, P. Sarah, and T. Olivier, "Air traffic control tracking systems performance impacts with new surveillance technology sensors," in *Aeronautics and Astronautics*, T. T. Arif, Ed. InTech, 2010, pp. 379–390.

[10] Shenzhen Anboshi Electronic Technology Co., Ltd, 2013, "Security alarm system." [Online]. Available: http://www.qrbiz.com/product/307242/GSM-wireless

[11] IEEE fraternity at YCCE, 2013, "Haptics robotic-arm." [Online]. Available: http://ieeeycce.blogspot.com/p/past-events.html

[12] Amazon, 2013, "Amazon prime air." [Online]. Available: http://www.amazon.com/b?ref_=tsm_1_fb_s_amzn_mx3eqp&node=8037720011

[13] Healthcare Global, 2013, "Remote health monitoring." [Online]. Available: http://www.healthcareglobal.com/sectors/medical-devices-products/3g-remote-health-monitoring-facilitated-sprint-and-bl-healthcare

[14] A. White, "India debuts manpack vtol uavs for hadr," 2013. [Online]. Available: http://www.shephardmedia.com/news/uv-online/india-debuts-manpack-vtol-uavs-hadr/

[15] Carbon-Based Technology Inc, 2013, "Radiation detection." [Online]. Available: http://www.uaver.com/uas-avian-r.html

[16] Big Blue Tech, 2013, "FAU's famed deep-sea exploration vehicles may be retired." [Online]. Available: http://bigbluetechnews.wordpress.com/2009/06/09/faus-famed-deepsea-exploration-vehicles-retired/

[17] Wikipedia, 2013, "Spirit(rover)." [Online]. Available: http://en.wikipedia.org/wiki/Spirit_%28rover%29

[18] National Science Foundation, 2013, "Cyber-physical systems (CPS) program solicitation." [Online]. Available: http://www.nsf.gov/pubs/2013/nsf13502/nsf13502.htm

[19] H. Chao and Y. Chen, *Remote Sensing and Actuation Using Unmanned Vehicles*. Hoboken, NJ: Wiley-IEEE Press, 2012.

[20] AggieAir, 2013, "Aggieair: A remote sensing unmanned aerial system for scientific applications." [Online]. Available: http://aggieair.usu.edu/aircraft

[21] AggieAir, 2014, "AggieAir visual mosaic of wetland." [Online]. Available: http://aggieair.usu.edu/vegetation

[22] AggieAir, 2013, "AggieAir map of evapotranspiration." [Online]. Available: http://aggieair.usu.edu/ag

[23] Friends of the Bear River Refuge website, 2013, "Bear river migatory bird refuge (MBR)." [Online]. Available: http://www.fobrr.org/refuge.php

[24] Australian Geographic, 2013, "Fishers, divers help track marine species." [Online]. Available: http://www.australiangeographic.com.au/journal/fishers-divers-help-with-marine-conservation.htm

[25] A. M. Jensen, M. Baumann, and Y. Q. Chen, "Low-cost multispectral aerial imaging using autonomous runway-free small flying wing vehicles," in *Proceedings of 2008 IEEE International Geoscience and Remote Sensing Symposium (IGARSS08)*, July 2008.

[26] Utah State University, 2013, "David G. sant engineering innovation building." [Online]. Available: http://www.usu.edu/celebration/buildings/

[27] Alaska Scenic Photos, 2013, "Algae growth." [Online]. Available: http://www.alaska-in-pictures.com/algae-growth-2478-pictures.htm

[28] Aerial Photography Specialists, 2013, "Powerline inspections." [Online]. Available: http://www.apspecialists.com.au/services/services_view/100

[29] Ropeworks, 2013, "Hoover dam inspection." [Online]. Available: http://www.ropeworks.com/service.htm

[30] L. Di, H. Chao, J. Han, and Y. Chen, "Cognitive multi-UAV formation flight: Principle, low-cost UAV testbed, controller tuning and experiments," in *Proceedings of the 2011 IEEE/ASME International Conference on Mechatronic and Embedded Systems and Applications (MESA11)*, Aug. 2011.

[31] J. Han, Y. Xu, L. Di, and Y. Chen, "Low-cost multi-UAV technologies for contour mapping of nuclear radiation field," *Journal of Intelligent and Robotic Systems*, vol. 70, no. 1-4, pp. 401–410, April 2013.

[32] Paparazzi, 2012, "Autopilot software." [Online]. Available: http://paparazzi.enac.fr/wiki/Software

[33] STARMAC, 2013, "Quadrotor helicopter UAV project." [Online]. Available: http://hybrid.eecs.berkeley.edu/starmac/

[34] P. Pounds, R. Mahony, and P. Corke, "Modelling and control of a quad-rotor robot," *Control Engineering Practice*, vol. 18, no. 7, pp. 691–699, July 2010.

[35] S. Bouabdallah, "design and control of quadrotors with application to autonomous flying," Ph.D. dissertation, Swiss Federal Institute of Technology in Lausanne, Lausanne, Switzerland, 2007.

[36] I. Kroo, "Prototype mesicopter with spinning rotors," 2014. [Online]. Available: http://adg.stanford.edu/mesicopter/imageArchive/

[37] Microdrones, 2012, "Industrial inspections." [Online]. Available: http://www.microdrones.com/index.php

[38] Parrot, 2012, "AR.Drone." [Online]. Available: http://ardroneparrotreview.com/

[39] V. Savov, "Minirad-v," 2010. [Online]. Available: http://www.engadget.com/2010/05/28/autonomous-quadrocopter-flies-through-windows-straight-into-our/

[40] Aerospace Controls Laboratory at MIT, 2013, "Closeup of flying quadrotors." [Online]. Available: http://vertol.mit.edu/photos.html

[41] S. Bouabdallah, M. Becker, V. de Perrot, and R. Siegwart, "Toward obstacle avoidance on quadrotors," in *Proceedings of the XII International Symposium on Dynamic Problems of Mechanics (DINAME07)*, Feb. 2007.

[42] Paparazzi, 2013, "Booz imu." [Online]. Available: http://paparazzi.enac.fr/wiki/Booz

[43] Transition Robotics, 2013, "Lia board." [Online]. Available: http://transition-robotics.com/products/lia

[44] Microstrain, 2012, "3dm-gx3." [Online]. Available: http://www.microstrain.com/3dm-gx3-25.aspx

[45] Paparazzi, 2013, "Sensors/gps." [Online]. Available: http://paparazzi.enac.fr/wiki/Gps

[46] Digi International, 2013, "XTend OEM RF modules." [Online]. Available: http://www.digi.com/products/wireless-wired-embedded-solutions/zigbee-rf-modules/point-multipoint-rfmodules/xtend-module

[47] Paparazzi, 2013, "Modems." [Online]. Available: http://paparazzi.enac.fr/wiki/Modems

[48] Model Motors, 2013, "Axi motors." [Online]. Available: http://www.modelmotors.cz/index.php?page=61

[49] Spektrum, 2013, "Dx7 ar7000." [Online]. Available: http://www.spektrumrc.com/Products/Default.aspx?ProdID=SPM2710

[50] Freescale Semiconductor, 2013, "3-phase bldc motor control with quadrature encoder using 56f800/e." [Online]. Available: http://www.freescale.com/files/dsp/doc

[51] S. Vorkoetter, "A tutorial introduction to motocalc," 2007. [Online]. Available: http://www.motocalc.com/tutorial.htm

[52] L. Di and Y. Chen, "Autonomous flying under 500 USD based on RC aircraft," in *Proceedings of 2011 IEEE/ASME International Conference on Mechatronic and Embedded Systems and Applications (MESA11)*, Aug. 2011.

[53] A. Geramifard, J. Redding, N. Roy, and J. P. How, "UAV cooperative control with stochastic risk models," in *Proceedings of the 2011 American Control Conference (ACC11)*, June 2011.

[54] A. NEmra and N. Aouf, "Robust cooperative UAV visual SLAM," in *Proceedings of the 9th IEEE International Conference on Cybernetic Intelligent Systems (CIS10)*, Sep. 2010.

[55] A. Abdessameud and A. Tayebi, "Formation stabilization of VTOL UAVs subject to communication delays," in *Proceedings of the 49th IEEE Conference on Decision and Control (CDC10)*, Dec. 2010.

[56] S. K. Gan and S. Sukkarieh, "Multi-UAV target search using explicit decentralized gradient-based negotiation," in *Proceedings of the 2011 IEEE International Conference on Robotics and Automation (ICRA11)*, May 2011.

[57] D. Casbeer, R. Beard, T. Mclain, S.-M. Li, and R. Mehra, "Forest fire monitoring with multiple small UAVs," in *Proceedings of the 2005 American Control Conference (ACC05)*, June 2005.

[58] The Engineer, 2010, "UAV for nuclear scouting missions." [Online]. Available: http://www.theengineer.co.uk/news/uav-for-nuclear-scouting-missions/1001237.article

[59] B. Carey, "Honeywell's micro-UAV monitors damaged nuclear plant," 2011. [Online]. Available: http://www.ainonline.com/?q=aviation-news/ain-defense-perspective/2011-05-02/honeywells-micro-uav-monitors-damaged-nuclear-plant

[60] I. Eliaz, "Nuclear radiation protection protocol," 2011. [Online]. Available: http://www.qmmc-wisdom.com/nuclear-radiation-protection-protocol.html

[61] H. Teimoori and A. Savkin, "Equiangular navigation and guidance of a wheeled mobile robot based on range-only measurements," *Robotics and Autonomous Systems*, vol. 58, no. 2, pp. 203–215, Feb. 2010.

[62] I. Manchester and A. Savkin, "Circular navigation missile guidance with incomplete information and uncertain autopilot model," *Journal of Guidance Control and Dynamics*, vol. 27, no. 6, pp. 1078–1083, 2004.

[63] A. Gadre and D. Stilwell, "Toward underwater navigation based on range measurements from a single location," in *Proceedings of the 2004 IEEE International Conference on Robotics and Automation (ICRA04)*, April 2004.

[64] A. Matveev, H. Teimoori, and A. Savkin, "Navigation of a non-holonomic vehicle for gradient climbing and source seeking without gradient estimation," in *Proceedings of the 2010 American Control Conference (ACC10)*, June 2010.

[65] B. J. Moore and C. C. de Wit, "Source seeking via collaborative measurements by a circular formation of agents," in *Proceedings of the 2010 American Control Conference (ACC10)*, June 2010.

[66] L. Di, T. Fromm, and Y. Chen, "A data fusion system for attitude estimation of low-cost miniature UAVs," *Journal of Intelligent and Robotic Systems*, vol. 65, no. 1-4, pp. 621–635, Jan. 2012.

[67] H. Chao, Y. Luo, L. Di, and Y. Chen, "Roll-channel fractional order controller design for a small fixed-wing unmanned aerial vehicle," *Control Engineering Practice*, vol. 18, no. 7, pp. 761–772, July 2010.

[68] D-tect Systems, 2012, "Minirad-v." [Online]. Available: http://www.dtectsystems.com

[69] ECE, USU, 2014, "Students launch an autonomous miniature uav." [Online]. Available: http://ece.usu.edu/

[70] C. Zhang, D. Arnold, N. Ghods, A. Siranosian, and M. Krstic, "Source seeking with non-holonomic unicycle without position measurement and with tuning of forward velocity," *Systems and Control Letters*, vol. 56, no. 3, pp. 245–252, March 2007.

[71] J. Cochran and M. Krstic, "Source seeking with a nonholonomic unicycle without position measurements and with tuning of angular velocity part I: Stability analysis," in *Proceedings of the 46th IEEE Conference on Decision and Control (CDC07)*, Dec. 2007.

[72] N. G. Jennie Cochran, Antranik Siranosian and M. Krstic, "Source seeking with a nonholonomic unicycle without position measurements and with tuning of angular velocity – part II: Applications," in *Proceedings of the 46th IEEE Conference on Decision and Control (CDC07)*, Dec. 2007.

[73] A. S. Matveev, H. Teimoori, and A. V. Savkin, "Navigation of a non-holonomic vehicle for gradient climbing and source seeking without gradient estimation," in *Proceedings of the 2010 American Control Conference (ACC10)*, June 2010.

[74] P. Ögren, E. Fiorelli, and N. E. Leonard, "Cooperative control of mobile sensor networks: adaptive gradient climbing in a distributed environment," *IEEE Transactions on Automatic Control*, vol. 49, no. 8, pp. 1292–1302, Aug. 2004.

[75] J. Daniel L. Stephens and A. J. Peurrung, "Detection of moving radioactive sources using sensor networks," *IEEE Transactions on Nuclear Science*, vol. 51, no. 5, pp. 2273–2278, Oct. 2004.

[76] M. A. Demetriou, "Process estimation and moving source detection in 2-d diffusion processes by scheduling of sensor networks," in *Proceedings of the 2007 American Control Conference (ACC07)*, July 2007.

[77] S. M. Brennan, A. M. Mielke, and D. C. Torney, "Radioactive source detection by sensor networks," *IEEE Transactions on Nuclear Science*, vol. 52, no. 3, pp. 813–819, June 2005.

[78] T. Zhao and A. Nehorai, "Detecting and estimating biochemical dispersion of a moving source in a semi-infinite medium," *IEEE Transactions on Signal Processing*, vol. 54, no. 6, pp. 2213–2225, June 2006.

[79] J. Cochran, N. Ghods, and M. Krstic, "3d nonholonomic source seeking without position measurement," in *Proceedings of the 2008 American Control Conference (ACC08)*, June 2008.

[80] J. Cochran, S. D. Kelly, H. Xiong, and M. Krstic, "Source seeking for a joukowski foil model of fish locomotion," in *Proceedings of the 2009 American Control Conference (ACC09)*, June 2009.

[81] S. ichi Azuma, M. S. Sakar, and G. J. Pappas, "Stochastic source seeking by mobile robots," *IEEE Transactions on Automatic Control*, vol. 57, no. 9, pp. 2308–2321, Sep. 2012.

[82] J. Han, L. Di, C. Coopmans, and Y. Chen, "Fractional order controller for pitch loop control of a vtol uav," in *Proceedings of the 2013 International Conference on Unmanned Aircraft Systems (ICUAS13)*, May 2013.

[83] M. Wheeler, B. Schrick, W. Whitacre, M. Campbell, RolfRysdyk, and R. Wise, "Cooperative tracking of moving targets by a team of autonomous UAVs," in *Proceedings of the 25th Digital Avionics Systems Conference (DASC06)*, Oct. 2006.

[84] S. Zhu, D. Wang, and C. B. Low, "Cooperative control of multiple UAVs for source seeking," *Journal of Intelligent and Robotic Systems*, vol. 70, no. 1-4, pp. 293–301, April 2013.

[85] F. Zhang and N. E. Leonard, "Cooperative filters and control for cooperative exploration," *IEEE Transactions on Automatic Control*, vol. 55, no. 3, pp. 650–663, March 2010.

[86] A. Jensen and Y. Chen, "Tracking tagged fish with swarming unmanned aerial vehicles using fractional order potential fields and kalman filtering," in *Proceedings of the 2013 International Conference on Unmanned Aircraft Systems (ICUAS13)*, May 2013.

[87] S. Zhu, D. Wang, and C. B. Low, "Cooperative control of multiple uavs for moving source seeking," in *Proceedings of the 2013 International Conference on Unmanned Aircraft Systems (ICUAS13)*, May 2013.

[88] J. Han and Y. Chen, "Cooperative source seeking and contour mapping of a diffusive signal field by formations of multiple uavs," in *Proceedings of the 2013 International Conference on Unmanned Aircraft Systems (ICUAS13)*, May 2013.

[89] J. Han and Y.Chen, "Multiple UAV formations for cooperative source seeking and contour mapping of a radiative signal field," *Journal of Intelligent and Robotic Systems*, vol. 74, no. 1-2, pp. 323–332, April 2014.

[90] W. Ren and E. Atkins, "Distributed multi-vehicle coordinated control via local information exchange," *International Journal of Robust and Nonlinear Control*, vol. 17, no. 10-11, pp. 1002–1033, July 2007.

[91] C. Hancer, K. T. Oner, E. Sirimoglu, E. Cetinsoy, and M. Unel, "Robust position control of a tilt-wing quadrotor," in *Proceedings of the 49th IEEE Conference on Decision and Control (CDC10)*, Dec. 2010.

[92] Y. Luo, L. Di, J. Han, H. Chao, and Y. Chen, "VTOL UAV altitude flight control using fractional order controllers," in *Proceedings of the 4th IFAC Workshop on Fractional Differentiation and Its Application (FDA10)*, Oct. 2010.

[93] L. R. Garcia-Carrillo, E. Rondon, A. Dzul, A. Sanchez, and R. Lozano, "Hovering quad-rotor control: A comparison of nonlinear controllers using visual feedback," in *Proceedings of the 49th IEEE Conference on Decision and Control (CDC10)*, Dec. 2010.

[94] A. Abdessameud and A. Tayebi, "Formation control of VTOL UAVs without linear-velocity measurements," in *Proceedings of the 2010 American Control Conference (ACC10)*, June 2010.

[95] S. Bouabdallah and R. Siegwart, "Full control of a quadrotor," in *Proceedings of the 2007 IEEE/RSJ International Conference on Intelligent Robots and Systems (IROS07)*, Oct. 2007.

[96] J. Escareo, A. Sanchez, O. Garcia, and R. Lozano, "Triple tilting rotor mini-UAV: Modeling and embedded control of the attitude," in *Proceedings of the 2008 American Control Conference (ACC08)*, June 2008.

[97] A. Tayebi and S. McGilvray, "Attitude stabilization of a vtol quadrotor aircraft," *IEEE Trasactions on Control Systems Technology*, vol. 14, no. 3, pp. 562–571, May 2006.

[98] C. A. Monje, Y. Chen, B. M. Vinagre, D. Xue, and V. Feliu, *Fractional-order Systems and Controls: Fundamentals and Applications*. New York City: Springer, 2010.

[99] Y. Chen, I. Petras, and D. Xue, "Fractional order control - a tutorial," in *Proceedings of the 2009 American Control Conference (ACC09)*, June 2009.

[100] Y. Luo and Y. Chen, *Fractional Order Motion Controls*. Hoboken, NJ: Wiley, 2012.

[101] J. Han, L. Di, C. Coopmans, and Y. Chen, "Pitch loop control of a VTOL UAV using fractional order controller," *Journal of Intelligent and Robotic Systems*, vol. 73, no. 1-4, pp. 187–195, Jan. 2014.

[102] N. V. Hoffer, C. Coopmans, A. M. Jensen, and Y. Chen, "Small low-cost unmanned aerial vehicle system identification: A survey and categorization," in *Proceedings of the 2013 International Conference on Unmanned Aircraft Systems (ICUAS13)*, May 2013.

[103] G. Milionis, "A framework for collaborative quadrotor c ground robot missions," Master's thesis, Naval Postgraduate School, Monterey, California, 2011.

[104] D. Xue and Y. Chen, *Linear Feedback Control: Analysis and Design with MATLAB*. Philadelphia, PA: Society for Industrial and Applied Mathematics, 2007.

[105] I. Podlubny, *Fractional Differential Equations*. Waltham, MA: Academic Press, 1999.

[106] C. Coopmans and Y. Han, "Aggieair: An integrated and effective small multi-uav command, control and data collection architecture," in *Proceedings of 2009 ASME/IEEE International Conference on Mechatronic and Embedded Systems and Applications (MESA09)*, August 2009.

[107] C. Coopmans, L. Di, A. Jensen, A. A. Dennis, and Y. Chen, "Improved architecture designs for a low cost personal remote sensing platform: Flight control and safety," in *Proceedings of 2011 ASME/IEEE International Conference on Mechatronic and Embedded Systems and Applications (MESA11)*, August 2011.

Vita

Jinlu Han

Education

- Ph.D. (Since September, 2009), Department of Electrical and Computer Engineering, Utah State University, Logan, Utah, U.S.A.
- M.S. (June, 2008), College of Control Theory and Control Engineering, Shandong University, Jinan, Shandong, China.
- B.S. (June, 2004), Department of Automation, Shandong University, Jinan, Shandong, China.

Journal Articles

- Jinlu Han, and YangQuan Chen, "Multiple UAV Formations for Cooperative Source Seeking and Contour Mapping of a Radiative Signal Field", *Journal of Intelligent and Robotic Systems*, 2014, Volume 74, Issue $1-2$, pp $323-332$.
- Jinlu Han, Long Di, Calvin Coopmans, and YangQuan Chen, "Pitch Loop Control of a VTOL UAV Using Fractional Order Controller", *Journal of Intelligent and Robotic Systems*, 2014, Volume 73, Issue $1-4$, pp $187-195$.
- Jinlu Han, Yaojin Xu, Long Di, and YangQuan Chen, "Low-cost Multi-UAV Technologies for Contour Mapping of Nuclear Radiation Field", *Journal of Intelligent and Robotic Systems*, 2013, Volume 70, Issue $1-4$, pp $401-410$.

Conference Papers

- Jinlu Han, and YangQuan Chen, "Cooperative source seeking and contour mapping of a diffusive signal field by formations of multiple UAVs", *The 2013 International Conference on Unmanned Aircraft Systems (ICUAS* 2013*)*, Atlanta, GA, USA, May 28 – 31, 2013.

- Jinlu Han, Long Di, Calvin Coopmans, and YangQuan Chen, "Fractional order controller for pitch loop control of a VTOL UAV", *The* 2013 *International Conference on Unmanned Aircraft Systems (ICUAS* 2013*)*, Atlanta, GA, USA, May 28 – 31, 2013.

- Jinlu Han, Yaojin Xu, Long Di and YangQuan Chen, "Low-cost Multi-UAV Technologies for Contour Mapping of Nuclear Radiation Field", 2012 *International Conference on Unmanned Aircraft Systems (ICUAS 2012)*, Philadelphia, PA, USA, June 12 – 15, 2012.

- Long Di, Haiyang Chao, Jinlu Han and YangQuan Chen, "Cognitive Multi-UAV Formation Flight: Principle, Low-Cost UAV Testbed, Controller Tuning and Experiments", *Proc. of* 2011 *IEEE/ASME International Conference on Mechatronic and Embedded Systems and Applications (IDETC/CIE* 2011*)*, Washington DC, USA, August 28 – 31, 2011.

- Ying Luo, Long Di, Jinlu Han, Haiyang Chao and Yangquan Chen, "VTOL UAV Altitude Flight Control Using Fractional Order Controllers", 4*th IFAC Workshop on Fractional Differentiation and Its Application (FDA* 2010*)*, Badajoz, Spain, October 18 – 20, 2010.

- Hu Sheng, Haiyang Chao, Calvin Coopmans, Jinlu Han, Mac McKee, and Yangquan Chen, "Low-cost UAV-based thermal infrared remote sensing: Platform, calibration and applications", *Proc. of* 2010 *IEEE/ASME International Conference on Mechatronics and Embedded Systems and Applications (MESA* 2010*)*, Qingdao, China, July 15 – 17, 2010.

Professional Presentations

- May 30, 2013: title of presentation "Fractional order controller for pitch loop control of a VTOL UAV", *The* 2013 *International Conference on Unmanned Aircraft Systems (ICUAS* 2013*)*, Atlanta, GA, USA.
- May 29, 2013: title of presentation "Cooperative source seeking and contour mapping of a diffusive signal field by formations of multiple UAVs", *The* 2013 *International Conference on Unmanned Aircraft Systems (ICUAS* 2013*)*, Atlanta, GA, USA.
- June 13, 2012: title of presentation "Low-cost Multi-UAV Technologies for Contour Mapping of Nuclear Radiation Field" for 2012 *International Conference on Unmanned Aircraft Systems (ICUAS* 2012*)*, Philadelphia, PA, USA.

Reviewer

- IEEE Transactions on Control of Network Systems (2014)
- International Journal of Advanced Robotic Systems (2014)
- The Aeronautical Journal (2014)
- IEEE International Conference on Robotics and Automation (ICRA 2014)
- International Journal of Advanced Robotic Systems (2013)
- ISA Transactions (2013)
- Information Sciences (2013)
- 52nd IEEE Conference on Decision and Control (CDC 2013)
- International Conference on Unmanned Aircraft Systems (ICUAS 2013)
- IEEE International Conference on Robotics and Automation (ICRA 2013)
- American Control Conference (ACC 2012)

- International Conference on Unmanned Aircraft Systems (ICUAS 2012)
- ASME 2011 International Design Engineering Technical Conferences (IDETC) and Computers and Information in Engineering Conference (CIE)
- International Conference on Control, Automation, Robotics and Vision (ICARCV 2010)

Service

Research Assistant, Center for Self-Organizing and Intelligent Systems (C-SOIS), Dept. of Electrical and Computer Engineering, Utah State University. Since September, 2009, worked as:

- Demonstrator: engineering week displays, "inverted pendulum, ball and beam", 2011, USU, Logan, UT, USA.
- Organizer and demonstrator: engineering state, "out of control", 2011, USU, Logan, UT, USA.
- Graduate research advisor: REU program, "introduction to quadrotor UAV", 2010, USU, Logan, UT, USA.
- Demonstrator: engineering state, "out of control", 2010, USU, Logan, UT, USA.